



Technische Universität München



Fakultät für Medizin

Institut für Diabetes und Adipositas

Novel disease entities and treatment strategies for leptin resistance and the metabolic syndrome

Luke Justin Harrison

Vollständiger Abdruck der von der Fakultät für Medizin der Technischen Universität München zur Erlangung des akademischen Grades eines

Doktors der Naturwissenschaften (Dr. rer. Nat.)

genehmigten Dissertation.

Vorsitzende/-r: Prof. Dr. Heiko Lickert

Prüfer der Dissertation: 1. Prof. Dr. Dr. h. c. Matthias Tschöp
2. Prof. Dr. Johann Josef Hauner

Die Dissertation wurde am 03.07.2019 bei der Technischen Universität München eingereicht und durch die Fakultät für Medizin am 05.11.2019 angenommen.

*“Nothing in life is to be feared,
It is only to be understood”*

Marie Curie

Abstract

In the past decades' obesity has evolved into a global disease of pandemic proportions, affecting over 650 million people. Being obese dramatically increases the risk of developing comorbidities such as type 2 diabetes, cardiovascular disease, osteoarthritis, various cancers as well as social burdens leading to psychosocial disease. The profound threat to human health and quality of life demands effective preventative measures, which currently are limited to risk-bearing surgical interventions. The discovery of leptin, a satiety signalling hormone derived from the adipose tissue, opened up a field of research with the aim of preventing obesity. A vast majority of obese subjects are suggested to have become leptin resistant, thus gaining excess weight, yet our understanding of this phenomenon is limited. This doctoral thesis discusses and explores the possible molecular mechanisms involved in leptin blood-brain-barrier transport, as an underlying cause for obesity. Moreover, further risk factors of obesity and the metabolic syndrome, namely hypothalamic gliosis and cranial irradiation are examined.

Here, using advanced light-sheet fluorescence microscopy and novel fluorescently labelled leptin, it is shown that leptin transport is likely not an underlying cause for leptin resistance. Furthermore, it is revealed that leptin transport is modulated by leptin receptor expression in the choroid plexus, highlighting a novel transport route for leptin to enter the brain. Hypothalamic gliosis, which has been shown to occur in response to obesity and high-fat diet feeding, was investigated in the context of chronic obesity and weight loss regimes. It was discovered that in chronic obesity, hypothalamic gliosis was no longer distinguishable from age-matched chow-fed counterparts, but that profound weight loss induced specific astrogliosis in the arcuate nucleus. This coincided with increased levels of circulating non-esterified fatty acids, hinting towards a possible disease mechanism of gliosis in early stage obesity. Finally, clinical evidence suggests a risk of developing obesity and the metabolic syndrome following high doses of childhood cranial irradiation. Here, the possibility that low-moderate doses could induce these maladies was studied. Using cranial irradiation directed towards the hypothalamus of

mice, it was demonstrated that, in addition to acute astrogliosis, latent onset disease phenotypes developed. Following 40 weeks, a body weight increase was recorded in female mice, with glucose intolerance developing after 18 months in male mice. Additionally, female mice presented with a decreased leptin response after only 2 months.

Together, this thesis has provided evidence that leptin resistance is unlikely due to deficits in leptin transport. Moreover, the nature of leptin resistance is discussed, ultimately questioning its current definition. These findings will most likely guide future work towards possible leptin sensitising therapies as treatment for obesity. Furthermore, the association of hypothalamic gliosis with profound weight perturbations but not with chronic obesity puts into question the translational future of this aspect. Lastly, first evidence was generated, indicating childhood cranial irradiation as a risk factor for the metabolic syndrome.

Zusammenfassung

In den letzten Jahrzehnten hat sich Fettleibigkeit zu einer globalen Krankheit entwickelt, von der über 650 Millionen Menschen betroffen sind. Fettleibigkeit erhöht das Risiko an Komorbiditäten wie Typ-2-Diabetes, Herz-Kreislauf-Erkrankungen, Arthrose, verschiedenen Krebsarten und sozialen Belastungen, die zu psychosozialen Erkrankungen führen, zu erkranken. Die Bedrohung der menschlichen Gesundheit und Lebensqualität erfordert wirksame Präventionsmaßnahmen, die derzeit auf risikobehaftete chirurgische Eingriffe beschränkt sind. Die Entdeckung von Leptin, einem aus dem Fettgewebe stammenden Sättigungshormon, eröffnete ein Forschungsfeld mit dem Ziel, Fettleibigkeit vorzubeugen. Es wird vermutet, dass die überwiegende Mehrheit übergewichtiger Personen eine Leptinresistenz entwickelt hat, die zur stetigen Gewichtszunahme beiträgt. Die Hintergründe dieses Phänomens sind jedoch größtenteils unbekannt. In dieser Doktorarbeit werden die möglichen molekularen Mechanismen des Blut-Hirn-Schranken-Transports von Leptin als Ursache für Fettleibigkeit diskutiert und untersucht. Darüber hinaus werden weitere Risikofaktoren für Adipositas und das Metabolische Syndrom, wie die hypothalamische Gliose und kraniale Bestrahlung untersucht.

Anhand der fortschrittlichen Lichtblatt-Fluoreszenzmikroskopie und des neuartigen fluoreszenzmarkierten Leptins wird gezeigt, dass der Leptintransport keine Ursache für die Leptinresistenz darstellt. Darüber hinaus wird gezeigt, dass der Leptintransport durch die Leptinrezeptorexpression im Plexus choroideus moduliert wird, was auf einen neuen hauptsächlichen Transportweg für Leptin in das Gehirn hinweist. Hypothalamische Gliose, die nachweislich als Reaktion auf Fettleibigkeit und fettreiche Ernährung auftritt, wurde im Zusammenhang mit chronischer Fettleibigkeit und Gewichtsverlust untersucht. Es wurde festgestellt, dass bei chronisch adipösen Tieren die hypothalamische Gliose im gleichen Maße auftritt wie in gleichaltrigen, mit fettarmer Diät gefütterten Kontrolltieren. Andererseits induzierte ein starker Gewichtsverlust eine spezifische Astrogliose im

Nucleus arcuatus. Dies ging mit einem Anstieg des Anteils an freien Fettsäuren im Blutkreislauf einher, was auf einen möglichen mechanistischen Zusammenhang der Gliose im Frühstadium der Adipositas hinweist. Klinische Belege deuten auf ein erhöhtes Risiko für die Entwicklung von Adipositas und des Metabolischen Syndroms nach hochdosierter kranialer Bestrahlung im Kindesalter hin. In dieser Arbeit wurden die möglichen Auswirkungen einer niedrig-moderaten Bestrahlung untersucht. Anhand von kranial bestrahlten Mäusen konnte gezeigt werden, dass zusätzlich zur akuten Astroglieose latente Krankheitsphänotypen auftraten. Bei weiblichen Mäusen konnte 40 Wochen nach der kranialen Bestrahlung ein erhöhter Anstieg des Körpergewichts beobachtet werden, diese zeigten zudem bereits zwei Monate nach Bestrahlung eine verminderte Leptinsensitivität. Bei männlichen Mäusen entwickelte sich nach 18 Monaten eine Glukoseintoleranz.

Zusammenfassend konnte in dieser Arbeit gezeigt werden, dass eine Leptinresistenz aufgrund von Defiziten im Leptintransport über die Blut-Hirn-Schranke unwahrscheinlich ist. Darüber hinaus wird das Thema Leptinresistenz diskutiert und letztendlich ihre derzeitige Definition in Frage gestellt. Diese Ergebnisse werden voraussichtlich zukünftige Ansätze der Leptinsensibilisierungstherapien zur Behandlung von Fettleibigkeit beeinflussen. Darüber hinaus stellt die Assoziation von hypothalamischer Gliose mit starken Gewichtsstörungen, jedoch nicht mit chronischer Adipositas, die translationale Zukunft dieses Aspekts in Frage. Zuletzt wurden erste Hinweise auf eine kraniale Bestrahlung im Kindesalter als Risikofaktor für das metabolische Syndrom gegeben.

Table of contents

1. Introduction	1
1.1. Obesity as a global burden	1
1.1.1. Type 2 Diabetes	3
1.2. Energy homeostasis imbalance	3
1.3. Central nervous system control of energy homeostasis	5
1.4. Discovery of leptin and the leptin receptor	7
1.5. Leptin receptor signalling	9
1.6. Leptin resistance and the metabolic syndrome	11
1.6.1. Leptin transport	12
1.6.2. Leptin signalling	12
1.7. Neuroinflammation – a common denominator for metabolic dysfunction	14
1.7.1. Reactive gliosis	15
1.7.2. Cranial irradiation as an exogenous risk factor for obesity and type 2 diabetes	17
2. Aims of the PhD thesis	19
3. Experimental approaches	21
3.1. Leptin coupling and visualisation	21
3.1.1. Choice of fluorophore	21
3.1.2. Tissue clearing and microscopy method	22
3.2. Reactive gliosis requires precise methodology	23
3.3. Irradiation source and calibration	24
4. Results	27
4.1. Fluorescent blood–brain barrier tracing shows intact leptin transport in obese mice	27
4.1.1. Aim and summary	27
4.1.2. Contribution	28
4.1.3. Publication information	28
4.2. Profound weight loss induces reactive astrogliosis in the arcuate nucleus of obese mice	43
4.2.1. Aim and summary	43
4.2.2. Contribution	44

4.2.3. Publication information.....	44
4.3. Low-medium dosed cranial irradiation in young mice induces sex specific metabolic disturbances later in life	53
4.3.1. Aim and summary	53
4.3.2. Contribution	53
4.3.3. Publication information.....	54
5. Summary of key findings.....	77
6. Discussion and future perspectives	79
6.1. Leptin transport across the BBB and our understanding of leptin resistance ...	79
6.2. Reactive gliosis in obesity.....	82
6.3. Moderate doses of cranial irradiation result in disturbed metabolic regulation.....	85
7. References	87
8. Abbreviations.....	103
9. List of figures	105
10. List of tables.....	105
11. Acknowledgements.....	107

1. Introduction

1.1. Obesity as a global burden

The earliest evidence for human obesity dates back to approximately 30,000 years ago in the form of an obese figurine known as the *Venus of Willendorf*, which was discovered in 1908 in Willendorf, Austria (Antl-Weiser 2000). Although obesity has been present throughout human history, it was reserved to sporadic and specific fractions of the population. It was not until the end of the 20th century that obesity started developing into a global health threat. The prevalence of obesity has tripled since 1975, with current numbers reaching over 1.9 billion adults classified as overweight, of which 650 million were obese (WHO 2018) (figure 1). The world health organization (WHO) has stated that currently over 2.8 million people die each year due to being overweight or obese. This surge not only affects adults (18 years and older), but is unfortunately also seen in children. In 2016 there were a staggering 41 million children under the age of 5 that were classified as overweight or obese. The general measure for a healthy body weight is typically determined using the body mass index (BMI) which is a measure of body weight relative to height and then classified into categories by the WHO, based on certain cut-off

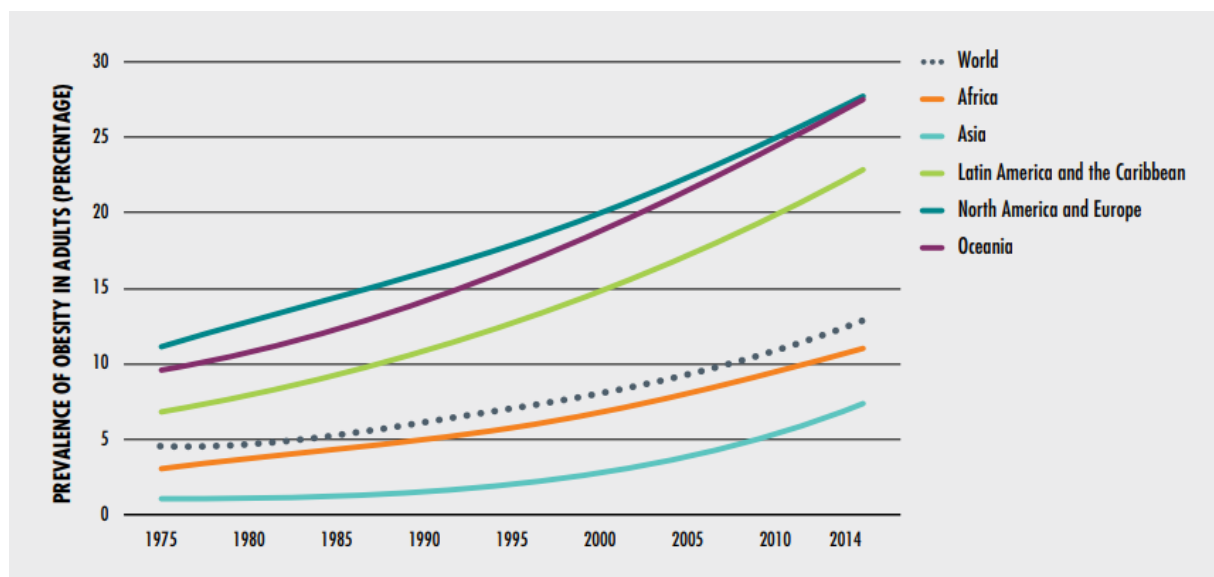


Figure 1: Prevalence of obesity in adults 18 years and older. Adapted from the WHO global health observatory data repository 2017 (FAO et al. 2017)

points (Table 1)(WHO 2004). Despite being the current determinant of obesity chosen by the WHO, the BMI scale has several limitations by not taking into account certain parameters such as age and lean mass (Rothman 2008). The next-in-line measurements of obesity are the waist-hip ratio and the waist-height ratio, which are simply the circumference in cm of the waist, divided by the circumference of the hip or height. Both waist-hip ratio and waist-height ratio have been used to better predict risk factors than BMI for certain cases (Huxley et al. 2009, Emdin et al. 2017, Liu et al. 2018). None of the mentioned scales are perfectly suited to measure obesity and often a combination of two or more are most beneficial (Emdin et al. 2017).

Classification	BMI(kg/m ²)	
	Principal cut-off points	Additional cut-off points
Underweight	<18.50	<18.50
Normal range	18.50 - 24.99	18.50 - 22.99
		23.00 - 24.99
Overweight	≥25.00	≥25.00
Pre-obese	25.00 - 29.99	25.00 - 27.49
		27.50 - 29.99
Obese	≥30.00	≥30.00
Obese class I	30.00 - 34.99	30.00 - 32.49
		32.50 - 34.99
Obese class II	35.00 - 39.99	35.00 - 37.49
		37.50 - 39.99
Obese class III	≥40.00	≥40.00

Table 1: Body weight classification defined by the World Health Organisation (WHO)

Obesity as such, is rarely the direct cause of death, however it is directly linked to a plethora of comorbidities such as coronary heart disease, stroke, hypertension, sleep apnea, osteoarthritis, insulin resistance and type 2 diabetes mellitus (T2D) (Khaodhiar et al. 1999). Abnormalities in lipid metabolism, typically described by reduced circulating high-density lipoproteins as well as increased serum low-density, very low-density lipoproteins and cholesterol are also common in obese subjects (Head 2015). Obesity also increases the likelihood of succumbing to stomach, liver, colorectal, gallbladder, pancreatic, kidney, prostate, oesophageal, breast, uterine, cervical and ovarian cancers, as well as leukaemia, multiple myeloma and non-Hodgkin’s lymphoma (Calle et al. 2003).

1.1.1. Type 2 Diabetes

Blood glucose levels are usually tightly regulated; as even slight disturbances can have severe impacts on health. Chronic high blood glucose (hyperglycaemia) may result in cardiovascular disease, diabetic nephropathy, diabetic neuropathy, diabetic retinopathy and reduced blood flow, typically to the lower extremities (Roglic et al. 2005). On the other end of the scale, hypoglycaemia can induce hunger, heart palpitations, loss of consciousness and eventually death (Frier et al. 2011). Insulin is the main regulator of blood glucose. It is secreted from beta cells located in the pancreas when blood glucose levels begin to increase. Insulin acts on many tissues in the body to regulate glucose levels, for example facilitating glucose uptake in muscle and fat, suppressing gluconeogenesis in the liver, preventing lipolysis in adipose tissue and decreasing food intake via the brain (Kleinridders et al. 2014, Lambadiari et al. 2015, Tokarz et al. 2018). T2D is clinically defined as having a fasting plasma glucose level of over 126 mg/dl or 200 mg/dl for 2 hours post 75 g oral glucose tolerance test or ad-libitum hyperglycaemia of over 200 mg/dl (American Diabetes Association 2015). The disease is mainly caused by insulin resistance in multiple tissues including skeletal muscle, liver and fat. These tissues have a blunted response to insulin, resulting in an increased insulin secretion by the pancreas and subsequent hyperinsulinemia (Groop 2000). The hyperinsulinemia in turn further aggravates the tissue resistance eventually ending in hyperglycaemia. Over time the elevated plasma glucose levels eventually lead to beta cell exhaustion and subsequent beta cell loss. The lack of insulin further worsens the hyperglycaemia which in time results in the maladies described above.

It is then clear that obesity has a strong negative impact on human health. Despite this, global obesity is on the rise and so great efforts need to be made to raise awareness as well as focus on understanding the underlying causes for obesity, and equally as important; how to avoid regaining lost weight. Understanding the bodies mechanisms for regulating energy homeostasis is key in this regard.

1.2. Energy homeostasis imbalance

One of the most basic functions of a living organism is the ability to sustain a constant metabolic balance which can adapt to changes in environment regarding energy availability. The system must be able to establish an energy reserve for times when

sources are low and fuel is required for high-demand activities such as hunting, foraging and other food seeking behaviours. During the evolution of the human species, a vast amount of time was spent in situations where phases of fasting for extended periods was commonplace and so homeostatic systems may have evolved to accommodate this by favouring energy storage at a time of energy surplus (Berbesque et al. 2014). The “thrifty genotype” hypothesis suggested that evolutionary pressure did precisely that (Neel 1962). However, these evolutionary adaptations do not fit into the current environment, where palatable high caloric food is readily available, thus suggesting a possible cause for the recent increase in obesity rates. Although this theory provides an attractive narrative for the current obesity epidemic, others have criticised its likelihood and have suggested other theories such as the “thrifty phenotype”, which suggests that a poor nutritional state in pre- and early postnatal stages are definitive, rather than later in life (Hales and Barker 1992). In these early developmental stages nutrient availability and source may influence where a body weight set-point is aligned. Alternatively, the “drifty genotype” argues that in fact there is little environmental pressure that would have caused the evolution of a homeostatic system that is cantered to one side, and that it is simply a result of genetic drift (Speakman 2008). Regardless of the current popular theory, it remains evident that the underlying causes involve complex homeostatic mechanisms, which are unable to cope with the current nutrient rich environment and subsequently result in detrimental energy balance handling.

Something that is widely agreed upon however, is that the two main contributors on either side of the energy balance scale are energy intake and energy expenditure (Cox et al. 2014). Energy intake is comprised mainly by the food we eat. Energy expenditure however has multiple outlets, most of which is in the form of our basal metabolism, required for normal physiological functions in a resting state. Aspects such as physical activity and thermogenesis also contribute to overall energy use (Trayhurn 1990). If these key factors are the tuning dials for energy homeostasis, then there must be mechanisms by which they can be up- and downregulated according to nutrient availability and current energy stores.

The regulation of energy homeostasis must be a dynamic process if it is to adjust for sudden changes in the environmental availability of food or acute physical activity demands. However, like many homeostatic systems, a chronic overstimulation of either

side of the scale will at some point reach a breaking point. This is the case in most of the western world, where there is a chronic situation of energy surplus due to ever increasing sedentary lifestyles, higher stress levels and easy access to palatable high caloric food. Over time, as body adiposity increases due to the chronic stress on the homeostatic system, the body undergoes adaptations which gradually recognise the now increased body weight as the new balanced homeostatic set-point (Keesey and Hirvonen 1997). As a result, the body will now defend the obese condition. For example; individuals that attempt to lose weight will typically reduce their caloric intake by eating less and placing a negative energy balance on the system. To counteract this negative energy balance the body decreases its energy expenditure, which is characterised by lowered resting metabolic rate, reduced exercise associated energy expenditure and diminished dietary induced thermogenesis required for digestion and calorie uptake (Johnson et al. 2016). Unfortunately, this decline in energy expenditure can persist for several years hindering long-term weight loss for most individuals (Fothergill et al. 2016). Understanding the mechanisms involved in these processes will remain fundamental in regards to understanding why we gain excess body fat and why losing this weight remains a global challenge.

1.3. Central nervous system control of energy homeostasis

The importance of the hypothalamus in the regulation of energy homeostasis was made clear by a series of elegant brain lesion experiments performed by John Brobeck in the middle of the 20th century. It was demonstrated, that lesions within the ventromedial hypothalamic nucleus (VMH) caused a reduction in food intake and weight loss, whereas lesions to the lateral hypothalamic area (LHA) resulted in increased food intake and weight gain (Brobeck 1946). Further experiments, such as those described by Coleman, which used parabiosis in combination with hypothalamic lesioned mice, confirmed that a circulating factor required certain hypothalamic nuclei as a sensor to regulate body adiposity (Hervey 1959, Coleman and Hummel 1969, Coleman 1973). The discovery of leptin (Zhang 1994), the leptin receptor (Tartaglia et al. 1995) and its expression in the brain (Maffei et al. 1995) was one of the main causes for an increase in interest as to how the brain controlled food intake and energy expenditure. Insulin too was a major player in the development of our understanding in how the central nervous system (CNS) regulates systemic glucose homeostasis. The insulin receptor was shown to be widely

expressed within the CNS with distinct expression patterns revealing brain centres relevant for metabolic sensing (Havrankova et al. 1978). Indeed intracerebroventricular (ICV) infusion of insulin resulted in reductions in food intake and was associated with a decrease in body weight (Woods et al. 1979).

The hypothalamus is a key brain region in regards to metabolic sensing and systemic metabolic control (Andermann and Lowell 2017). In particular, the arcuate nucleus of the hypothalamus (ARC), which is located in the mediobasal region of the hypothalamus (MBH), displays a high concentration of both insulin and leptin receptors. In the ARC there are a number of neuronal populations that are involved in controlling energy homeostasis. The two most well described types, express either the neuropeptide agouti-related protein (Agrp) (Horvath et al. 1992) or pro-opiomelanocortin (POMC) (Mountjoy et al. 1992). These neurons are capable of sensing metabolic factors such as leptin or insulin by expression of the respective receptors. Activation of these neurons leads to the release of Agrp, neuropeptide Y (NPY) (which is co-expressed with Agrp) and a cleaved

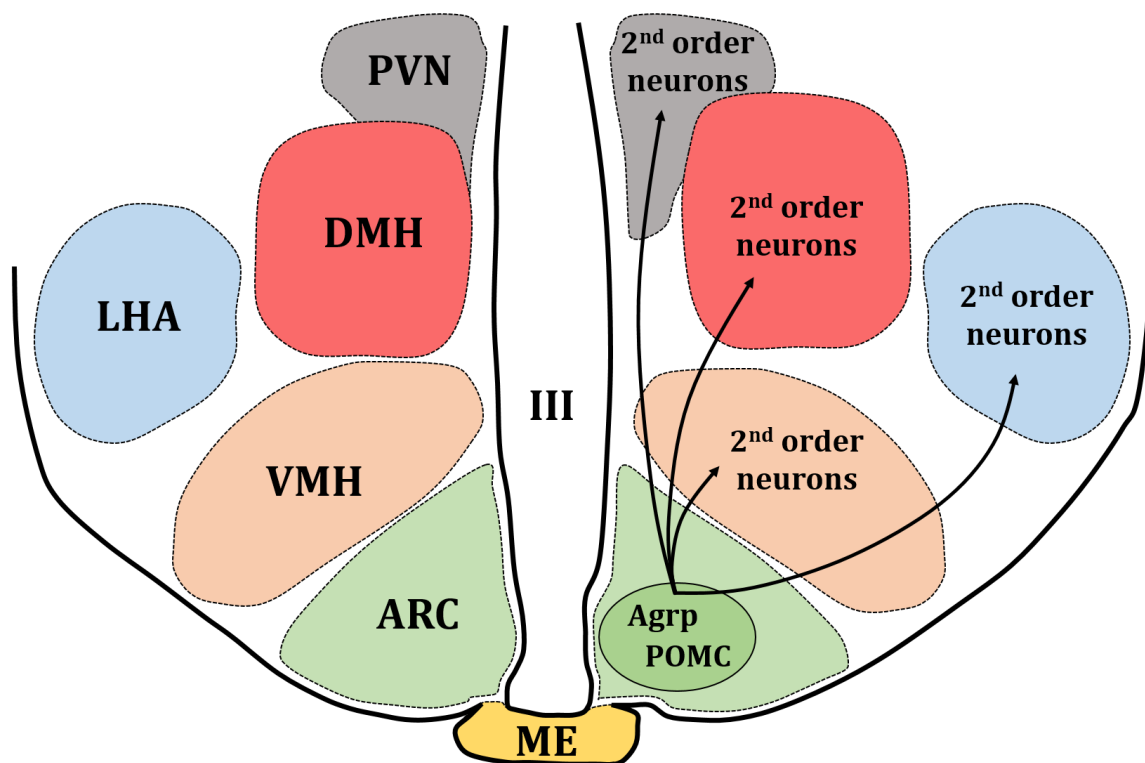


Figure 2: Murine hypothalamic organisation. Agrp and POMC expressing neurons in the ARC extend their processes to the VMH, LHA, DMH and PVN, whilst close proximity to the ME enables sensing of circulating factors. III = 3rd ventricle

form of POMC; α -melanocyte-stimulating hormone. AgRP and POMC neurons extend their processes to various other hypothalamic nuclei such as the paraventricular nucleus (PVN), the VMH, the LHA and the dorsomedial hypothalamus (DMH) (figure 2). Second-order neurons in these regions express the melanocortin receptor 3 and 4 (MC3/4R) and project to more distant regions such as the cortex and brainstem to facilitate behavioural and systemic regulation of food intake and energy expenditure.

The ARC is situated ideally within the brain to be able to sense circulating metabolic factors. The median eminence (ME) lies directly adjacent to the ARC and is one of the circumventricular organs of the brain. Circumventricular organs are not protected by a traditional blood-brain-barrier (BBB) and thus come into direct contact with factors present in the blood (Knigge and Scott 1970, Rodriguez et al. 2010). Projections from ARC neurons reach into the ME and thus able to directly sense acute changes in hormones, nutrients and other signalling molecules (Kiss et al. 1985). Furthermore, the ARC is in close proximity to the third ventricle, separated by a single cell layer of specialised glial cells known as tanycytes (Langlet et al. 2013). Metabolic factors present in the cerebrospinal fluid (CSF) may be sensed by tanycytes (Bolborea and Dale 2013) or even passively diffuse into the ARC (Whish et al. 2015) and be capable of regulating the neurons located here.

1.4. Discovery of leptin and the leptin receptor

In the late 1940's researchers at the Jackson laboratory in Maine, USA, discovered a strain of mice that were massively obese (Ingalls et al. 1950). They realised that a recessive mutation in a gene they called "obese" (ob) was causing the severe obesity in these animals. The most prominent phenotype of these mice was extreme hyperphagia, resulting in mutants weighing up to three times more than wild type littermates (Ingalls et al. 1950). The fact that a single gene could result in such an extreme dysregulation of food intake and obesity indicated the presence of a powerful regulator. 15 years later another strain was discovered, which also rapidly developed obesity driven by a voracious appetite. This strain however, differed to the ob/ob mouse in that it developed severe diabetes, thus the gene was named "diabetes" (db) (Hummel et al. 1966). The rate at which the ob/ob and the db/db mouse became obese was almost identical. Douglas

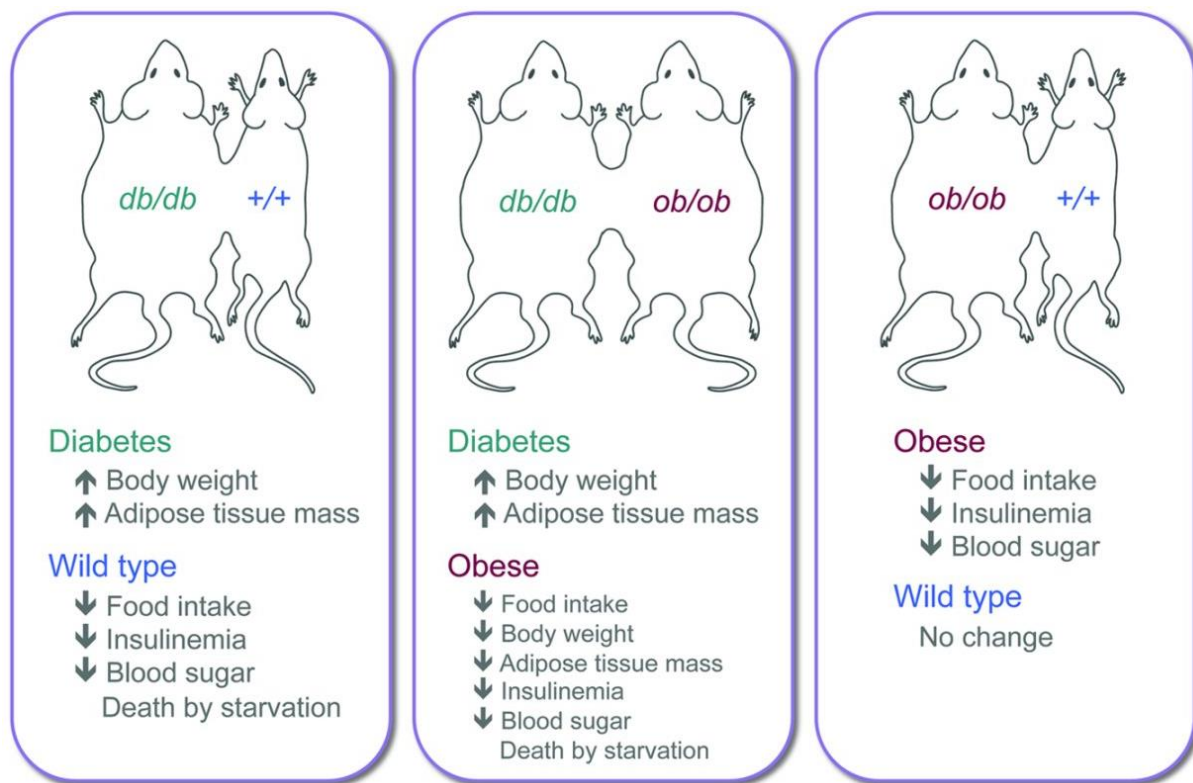


Figure 3: Parabiosis experiments performed by Douglas Coleman. Illustrated are the experimental designs for the parabiosis experiments leading to the discovery of a circulating satiety factor, which would eventually be discovered and named leptin. Figure adapted from (Neill 2010).

Coleman was working at the Jackson laboratory and set about trying to understand the underlying mechanisms driving the similar phenotypes. Displaying elegant experimental design, Coleman used parabiosis experiments to tease out the functions of the obese and diabetes genes after he wondered if a circulating factor might be causing the metabolic abnormalities (figure 3). This involved joining mice by their skin from the shoulder to the hip, which after several days resulted in a shared blood circulation. In the initial experiments a *db/db* mouse was joined to a wild type mouse. Although no changes were noted in the *db/db* mouse, the wild type mouse displayed dramatically reduced food intake and severe hypoglycaemia that ultimately led to death by starvation (Coleman and Hummel 1969). This suggested that the *db/db* mouse was producing a circulating factor that was a potent stimulator of satiety. When Coleman parabiosed the *db/db* mouse with the *ob/ob* mouse, the situation repeated itself and the *ob/ob* mouse stopped eating and died of starvation 20 – 30 days later (Coleman 1973). Finally, when *ob/ob* mice were paired to wild type mice, the *ob/ob* mice again decreased their food intake and lost weight, but importantly, not to the point of starvation (Coleman 1973). This led to the

hypothesis that the db/db mouse was secreting high concentrations of an unknown molecule that could powerfully suppress food intake, but had no effect in the db/db mouse itself and that this molecule was present at lower concentrations in wild type mouse. The ob/ob mouse on the other hand could respond to this molecule but was not able to produce it. It was not until 1994, when the responsible molecule was finally discovered by a technique known as positional cloning in Jeffery Friedman's lab (Zhang 1994). The protein was named leptin, originating from the Greek "leptos" meaning thin. They also showed that leptin was synthesised exclusively in the white adipose tissue (Zhang 1994). Just a year later in 1995 the leptin receptor was identified by Millennium Pharmaceuticals (Tartaglia et al. 1995). Shortly after its discovery, the leptin receptor was shown to be expressed in the brain, and particularly in the hypothalamus, known to play a role in energy homeostasis (Maffei et al. 1995).

These discoveries not only led to a global explosion in leptin related research, but also changed our understanding of obesity as a disease. No longer was lack of will power or laziness the prevailing theory for why people became obese. It had been shown that hormone signalling could dramatically affect body weight homeostasis, offering underlying genetic causes for obesity. It was now also clear that adipose tissue was a key endocrine organ, rather than a simple depot for long term energy storage (Coleman 2010).

1.5. Leptin receptor signalling

In the CNS a specific isoform of the leptin receptor (LepR) is responsible for mediating leptin's role in energy homeostasis. LepRb is one of six leptin receptor isoforms (LepR a, b, c, d, e or f) encoded by the same leptin receptor gene (Fei et al. 1997). All of the isoforms contain the extracellular N-terminal leptin binding domain but differ in their C-terminal domains. The receptor isoforms can be grouped into three main categories; short forms (LepRa, c, d and f) which lack the full length C-terminal intracellular signalling domain, the long form (LepRb) and the secreted form (LepRe) (Fei et al. 1997). The long form LepRb has an extracellular, a membrane spanning, and intracellular domain and belongs to the interleukin 6 (IL-6) type cytokine receptor family (Baumann et al. 1996) (figure 4). Upon leptin binding, Janus kinase 2 (JAK2), a tyrosine kinase associated to the leptin receptor, becomes activated via auto-phosphorylation (Banks et al. 2000). JAK2 in turn

then phosphorylates three tyrosine residues on the leptin receptor. Phospho-Tyr⁹⁸⁵, -Tyr¹⁰⁷⁷, -Tyr¹¹³⁸ recruit further signalling molecules containing an Src-homology 2 domain such as signal transducer and activator of transcript 3 (STAT3), signal transducer and activator of transcript 5 (STAT5) and protein tyrosine phosphatase 2 (SHP2) (Zhou and Rui 2013). Phosphorylation of STAT3 and the subsequent transcriptional regulation is thought to be the main driver for leptin's hypothalamic anorectic effects (Bates et al. 2003). The leptin signalling cascade is inhibited by a negative feedback loop driven mainly by suppressor of cytokine signalling 3 (SOCS3) (Bjørnbæk et al. 1998), but also by protein tyrosine phosphatase 1B (PTP1B) (Kaszubska et al. 2002) and T cell protein tyrosine phosphatase (TCPTP) (Loh et al. 2011), all of which inhibit the activation of either SHP2, JAK2 or STAT3.

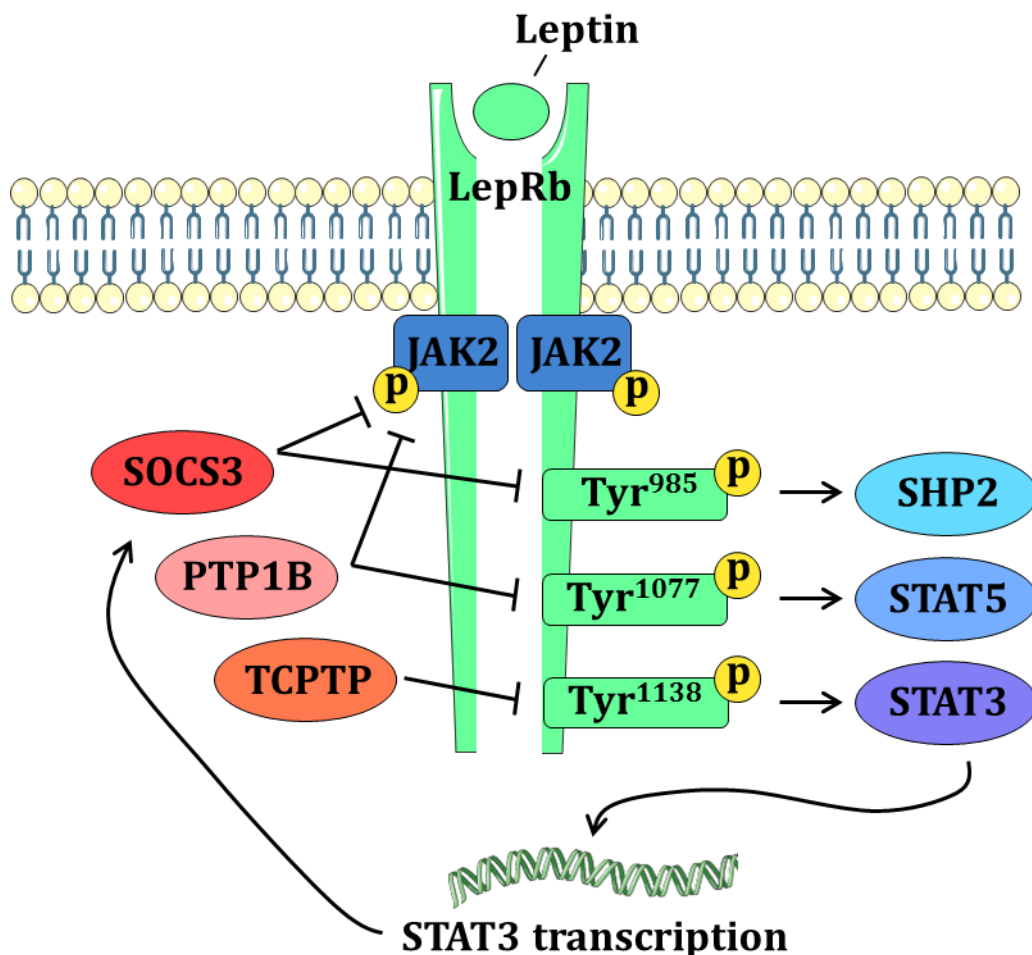


Figure 4: Leptin receptor signalling mechanism. The binding of leptin to the leptin receptor LepRb results in a signalling cascade ultimately resulting in STAT3 mediated transcription of target neuropeptides and negative feedback regulators such as SOCS3.

1.6. Leptin resistance and the metabolic syndrome

The discovery that leptin potently inhibits food intake in leptin deficient ob/ob mice raised hopes that leptin therapy could be the answer to the obesity epidemic. Amgen Pharmaceuticals carried out a clinical trial using daily leptin injections as a monotherapy for the treatment of obesity (Heymsfield et al. 1999). Within the first 4 weeks of the study both lean and obese patients lost similar amounts of weight which was significantly more than the placebo group. Obese subjects alone then continued the study for a further 20 weeks and results varied heavily. Only patients receiving the highest dose of leptin displayed a significant weight loss compared to the placebo, however some patients in the high dose group even gained weight and significant side effects were also observed. Overall the results were so varied that no further studies were performed and the hopes of using leptin as a simple one-shot treatment for obesity quickly faded.

Obese individuals actually present circulating leptin levels which are close to 10-fold higher than lean counterparts (Considine et al. 1996). The fact that leptin therapy was not able to mediate food intake driven weight loss is then perhaps not as surprising. Studies on mice that were made obese by feeding them with a high-fat diet (HFD) (diet induced obesity (DIO)) replicated the findings in humans that when treated with leptin there was no change of their food intake or bodyweight (El-Haschimi et al. 2000). This finding led to the term “leptin resistance”. In obesity, leptin resistance broadly describes the inability of leptin to reduce energy intake and increase energy expenditure. Leptin resistance is typically assessed by the use of two different tests. The first uses a simple approach which is to treat fasted mice with leptin or vehicle and then measure the food intake over the following 24 hours. Leptin sensitive animals should reduce their food intake significantly to that of the vehicle treated mice. The second readout of leptin sensitivity is to determine the downstream signalling magnitude in the ARC of the hypothalamus after leptin injection, as measured by phosphorylation of STAT3.

There are several proposed possible mechanisms responsible for leptin resistance, which fall into three groups:

1.6.1. Leptin transport

As leptin is released by the white adipose tissue it must travel via the circulation to reach its target neurons in the brain. To gain access to the hypothalamus and other regions in the brain, leptin must cross the blood brain barrier (BBB). The BBB is formed by specific tight junctions between the endothelial cell layer of blood vessels, but is a dynamic system that is maintained and regulated by what is known as the neurovascular unit, comprising of endothelial cells, astrocytes, neurons and pericytes (Bauer et al. 2014). In essence the BBB prohibits the passage of unwanted molecules or pathogens into the brain parenchyma, but allows for the diffusion of smaller required substances such as oxygen or ions (Daneman and Prat 2015). Leptin, being comparatively large, must then be transported via an active transportation route (Hileman et al. 2002) to reach the hypothalamic regions and LepRa is the likely candidate responsible for this (Kastin et al. 1999, Hileman et al. 2002). There are several lines of evidence that suggest inhibited or blunted leptin transport across the BBB may be a cause for leptin resistance. Some suggest a reduced transfer of leptin across the BBB due to decreased plasma : CSF concentrations (Banks et al. 1999), possibly induced by increased circulating triglycerides (Banks et al. 2004), whilst others have proposed more specific mechanisms involving a tanycyte-mediated uptake (Balland et al. 2014). However, more evidence is required to support these findings as a definitive answer is still missing.

1.6.2. Leptin signalling

A perhaps more direct cause for leptin resistance is the misregulation of intracellular leptin signalling. A decreasing leptin action would be expected if any stage of the leptin signalling process would be impaired.

1.6.2.1. Receptor trafficking

According to immunohistochemistry studies, the highest proportion of leptin receptor is located within the Golgi apparatus, and not at the plasma membrane (Diano et al. 1998). This indicates that leptin receptor turnover at the membrane is high and so must be tightly regulated. Changes to leptin receptor trafficking would likely result in diminished leptin signalling due to a decreased presence of the leptin receptor at the membrane. Indeed, mouse models of the Bardet-Biedl syndrome, which have impaired Golgi – membrane trafficking, result in obesity (Rahmouni et al. 2008) and a lack of leptin

signalling (Bugge et al. 2009). Conversely a decrease in leptin receptor internalisation from the membrane may also lead to a blunted response.

1.6.2.2. Negative regulators

The inhibition of leptin signalling is tightly controlled via a negative feedback loop involving SOCS3, PTP1B and TCPTP. Not only does SOCS3 inhibit leptin signalling by binding to the intracellular domain of the leptin receptor, but also by directly binding JAK2 (Bjørnbæk et al. 1998). Accordingly, a global heterozygous deletion of SOCS3 increases leptin signalling, sensitivity to exogenous leptin and blunts weight gain in HFD fed mice (Howard et al. 2004). When SOCS3 was deleted from neurons exclusively, mice were protected from DIO and had improved leptin sensitivity (Mori et al. 2004). Furthermore, experiments where SOCS3 levels were genetically increased in POMC neurons, resulted in severe obesity and blunted leptin sensitivity (Reed et al. 2010). In mice that are overweight due to age or in models of obesity, there is a chronic increase in SOCS3 levels, providing physiological evidence for a SOCS3-dependant leptin resistance (Bjørnbæk et al. 1998). Similar data can be found for both PTP1B (Zabolotny et al. 2002, Bence et al. 2006, Zimmer et al. 2012) and TCPTP (Loh et al. 2011, Pfuhlmann et al. 2018), indicating that any of these signalling pathways could be a possible cause for leptin resistance.

1.6.2.3. Second-order resistance

Agrp/NPY and POMC neurons in the ARC that express the leptin receptor are only the initial step in the signal transduction pathway leading to leptin's anorectic effects. The primary neurons in the ARC project to second-order neurons in the VMH, PVN, DMH and LHA. The expression of the MC3/4R in the second-order neurons is critical for functional leptin signalling in the hypothalamus, which if lacking, results in morbid obesity in animal models and in humans (Yeo et al. 1998, Marsh et al. 1999, Farooqi et al. 2003). A number of other signalling pathways in second-order neurons are known to be involved with leptin signalling, such as the brain-derived neurotrophic factor (BDNF) signalling cascade. BDNF located in DMH neurons is activated following the presence of leptin or insulin in the ARC, and when mutated to a non-functional truncated form, results in severe hyperphagia and weight gain (Liao et al. 2012). BDNF's significance was confirmed in humans when BDNF gene mutations were linked to obesity (Liao et al. 2012).

1.7. Neuroinflammation – a common denominator for metabolic dysfunction

Obesity and other metabolic disorders have been associated with a low-grade chronic inflammation (Gregor and Hotamisligil 2011, Thaler et al. 2013, Zhou and Rui 2013). Overnutrition and consumption of HFD promotes inflammation in various tissues, resulting in tissue specific insulin resistance (Gregor and Hotamisligil 2011). Nuclear factor kappa-light-chain-enhancer of activated B-cells (NF- κ B) is known to be a master regulator of inflammation in peripheral tissues (Lehrke and Lazar 2004, Hotamisligil 2006). This phenomenon is also present in the hypothalamus, where pro-inflammatory signals and responses are upregulated in response to HFD feeding (De Souza et al. 2005). Here, NF- κ B signalling has been described in Agrp neurons, where, similarly to in POMC neurons, it was activated in response to hypothalamic inflammation, inducing SOCS3 expression and causing insulin and leptin resistance (Zhang et al. 2008, Velloso and Schwartz 2011). Obesity and HFD feeding also increase the concentrations of circulating non-esterified fatty acids (NEFA), which can bind the toll-like receptor 4 (TLR4) (Shi et al. 2006) to further mediate NF- κ B signalling (Zhang et al. 2008) and induce endoplasmic reticulum (ER) stress. Accordingly, when TLR4 neutralising antibodies were injected ICV into rats, they blunted the hypothalamic inflammation in response to circulating NEFAs (Milanski et al. 2009).

The ER is an organelle and is the primary site of protein synthesis, protein folding and lipid synthesis. It can also be referred to as the sorting station of the cell, as proteins located in the ER are organised in regards to their destination. Short N-terminal amino acid sequences act as identifiers for where proteins are transported to and are distributed accordingly within the ER (Kaufman 1999). ER stress is described as a situation where there is an accumulation of misfolded or unfolded proteins within the ER, resulting in cellular malfunction. Overnutrition has been strongly linked to ER stress, which can be activated by circulating inflammatory factors such as IL-6 and TNF- α (Zhang et al. 2006) and is implicated in leptin resistance (Ozcan et al. 2009). Moreover, ER stress also induces the inhibitor of nuclear factor kappa-B kinase subunit beta / NF- κ B pathway, which can in turn further exacerbate the level of ER stress (Zhang et al. 2008).

A further key regulator of inflammation, c-Jun amino-terminal kinase 1 (JNK1), is also clearly involved in hypothalamic inflammation. When deleted, either globally or specifically in hypothalamic neurons, it prevents the development of obesity in HFD fed mice (Hirosumi et al. 2002). Furthermore, low-grade inflammation increased the expression of hypothalamic JNK1, resulting in central insulin resistance (Rorato et al. 2017).

Although much of the evidence described so far points towards a positive correlation between inflammation and a worsened metabolic state, there are examples of the reverse effect. For example, knock-out mice for pro-inflammatory mediators such as interleukin-1 (IL-1), IL-6 or TNF- α display an increased susceptibility to obesity rather than a decrease (Schreyer et al. 1998, García et al. 2006). Similarly, pharmacologically increasing pro-inflammatory reactive oxygen species was shown to prevent DIO (Findeisen et al. 2011). Another example comes from an experiment where after HFD feeding, DIO rats were switched back to a normal chow diet and after 2 months normalise their bodyweight, but preserve an increased level of hypothalamic inflammation (Wang et al. 2012). More recently, the effects of celastrol (a potent anti-obesity agent (Liu et al. 2015)) were shown to be driven by activation of the IL-1 receptor 1 (Feng et al. 2019) and this is well known to induce pro-inflammatory signalling (O'Neill 2008, Dinarello 2011).

Although in many cases of HFD feeding and obesity it seems that hypothalamic inflammation plays a key role, whether or not the inflammatory response is more a consequence rather than a cause needs to be further elucidated. A likely scenario is that, as so often in obesity, hypothalamic inflammation may be one of many physiological changes that contribute to the development of the disease and that the additive effects of these changes are required for a fully developed disease phenotype (Thaler et al. 2013). Indeed, recent evidence suggests that glia cells may comprise a further potential component of this puzzle by becoming activated in response to obesity and HFD feeding (Thaler et al. 2012).

1.7.1. Reactive gliosis

Glial cells, which consist mainly of astrocytes, microglia and oligodendrocytes, but to a lesser extent also include tanycytes, Schwann cells and satellite cells (Jäkel and Dimou 2017) respond to a wide range of stimuli. A classical response for example, is the

involvement of microglia in the so-called scar formation following physical damage to the CNS (Fitch and Silver 2008). Here microglia and astrocytes undergo a process known as reactive gliosis (RG) in order to carry out their wound healing and neuroprotective roles (Norton et al. 1992). RG includes morphological changes such as hypertrophy and hyperplasia, cell migration, transcriptional changes and cytokine release (e.g. IL-6, transforming growth factor beta, IL-1 β and TNF α (Burda and Sofroniew 2014)) (Kreutzberg 1996, Ridet et al. 1997). Astrocytes are stellate in structure and extend their processes to reach nearby neurons, blood vessel endothelial cells or other astrocytes. Here, the process terminating end-feet wrap around or make contact with the target cells. For neurons this takes place either at the synapse or along the axon (Bushong et al. 2004, Oberheim et al. 2006, Freeman 2010). Glial fibrillary acidic protein (GFAP) is expressed almost exclusively by astrocytes. It provides an intermediate structural component and is up regulated during RG (Ridet et al. 1997).

Microglia on the other hand are smaller in size and are often referred to as the macrophages of the brain as they have been shown to perform phagocytosis within the CNS (Fu et al. 2014). Upon activation and RG, microglia increase their expression of certain factors such as the major histocompatibility complex 2 and inducible nitric oxide (Banati et al. 1993, Kreutzberg 1996). Ionised calcium-binding adapter molecule 1 (Iba1) is a microglia specific marker, which is also upregulated during RG and is often used as a marker for microglial identification.

Astrocytes and microglia become activated in certain disease states, having beneficial and anti-inflammatory effects. Long-term RG however has been shown to be detrimental and reflect a pro-inflammatory state. Chronic release of pro-inflammatory factors causes tissue damage and is the underlying malfunction of the CNS in many diseases (Sheng et al. 1996, Johnstone et al. 1999, Knott et al. 2000). This has been suggested for astrocytes and microglia in the hypothalamus in obesity where they may contribute to hypothalamic inflammation (Dong and Benveniste 2001, Streit et al. 2004, García-Cáceres et al. 2012). Astrocytes and microglia become activated in as little as 24 h after the start of HFD feeding (Thaler et al. 2012) and have been observed to remain in this activated state for longer periods of chronic hyper-caloric feeding (Thaler et al. 2012, Buckman et al. 2014, Valdearcos et al. 2014). It is known that astrocytes sense the metabolic and dietary environment, firstly due to their close proximity to circulating factors via the ME, and

second due to the expression of receptors such as glucose transporter 1 (Chari et al. 2011) and glucose transporter 2 (Marty et al. 2005), hormone receptors such as the LepR, growth hormone secretagogue receptor (GhsR) and insulin receptor (InsR) (Garcia-Caceres et al. 2019).

It is then clear that glial cells of the brain, in particular astrocytes and microglia are equipped to play a key role in metabolic sensing and regulation, making them interesting candidates for further study in respect to the metabolic syndrome (MetS).

1.7.2. Cranial irradiation as an exogenous risk factor for obesity and type 2 diabetes

The brain is a, if not *the* key organ involved in regulating our metabolic demands and adjusting these to the environment. Hypothalamic damage and inflammation are clearly indicated in obesity. It is then perhaps not surprising that high doses of cranial irradiation (CrI) during adolescence have been shown to significantly increase the risk of obesity and the MetS. Evidence comes primarily from childhood leukaemia survivors who received CrI as a preventative measure to avoid brain metastasis (Gurney et al. 2003, Garmey et al. 2008, Meacham et al. 2009, Miller et al. 2010, van Waas et al. 2013). These individuals had a 2-fold increased risk to develop hypertension, T2D and dyslipidaemia when compared with their siblings (Gunn et al. 2015). As a consequence, their cardiovascular health was also impaired, resulting them being 4 times more likely to succumb due to complications such as heart attack and stroke (Oeffinger et al. 2006). As radiation therapy and other cancer treatments improve and the life expectancy of cancer patients increases, long term complications are becoming more evident. The underlying causes of CrI induced MetS have yet to be fully understood, but are becoming more clinically relevant, especially as there is currently no alternative to radiotherapy for the vast majority of brain tumours or brain metastases (Lannering et al. 2012).

2. Aims of the PhD thesis

In the face of an ever increasing global obesity risk, the work presented here aids in our understanding of the disease and the data generated may serve to assist in preventing obesity in the future. The overall aim of this thesis was to deepen our understanding of the enigma that is leptin resistance by elucidating potential causes for the syndrome and furthermore by revealing other risk factors for leptin resistance which ultimately contribute to obesity and the MetS. This work is divided into three projects which are divided into three chapters within this thesis.

The role of leptin transport in leptin resistance

Leptin transport has previously been proposed as one of the underlying causes for leptin resistance (Banks et al. 1999, El-Haschimi et al. 2000, Banks et al. 2004). However, the data on this subject matter remains unconvincing. The objective here was to assess leptin transport with the use of fluorescently labelled leptin, advanced three-dimensional light-sheet fluorescence microscopy in leptin resistant DIO mice and three models of weight loss.

Evaluation of hypothalamic gliosis as a result of chronic obesity and weight loss

The involvement of astrocytes and microglia in metabolic sensing, obesity, and hypothalamic inflammation have been described in the literature (Thaler et al. 2012, Garcia-Caceres et al. 2016, Valdearcos et al. 2017). The aim of this project is to understand how the RG state of the hypothalamus is affected by long term obesity, weight loss by pharmacological treatment, calorie restriction or diet type. According to a well-designed scoring system, the reactive nature of both astrocytes and microglia was examined.

Low-moderate dose cranial irradiation as a risk factor for obesity and the metabolic syndrome

High-dose CrI has been strongly linked to development of obesity, T2D and other aspects of the MetS (Oeffinger et al. 2006). This chapter was aimed at revealing whether or not lower more commonly found doses of CrI would increase the risk of developing metabolic dysfunction. The goal was to closely monitor the metabolic status of mice receiving low-

moderate dosed CrI to the hypothalamus for changes in metabolic function by checking body weight, blood chemistry, leptin sensitivity, hypothalamic inflammation and metabolic rate.

3. Experimental approaches

This section will outline and discuss the major experimental methods chosen and briefly describe how they were performed. Detailed methodology is provided in the individual publications.

3.1. Leptin coupling and visualisation

To be able to study leptin transport it was necessary to accurately detect the protein. Protein detection is available in a wide range of modalities. Classical methods such as the antibody dependent methods western blot, enzyme-linked immunosorbent assay or immunoprecipitation provide highly sensitive quantitative methods capable of detecting low concentrations of the desired protein (Mahmood and Yang 2012). A major drawback of this method however is that tissue must be destroyed or lysed in order to extract the protein. Clearly then this method is ill-suited to tracing studies within the brain, as an intact anatomical structure is required for precise localisation within the tissue. A further complication with these methods is that a viable antibody must be available which is unfortunately often not the case (Kusnezow and Hoheisel 2002). Here, to overcome these issues, the method of protein tagging was employed. Typically, proteins are tagged with the use of genetically engineered protein sequences to encode the tag, such as hemagglutinin (Kimple et al. 2013) or fluorescent proteins like green-fluorescent protein (Chalfie et al. 1994). The use of chemical fluorescent dyes presents several advantages over the protein alternative, such as dye stability, fluorescence intensity, small size and range of emission spectra. A review of the available options revealed that chemical tagging using the N-hydroxysuccinimide (NHS) esters would allow for fast, efficient tagging of the leptin protein. The NHS ester reacts with primary amines found on the N-terminus of the polypeptide chain, as well as on lysine residues (Nanda and Lorsch 2014). Leptin was coupled using the commercially available IRDye® 800CW NHS ester kit (LI-COR) according to the provided handbook.

3.1.1. Choice of fluorophore

The 800CW dye has an excitation peak at 774 nm and an emission peak at 790 nm which is in the near infrared range of the spectrum. There are many advantages to using so-

called long wavelength fluorescent dyes. First, longer wavelengths are able to penetrate deeper into biological tissues (Smith et al. 2009, Ash et al. 2017). This is of critical importance when imaging larger samples, such as the murine brain. Second, the amount of auto fluorescence detected in this particular range is significantly lower than at shorter wavelengths (Gao et al. 2014). This allows for greater signal-to-noise ratios and thus far clearer images.

To be able to determine leptin transport from the circulation into the brain parenchyma it was necessary to not only visualise leptin, but also the blood vessels of the brain. In order to achieve this a fluorescent-lectin was chosen. Lectins bind carbohydrate components of the inner lining of blood vessels. Lectin-647 was selected due to the far-red spectrum of fluorescence, which, similar to CW800 would allow for improved light penetration.

3.1.2. Tissue clearing and microscopy method

Although near infrared light can penetrate tissues up to 5 mm, shorter wavelengths in the far-red region can only penetrate 3 mm (Teraphongphom et al. 2017), which is not sufficient for murine brain imaging. Regardless, improving image quality by reducing light absorption and scattering is always likely to be beneficial. A method known as tissue clearing dramatically reduces light absorption and scattering by unifying the refractive indices within a sample. Briefly, this involves de-lipidation of the tissue and a subsequent matching of refractive indices. Although other methods exist that require much shorter clearing times (Silvestri et al. 2016), the solvent based benzylalcohol-benzylbenzoate (BABB) method was selected due to the superior clearing quality (Dodt et al. 2007). Following fixation in PAXgene fixative, clearing was performed by placing brains in increasing concentrations of tetrahydrofuran for 12 hours per step. Initially in 50 %, followed by 70 %, 80 % and 100 %. The 100 % step was repeated two further times. Finally, the brain was placed in BABB for 2 days.

Selecting the ideal method of microscopy is usually dependent on the requirements such as resolution, magnification, sample size, fluorophores and cost (Sanderson et al. 2014). Traditional wide-field microscopy would enable imaging of larger samples, such as the murine brain, but suffer from low resolution and contrast due to the epi-illumination of the sample and noise from out of focus layers. Although conventional setups such as

confocal laser scanning microscopy and more advanced super-resolution systems such as 2-photon microscopy offer dramatic increases in image resolution, they suffer from slower imaging times, are in most cases limited to smaller samples and reside at the higher end of the cost scale (Sanderson et al. 2014). Sample size can be overcome by the cutting of samples into thinner sections, however this is labour intensive and requires extensive methodological skill. Additionally, the complicated reconstruction of the multiple sections to form a full organ image is very challenging and sometimes even no longer feasible. For the requirements of the current study, light-sheet fluorescence microscopy offers the perfect balance of all parameters. Image acquisition by a charge-coupled device camera and illumination via a sheet of light in the entire focal plane allows for rapid imaging of large samples. Illumination using a narrow light-sheet also reduces whole sample photo toxicity and simultaneously increases the signal-to-noise ratio due to fluorophore excitation localised solely to the focal plane. The matching of tissue clearing and light-sheet fluorescence microscopy has been highlighted by many as an ideal combination for investigating of large biological samples, resulting in novel insights and remarkable images (Keller and Dodt 2012).

3.2. Reactive gliosis requires precise methodology

RG may be characterised in a number of varying methodologies. The most common method is the quantification of the proteins GFAP in astrocytes and Iba1 in microglia, which are either performed as western blots, immunohistochemical analysis or by quantitative polymerase chain reaction (qPCR) of messenger ribonucleic acids (Deren et al. 2010). In cases of profound reactive astrocytosis and microgliosis such as hydrocephalus, these methods can robustly detect significant changes (Deren et al. 2010). However, when the gliosis is subtler, which is the case in obesity related RG, these differences can be harder to detect. An example of this can be found in a study by Berkseth and colleagues, who found no difference in Iba1 cell number, but when multiple morphological factors were taken into account a significant difference became clear (Berkseth et al. 2014). Several publications have quantified RG by measuring the overall or average staining intensities in the region of interest. However, this method is susceptible to variations such as unspecific background intensity, section thickness and staining variability. Overall, the most precise method for detection of subtle changes in RG appeared to be evaluation of morphological differences. For the current study a 5-step

ranking score was designed based on morphological characteristics for microglia and for astrocytes (Harrison et al. 2019). This took into account the factors size of cell body, membrane smoothness, process thickness and complexity. In addition, the staining intensity was evaluated and incorporated into the rank, as this adds the qualitative additional information of GFAP or Iba1 expression levels. These parameters were in agreement with published ranking scores used for RG (Deren et al. 2010, Berkseth et al. 2014). Using this method, it was possible to detect subtle changes in astrocytosis upon weight loss, which otherwise would likely have gone unnoticed (Harrison et al. 2019).

3.3. Irradiation source and calibration

There are two main sources of irradiation typically used in small animal research, X-ray or gamma irradiation. The decision of which method is more suitable is often made based on the availability of the device. There are however some considerations which should be taken into account when a selection is made, as gamma and X-ray irradiation have different properties. Although the radiation dosage may be the same in terms of delivered dose (measured in gray (Gy)) the relative biological effect is in fact different. The precise difference is subject to variability, however it can be estimated that X-ray irradiation will result in a 30% increased relative biological effect compared to the same dose originating from gamma irradiation (Storer et al. 1957). The work presented here made use of a ^{60}Co therapy machine (ELDORADO, AEC), emitting gamma rays. Dosage rates are another important aspect that must be accurately calculated prior to irradiation, as many factors will influence the dose achieved in the target tissue (Yoshizumi et al. 2011). To allow for accurate dose delivery, the current work employed a highly sensitive dose calibration pre-testing. Thermoluminescent dosimeters (TLD) are small sensors that when heated to high temperatures of max. 300 °C emit photons in proportion to the amount of irradiation dose received (Stadtman et al. 2006). Following TLD calibration, a TLD was placed directly below the hypothalamus and other organs in a mouse cadaver and irradiated. Based on these measurements the irradiation time was determined to achieve doses of either 2 Gy or 0.5 Gy. Due to the nature of the study in this thesis, the irradiation was focused towards the hypothalamus. Modern equipment such as the small animal radiation research platform allow for a precise stereotactic irradiation of specific regions with very low dose to surrounding regions (Deng et al. 2007). As this option was not available, a custom irradiation chamber was designed and built (figure 5). The chamber included the option

for mouse isoflurane sedation, head fixation and heating to 37 °C. An additional 50 mm thick lead shield, with a bore hole of 4 mm allowed for irradiation with a 4 mm beam, directed at the hypothalamus. Importantly, this meant that further brain regions in a column above the hypothalamus were also irradiated, including the cortex, corpus callosum, hippocampus and thalamus.



Figure 5: Custom-built irradiation chamber. The upper panel depicts the chamber with Plexiglas lid, creating sterile sealed unit. In the lower panel a mouse is fixed in place using the mouth guide from the isoflurane delivery unit, and plastic covered head stabilisation pins.

4. Results

4.1. Fluorescent blood–brain barrier tracing shows intact leptin transport in obese mice

4.1.1. Aim and summary

Leptin transport has been suggested as one of the possible underlying causes of leptin resistance. The aim of this study was to make use of a near infrared fluorescently labelled leptin (leptin-CW800) combined with tissue clearing and light-sheet fluorescence microscopy to trace leptin in the entire intact murine brain. This method was then applied to mice that were either lean or DIO. Furthermore, leptin accumulation in the MBH was quantified using western blotting of micro-dissected MBH samples. The results of this study showed that most of the leptin-CW800 accumulated in the choroid plexus (CP), followed by the ME. A closer analysis of the choroid plexus using a far-red fluorescently labelled leptin (leptin-650) revealed that leptin-650 was being specifically transported into the ependymal cells of the CP. It is presumed that from here leptin is transported into the CSF. A comparison of leptin-CW800 accumulation in the CP and ME between lean, chow-fed and obese, HFD-fed mice revealed no differences. To verify these findings, a diet intervention study experiment was performed where HFD-fed DIO mice were subjected to weight loss via a diet-switch to chow, calorie restriction or pharmacological treatment with exendin-4. The latter has been shown to restore leptin sensitivity. After the intervention, leptin accumulation in the MBH was measured. In support of the initial findings, there was no difference in MBH leptin accumulation between lean and DIO mice. Unexpectedly however, an increase in leptin accumulation was detected in the MBH of both calorie restriction (CR) and exendin-4 (EX4) groups that lost approximately 30 % bodyweight. This increase corresponded to an upregulation of the leptin receptor in the choroid plexus suggesting a mechanism by which leptin transport from circulation to the MBH may be regulated.

Thus, using a novel fluorescent leptin and advanced microscopy, it was shown that leptin transport does not appear to be dysregulated during obesity and as such is unlikely to play a role in leptin resistance. Nonetheless, dramatic weight loss results in an

upregulation of the leptin receptor in the CP, which ultimately leads to an increased leptin accumulation in the MBH.

4.1.2. Contribution

The in-vivo studies were performed primarily by myself with the support of Dr. Sonja C. Schriever, Peter Baumann, Dr. Katrin Pfuhlmann and Dr. Paul T. Pfluger. Moreover, I performed all of the immunohistochemistry experiments, qPCR and western blots. Tissue clearing was performed in collaboration with Dr. Annette Feuchtinger and Dr. Axel Walch. Furthermore, Dr. Eleni Kyriakou, Dr. Ana C. Messias and I performed the ion-exchange chromatography experiments. Light-sheet fluorescence microscopy and subsequent analysis was performed by myself. I designed all figures and performed all the statistical analyses of the data. Finally, I wrote the manuscript with support from Dr. Paul Pfluger and Dr. Sonja Schriever. All co-authors were involved in aspects of the scientific discussion, interpretation of the results and reviewed the manuscript.

4.1.3. Publication information

The completed manuscript and data were submitted to the International journal of obesity on the 28th of February 2018 and accepted on the 2nd of September 2018.

Fluorescent blood-brain barrier tracing shows intact leptin transport in obese mice

Luke Harrison, Sonja C. Schriever, Annette Feuchtinger, Eleni Kyriakou, Peter Baumann, Katrin Pfuhlmann, Ana C. Messias, Axel Walch, Matthias H. Tschöp and Paul T. Pfluger

<https://doi.org/10.1038/s41366-018-0221-z>



Physiology

Fluorescent blood–brain barrier tracing shows intact leptin transport in obese mice

Luke Harrison^{1,2,3,4} · Sonja C. Schriever^{1,2,3} · Annette Feuchtinger⁵ · Eleni Kyriakou^{6,7} · Peter Baumann^{1,2,3,4} · Katrin Pfuhlmann^{2,3,4} · Ana C. Messias^{6,7} · Axel Walch⁵ · Matthias H. Tschöp^{2,3,4} · Paul T. Pfluger^{1,2,3}

Received: 28 February 2018 / Revised: 20 July 2018 / Accepted: 2 September 2018
© The Author(s) 2018. This article is published with open access

Abstract

Background/objectives Individuals carrying loss-of-function gene mutations for the adipocyte hormone leptin are morbidly obese, but respond favorably to replacement therapy. Recombinant leptin is however largely ineffective for the vast majority of obese individuals due to leptin resistance. One theory underlying leptin resistance is impaired leptin transport across the blood–brain-barrier (BBB). Here, we aim to gain new insights into the mechanisms of leptin BBB transport, and its role in leptin resistance.

Methods We developed a novel tool for visualizing leptin transport using infrared fluorescently labeled leptin, combined with tissue clearing and light-sheet fluorescence microscopy. We corroborated these data using western blotting.

Results Using 3D whole brain imaging, we display comparable leptin accumulation in circumventricular organs of lean and obese mice, predominantly in the choroid plexus (CP). Protein quantification revealed comparable leptin levels in micro-dissected mediobasal hypothalami (MBH) of lean and obese mice ($p = 0.99$). We further found increased leptin receptor expression in the CP ($p = 0.025$, $p = 0.0002$) and a trend toward elevated leptin protein levels in the MBH ($p = 0.17$, $p = 0.078$) of obese mice undergoing weight loss interventions by calorie restriction or exendin-4 treatment.

Conclusions Overall, our findings suggest a crucial role for the CP in controlling the transport of leptin into the cerebrospinal fluid and from there to target areas such as the MBH, potentially mediated via the leptin receptor. Similar leptin levels in circumventricular organs and the MBH of lean and obese mice further suggest intact leptin BBB transport in leptin resistant mice.

Introduction

Maintenance of energy homeostasis is the keystone in preventing obesity and the metabolic syndrome. The brain plays an important role in orchestrating this homeostasis by receiving inputs from peripheral tissues and responding by regulating various sensations such as reward and satiety. In addition to this, direct innervation as well as indirect signaling via hormones allows for a feedback system back to the peripheral organs [1]. The transport of these peripheral signals into the brain and the target regions is regulated in a

controlled manner by the blood–brain barrier, in essence a layer of endothelial cells that divides the microvasculature from the brain compartment. Several cell types such as pericytes and astrocytes contribute to the architecture and function of the blood–brain barrier (BBB), which ultimately protects the brain from neurotoxins while governing the passive diffusion of gases and hydrophobic molecules as well as the active transport of hydrophilic nutrients, amino acids and large-scale peptide hormones [2, 3].

One such peptide hormone which requires active BBB transport is leptin, a 16 kDa hormone that is synthesized in white adipose tissue and released into circulation in direct proportion to the amount of body fat [4, 5]. Leptin serves as an adipostat, i.e., it has the capacity to inform the rest of the body on available fat stores. The importance of leptin in the control of systemic energy homeostasis is demonstrated by clinical observations in people with genetic loss of leptin, which develop hyperphagia and morbid obesity in early childhood that can be reversed by leptin replacement

Electronic supplementary material The online version of this article (<https://doi.org/10.1038/s41366-018-0221-z>) contains supplementary material, which is available to authorized users.

✉ Paul T. Pfluger
paul.pfluger@helmholtz-muenchen.de

Extended author information available on the last page of the article

therapy [6]. Most obese subjects are however not deficient in leptin, but rather leptin resistant. Despite high circulating leptin levels, leptin resistant individuals typically experience a drive to eat extra calories, which impedes sustainable weight loss [7]. Molecular reasons for leptin resistance are not yet entirely clear, but may entail impaired signaling linked to SOCS3 expression [8], elevated levels of circulating c-reactive protein [9] or impaired histone deacetylase 5 activity in the hypothalamus [10]. Moreover, impaired transport of leptin into the brain is viewed as important contributor to leptin resistance [11]. This is mainly supported by leptin transport studies that used radioactively labeled leptin and showed a decrease in blood–CSF leptin ratios, suggesting blunted leptin transport kinetics and thus a cause for leptin resistance [12]. Similarly, El-Haschimi and colleagues performed a series of intracerebral ventricular (ICV) leptin injection experiments, which also indicated a decrease in leptin BBB transport [13].

Leptin must cross the BBB to reach its neuronal targets in the mediobasal hypothalamus (MBH) and other brain areas. How leptin is transported across the BBB and to its responder neurons, defined by their expression of the leptin receptor (LepR), is still a matter of debate [14]. Past work hints that leptin BBB transport is facilitated by tanycytes, i.e., specialized ependymal cells in the median eminence (ME), a circumventricular organ at the bottom of the MBH involved in secreting brain derived signals to the pituitary and peripheral organs via the circulation [15, 16]. In the ME, leptin can freely diffuse into the ME parenchyma due to the fenestration of capillaries and lack of a functional BBB. Subsequently, leptin is transported via tanycytes into the cerebrospinal fluid (CSF) of the ventricular space, from where it then laterally diffuses into the MBH [17]. More recent work points towards a crucial direct involvement of endothelial cells of the BBB as major mechanism of leptin transport [18]. The knockdown of LepR specifically in endothelial cells of the BBB was functionally linked to impaired transport of leptin into the CSF and LepR positive brain regions, and aggravated obesity when mice were exposed to high fat diet [18]. Dense LepR expression is especially found in the choroid plexus (CP) [19], an important component of the BBB anchored to the walls of the lateral, central and fourth ventricles. Although the production of CSF is the most described role of the CP, it also acts as an important selective gateway to the CSF. Molecules that enter the CSF can freely diffuse into many brain regions that line the ventricles [20]. Accordingly, the CP has been strongly linked to leptin transport into the brain [21].

Here, we aimed to gain new understanding in leptin BBB transport by visualizing and comparing leptin transport into the brain via whole mouse brain 3D imaging from lightsheet fluorescence microscopy. We furthermore aimed to address

the question of whether leptin transport into the CP, ME and MBH is altered in diet-induced obese (DIO) and thus leptin resistant mice, compared to chow-fed and leptin sensitive lean control mice. Moreover, we compared leptin levels in the ME and MBH of DIO mice subjected to weight loss by either modest dieting, profound calorie restriction or repeated treatment with exendin-4, to clarify whether altered leptin transport into the MBH can explain the superior restoration of leptin sensitivity by pharmacology [22].

Materials and methods

Animals

All experiments were performed in adult male C57BL/6 J mice purchased from Janvier Labs (Saint-Berthevin, Cedex, France). Mice were maintained on a 12 h-light–dark cycle with free access to water and standard chow diet (Altromin, #1314) or 58% high fat diet (HFD) (Research Diets, D12331). Diet induced obese (DIO) mice were subjected to HFD for at least 20 weeks. Body composition was determined using nuclear magnetic resonance (NMR) technology (EchoMRI, Houston, TX, USA). For the diet intervention study, DIO mice were subdivided into 4 experimental groups. The group termed HFD was kept on HFD during the study. The remaining 3 groups of DIO mice were switched to chow on day 0 of the study and divided as follows: Diet switch (H>C) animals received ad libitum access to chow diet. Calorie restricted (CR) mice were restricted to the average food intake of the exendin-4 (EX4) group and EX4 treated animals were subjected to daily injections of exendin-4 (0.08 mg/kg) (Tocris biosciences, Bristol, UK) in the morning for up to 10 days. Age-matched mice fed chow were used as a control group. At the end of the diet-intervention study, all mice were first subjected to a single intraperitoneal (i.p.) injection of either vehicle or leptin, 45 min before being sacrificed by cervical dislocation for organ withdrawal. Brains were extracted swiftly and the ME and MBH dissected as described below. Recombinant murine leptin was reconstituted in 20 mM Tris-HCl, pH 8.0 at a concentration of 5 mg/ml. This was then further diluted in saline (0.9 % NaCl) to a final concentration of 1 mg/ml and injected at a dose of 5 mg/kg body weight. Mice were distributed into treatment groups based on their starting body weight. We thereby aimed to assure an equal distribution of starting body weights at the beginning of the study, which allows for better dissection of longitudinal treatments effects on body weight. In vivo experiments were performed without blinding of the investigators. All studies were based on power analyses to assure adequate sample sizes, and approved by the State of Bavaria, Germany.

Leptin coupling

Leptin was coupled to either infrared IRDye® CW-800 (LICOR #929-71012) or far-red IRDye® 650 (LICOR #929-70020) fluorescent dyes. Coupling was carried out according to the IRDye® CW-800 kit handbook. Lyophilized recombinant mouse leptin (R&D systems Cat.# 498-OB-05M) was reconstituted in PBS with a pH of 8.5 to a final concentration of 1 mg/ml. The dye was reconstituted in RNase-free water and the appropriate volume was added to 1 ml of 1 mg/ml leptin, then incubated at 20 °C for 2 h. Coupled leptin was separated from unbound dye by size exclusion column filtration (Pierce Zebra™ desalting spin columns, Life Technologies #89891). Dye solution not used for coupling was diluted to the same absorption value as that of the coupled leptin sample and used as a control. Largely avoiding freeze-thaw cycles, coupled leptin was stored in dark tubes and kept at 4 °C for short-term storage and –20 °C for long-term storage.

Ion exchange purification

To separate coupled from uncoupled leptin, we performed Ion Exchange Chromatography (IEX) using a Resource Q anion-exchange column with 1 ml volume (RESOURCE™ Q, GE Healthcare) at pH 8. The leptin-CW800 sample underwent a buffer exchange, by sequential concentration/dilution steps into 20 mM TRIS-HCl pH 8 (Buffer A). After loading the sample onto the column, the column was washed with 10 column volumes of Buffer A. Separation was then achieved by applying a salt gradient based on increasing ionic strength to 0.5 M NaCl (50% Buffer B; 20 mM TRIS-HCl buffer pH 8, 1 M NaCl) at a flow rate of 4 ml/min and eluent volume of 20 columns. Finally, the column was washed with 5 column volumes of 100% Buffer B. For each fraction the purity and molecular weight was assessed by a Pierce BCA protein assay kit (Thermo Fisher Scientific Inc., Rockford, IL, USA) and SDS-PAGE, as described below.

Median eminence and mediobasal hypothalamus dissection

Under a dissecting microscope the ME can be seen as a thin structure following the sagittal plane, lying on top of the hypothalamus. It was possible to see the fenestrated blood vessels running along the ME. Using very fine forceps (Dumont, 5SPSF – Inox – B), and applying light pressure parallel to either side of the ME, the ME was pinched away from the hypothalamus. Removing the ME causes a break in the third ventricle wall, and a small amount of fluid was seen leaving the ventricle. This may serve as confirmation that the ME was removed. To remove the MBH the brain

was cut with a scalpel coronally, directly through the center of the hypothalamus. The two brain halves are then laid flat, to expose the hypothalamus face upwards. If the ME dissection was done correctly, the MBH will have a flat surface. If too much tissue was removed, it will have a concave surface. Using fine forceps, two 45° cuts were made vertically on either side of the MBH. A third cut was then made horizontally below the MBH, allowing the MBH to be lifted from the brain. Tissues were snap frozen in liquid nitrogen and stored at –80 °C.

Protein extraction and western blotting

As ME and MBH samples only provide a very small amount of tissue, samples from 2 mice were pooled to provide sufficient protein levels for detection. Tissue lysis buffer consisted of RIPA buffer (Thermo Fisher Scientific Inc., Rockford, IL, USA) with the addition of 1× phosphatase- and protease-inhibitors (Thermo Fisher Scientific Inc., Rockford, IL, USA) and 1 mM phenyl-methanesulfonyl fluorid (PMSF). Using 200 µl of lysis buffer for MBH samples and 50 µl of lysis buffer for ME samples resulted in the most efficient protein extraction. Samples were lysed via sonication then rotated on a wheel for 30 min to ensure full suspension of the tissues in lysis buffer. Samples were then centrifuged at 12,000×g for 7 min and the supernatants collected. Protein concentrations were measured using the Pierce BCA protein assay kit (Thermo Fisher Scientific Inc., Rockford, IL, USA), samples were then diluted to equal concentrations in 4× NuPage buffer + DTT (Thermo Fisher Scientific Inc., Rockford, IL, USA). After boiling at 95 °C for 5 min, equal amounts of protein were loaded onto 4–20% gradient Criterion™ TGX™ Precast Gels (Biorad, Hercules, CA, USA). Samples were transferred to a nitrocellulose membrane using the Trans-Blot® Turbo™ Transfer System (Biorad, Hercules, CA, USA). Membranes were blocked in Tris-buffered-saline with 0.05% Tween 20 (TBS-T) containing 5% BSA (VWR, Vienna, Austria) for 1 h. For leptin detection, membranes were blocked in 5% skim milk powder (Sigma-Aldrich, St. Louis, Missouri, USA) in TBS-T. Primary antibodies were anti-pSTAT3^{T705} (rabbit polyclonal, 1:1000, Cat #9145), anti-STAT3 (mouse monoclonal, 1:1000, Cat #9139), anti-β-actin (rabbit polyclonal, 1:10000, Cat #4970) (all antibodies purchased from Cell Signaling Technology (Cell Signaling, Danvers, MA, USA)) or anti-murine-leptin (rabbit polyclonal, 1:1000, Cat #500-P68, Peprotech, Rocky Hill, NJ, USA). Antibodies were diluted in blocking buffer (5% skim milk powder for leptin antibodies, 5% BSA for all others) and incubated on the membranes overnight at 4 °C. Detection was achieved using ECL Clarity (Biorad, Hercules, California, USA) and exposure to high-sensitivity films (Amersham Hyperfilm ECL (GE Healthcare Bio-

Sciences, Pittsburgh, PA, USA)). Densitometric analysis was performed using ImageJ 1.51 (NIH, Bethesda, Maryland, USA).

Cell culture

HEK293 cells were cultured in a 6-well plate with low glucose DMEM, with 10% FBS and 1% Pen/Strep. Transfection of pCAG-2A-H2B Venus_mOBRb-HA was carried out using the FuGene[®] HD transfection reagent (Promega, Madison, WI, USA) as per the kit's instructions with 1.5 µg of mLepRb plasmid DNA and 4.5 µl of transfection reagent. 48 h post transfection, cells were placed in starvation medium (DMEM, with 0.1% FBS) for 4 h prior to leptin stimulation. Recombinant murine leptin was added to the cells at a final concentration of 10 nM. Cells were stimulated for 30 min with vehicle, leptin, CW-800 dye or leptin-CW800, washed twice with ice cold PBS and then snap frozen at -80°C . Cellular proteins were isolated by adding 100 µl RIPA buffer with inhibitors and PMSF, and further treated as described above.

RNA extraction and qPCR

RNA was extracted from tissue using the NucleoSpin RNA isolation kit (Macherey-Nagel, Düren, Germany). Equal amounts of RNA were reverse transcribed to cDNA using the QuantiTect Reverse Transcription kit (Qiagen, Hilden, Germany). Gene expression was analyzed using TaqMan probes for LRP2 (Mm01328171_m1), murine leptin receptor (Mm00440181_m1), and Hprt (Mm01545399_m1) as the housekeeping gene with the respective TaqMan mastermix (Thermo Fischer Scientific, Inc., Rockford, IL USA). qPCRs were carried out using a ViiA[™] 7 Real Time PCR System (Applied Biosystems). Gene expression was evaluated using the $\Delta\text{-}\Delta$ Ct method.

Tissue clearing and light-sheet fluorescence microscopy

The dissected brain was fixed in PaxGene (PreAnalytiX, Hombrechtikon, Switzerland) according to the manufacturer's recommendations and thereafter underwent a chemical procedure of optical clearing as described before [23]. Afterwards cleared whole mouse brains were imaged on a light-sheet fluorescence microscope (UltraMicroscope II, LaVision BioTec, Bielefeld, Germany). In order to visualize the lectin-647 (Thermo Fisher Scientific Inc., Rockford, IL, USA, Cat# L32451) a bandpass filter set with an excitation range of 640/30 and emission range of 690/50 was used in combination with an additional filter set (excitation: 740/35; emission: 795/50) for detection of leptin-CW800 signals. 3D-reconstruction and rendering was

performed using Imaris vers.7.3 (Bitplane, Concord, MA, USA). Volume analysis was performed using Arivis Vision4D (Arivis, Munich, Germany).

Immunohistochemistry

Brains were extracted after cervical dislocation and incubated in 4% paraformaldehyde at 4°C overnight. Brains were then transferred to 20% sucrose in 0.1 M tris-buffered-saline (TBS) for 24–48 h. Brains were frozen at -20°C , mounted with OCT and cut coronally on a cryostat into 30 µm sections. Free-floating sections were subjected to pre-treatment with ice-cold 100% methanol for 10 min at -20°C , then to blocking for 1 h at RT in a buffer containing 0.25% gelatin and 0.5% Triton X 100 in 1x TBS. Primary anti-pSTAT3^{T705} antibody was incubated with brain sections overnight at 4°C . After 3×5 min washing steps with TBS, the secondary donkey anti-rabbit-568 antibody (1:500 in blocking buffer, Thermofischer Scientific, Cat # A10042) was incubated with brain slices for 1 h at RT. After washing, the sections were counterstained with DAPI (1:10000) and mounted on slides. Images were captured with a Leica TCS SP5 microscope. Stack and overlay pictures were created using ImageJ image analysis software (v. 1.51, NIH, Bethesda, Maryland, USA). Brain regions were defined with the use of the DAPI counterstaining and the Allen brain Atlas (<http://mouse.brain-map.org/static/atlas>).

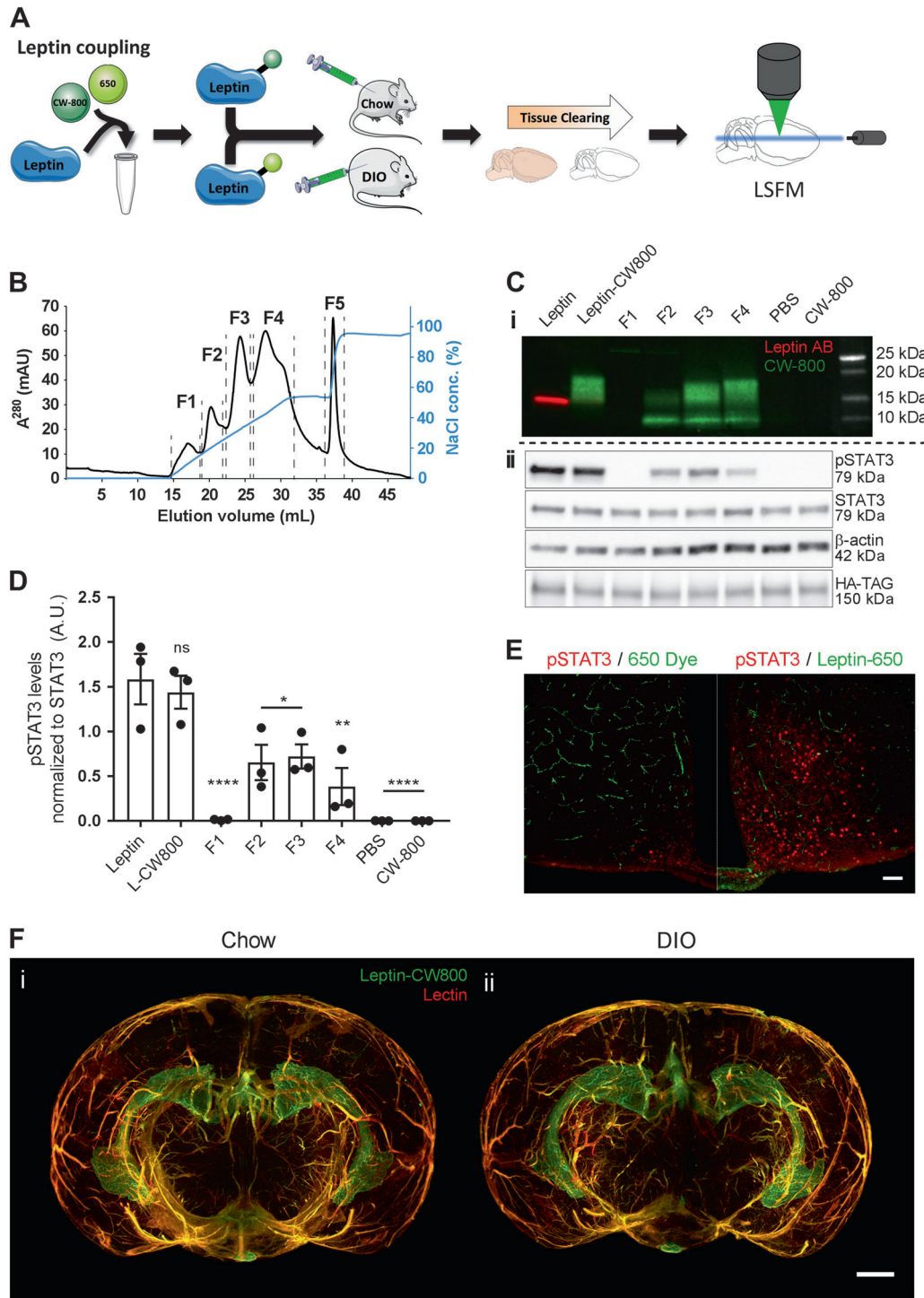
Statistical analyses

Statistical analyses were performed using GraphPad Prism (GraphPad Software, Inc. La Jolla, CA, USA). Two-tailed Student's t-tests or One-Way ANOVA with Bonferroni's post tests were used to compare differences between phenotypes. P-values lower than 0.05 were considered significant. Significances were indicated as follow: $**p < 0.01$, $***p < 0.001$, $****p < 0.0001$ or, groups with significantly different values were indicated as different characters and groups not significantly different from each other were indicated with the same characters. All results are presented as means \pm SEM. Gaussian distribution was analyzed with the D'Agostino-Pearson omnibus test.

Results

Fluorescently labeled leptin allows for visualization of leptin distribution in the whole mouse brain

To visualize how exogenous leptin distributes in the brain after injection (i.p., 5 mg kg^{-1}), we coupled an infrared fluorescent dye (CW800) or a far-red fluorescent dye (650) to recombinant murine leptin (Fig. 1a). The product leptin-



CW800 was subsequently subjected to anion exchange chromatography (Fig. 1b), and the resulting fractions 1 to 4, washout fraction 5 as well as the naïve unlabeled leptin and the labeled product leptin-CW800 were assessed by SDS page and Western Blotting (Fig. 1c). Immunolabeling with an antibody against leptin, and the simultaneous direct detection of infrared CW800 fluorescence revealed a full

conversion of unlabeled leptin to leptin-CW800, i.e., the absence of unlabeled leptin in the reaction product (Fig. 1c-i). Moreover, fractions 2 to 4 contained leptin-CW800 bands that appeared to be larger in size (ca. 17–20 kDa) compared to naïve unlabeled leptin at 16 kDa. Notably, the antibody against leptin had a profoundly reduced affinity against leptin-CW800 (Fig. 1c-i), and leptin-

Fig. 1 Labeled leptin combined with tissue clearing and light-sheet fluorescence microscopy allows for 3D visualization of leptin distribution in the intact mouse brain. **a** Leptin was coupled to either an infrared fluorescent dye (CW800) or a far-red fluorescent dye (650). Labeled leptin was then injected into chow-fed lean mice or age-matched diet-induced obese (DIO) mice fed with HFD for 20 weeks. Brains were collected 45 min after leptin injections and subjected to tissue clearing followed by LSFM to obtain 3D whole brain images. **b** Anion exchange chromatography was used to purify CW800 labeled leptin. Individual fractions F1–F4 were collected based on UV absorption (280 nm). A final fraction (F5) was collected by increasing the NaCl concentration above 50%, which is known to remove any remaining bound substances from the column. **c–i** Leptin, leptin-CW800, fractions F1–F4, PBS and CW800 alone were subjected to SDS-Page and Western blotting. Leptin bands were detected by either immunolabeling with a leptin antibody (red) or infrared fluorescence (green). **c–ii** Murine LepRb overexpressing HEK293 cells were

incubated for 30 min with native leptin, leptin-CW800, fractions F1–F4, CW800 alone, or PBS to measure pSTAT3 levels as a marker for leptin bioactivity. **d** Densitometric analysis of the pSTAT3 signal from the western blots seen in **c–ii**. **e** Bioactivity was further confirmed *in vivo* by injecting leptin-650 (i.p., 5 mg kg⁻¹) in mice and analyzing pSTAT3 45 min after leptin administration (pSTAT3 shown in red, leptin-650 or the 650 dye alone shown in green). **f** Mice, either chow-fed and lean (**i**) or HFD-fed and DIO (**ii**), were injected with leptin-CW800 (i.p., 5 mg kg⁻¹) and lectin-647 (i.v., 250 µg). 3D-reconstruction of the brains reveals leptin accumulation in the ME and CP (Lectin-647 shown in red, leptin-CW800 shown in green). Scale bars for **e** and **f** are 100 and 1000 µm, respectively. Data in **D** are means ± SEM for 3 independent experiments. Significance was determined using One-Way ANOVA and Bonferroni's post-hoc testing. Significance is depicted as **p* < 0.05, ***p* < 0.01, ****p* < 0.0001

CW800 could only be visualized when the signal intensity was strongly enhanced (Supplementary Figure 1A).

Next, to test if labeled leptin-CW800 was still bioactive, we overexpressed the long, signal transducing form of the murine leptin receptor (mLepRb) in HEK293 cells and stimulated these cells with either native leptin, leptin-CW800, the isolated fractions, vehicle (PBS) or CW800-dye alone. Labeled leptin-CW800 was capable of activating LepRb downstream signaling to the same extent as native leptin, indicated by comparable phosphorylation of signal transducer and activator of transcription 3 (STAT3, pSTAT3) (Fig. 1c–ii and 1d). Fractions 2–4 displayed significant leptin bioactivity as well, but proteolytic cleavage with the occurrence of a 10 kDa leptin fragment during anion exchange chromatography slightly diminished their bioactivity compared to native or labeled leptin-CW800. Accordingly, to confirm the bioactivity of labeled leptin *in vivo*, we injected 5 mg kg⁻¹ of unfractionated leptin-650 into chow fed control mice and confirmed an increased staining for pSTAT3 nuclei in the hypothalamus compared to injection of the 650 dye alone (Fig. 1e). Having established that labeled leptin is functional *in vitro* and *in vivo*, we next injected unfractionated leptin-CW800 (i.p., 5 mg kg⁻¹, 45 min prior to sacrifice) into mice fed either chow or a high fat diet (HFD). We also injected fluorescent lectin-647 (i.v., 250 µg, 5–10 min prior to sacrifice), which marks blood vessels by binding glycoproteins on the vascular endothelial layer [24].

Tissue clearing and light-sheet fluorescence microscopy (LSFM) (Fig. 1a) allowed us to visualize precisely where exogenous leptin-CW800 accumulates in the brain (Fig. 1f). Leptin-CW800 that has entered the brain parenchyma is clearly distinct from leptin that is in circulation, which colocalizes with lectin in the blood vessels (yellow/orange signal) (Figs. 1f & 2a). 3D rendering of LSFM images allowed for further appreciation of the leptin-CW800

distribution in the brain. Using 3D visualization we could demonstrate, based on signal strength and overall size, that the majority of leptin-CW800 is seen in the lateral CP (Supplementary Video SV1, SV2 and SV5). Leptin-CW800 is predominantly found in the circumventricular organs such as the ME or the CP in the lateral ventricle (Fig. 2a). In 3D rendered LSFM images (Supplementary Video SV2), other circumventricular organs such as the CP in the 4th ventricle also showed high leptin-CW800 signal. In contrast, the arcuate nucleus (ARC) appears to be protected from circulating molecules that leak into the ME, evidenced by the restricted signal of leptin-CW800 within the ME and a lack of penetration into the ARC 45 min post leptin i.p. injection (Fig. 2a–i & ii). In the lateral ventricle CP the leptin signal was not only present in the blood vessels, but also outside the capillaries within the CP ependymal cell layer (Fig. 2a–ii, iv & Supplementary Video SV5). When compared to other microvessels of the brain, leptin-CW800 signal is found only colocalized within lectin-647 (Supplementary Video SV5). Interestingly, when comparing leptin-CW800 accumulation in chow and DIO mice, there appears to be no difference in signal intensities across all areas positive for leptin-CW800. DIO mice display no differences in leptin accumulation in the ME or CP ependymal layers (Fig. 1f, Fig. 2a, Supplementary Video SV1, SV3 and SV4). This was quantified using volumetric calculations based on signal intensity for the ME (Fig. 2b) and showed no difference between lean chow fed and HFD fed DIO mice (Fig. 2c).

Due to resolution limitations of the LSFM setup, it was not possible to distinguish whether or not the leptin-CW800 signal was in the CP interstitium, or had been taken up by the ependymal cells themselves. The latter would indicate a specific uptake, due to the fact that the ependymal cells are connected by tight-junctions and thus form the blood–CSF barrier in the CP. To overcome this we injected mice with leptin-650 (i.p., 5 mg kg⁻¹) and lectin-488 (i.v., 250 µg),

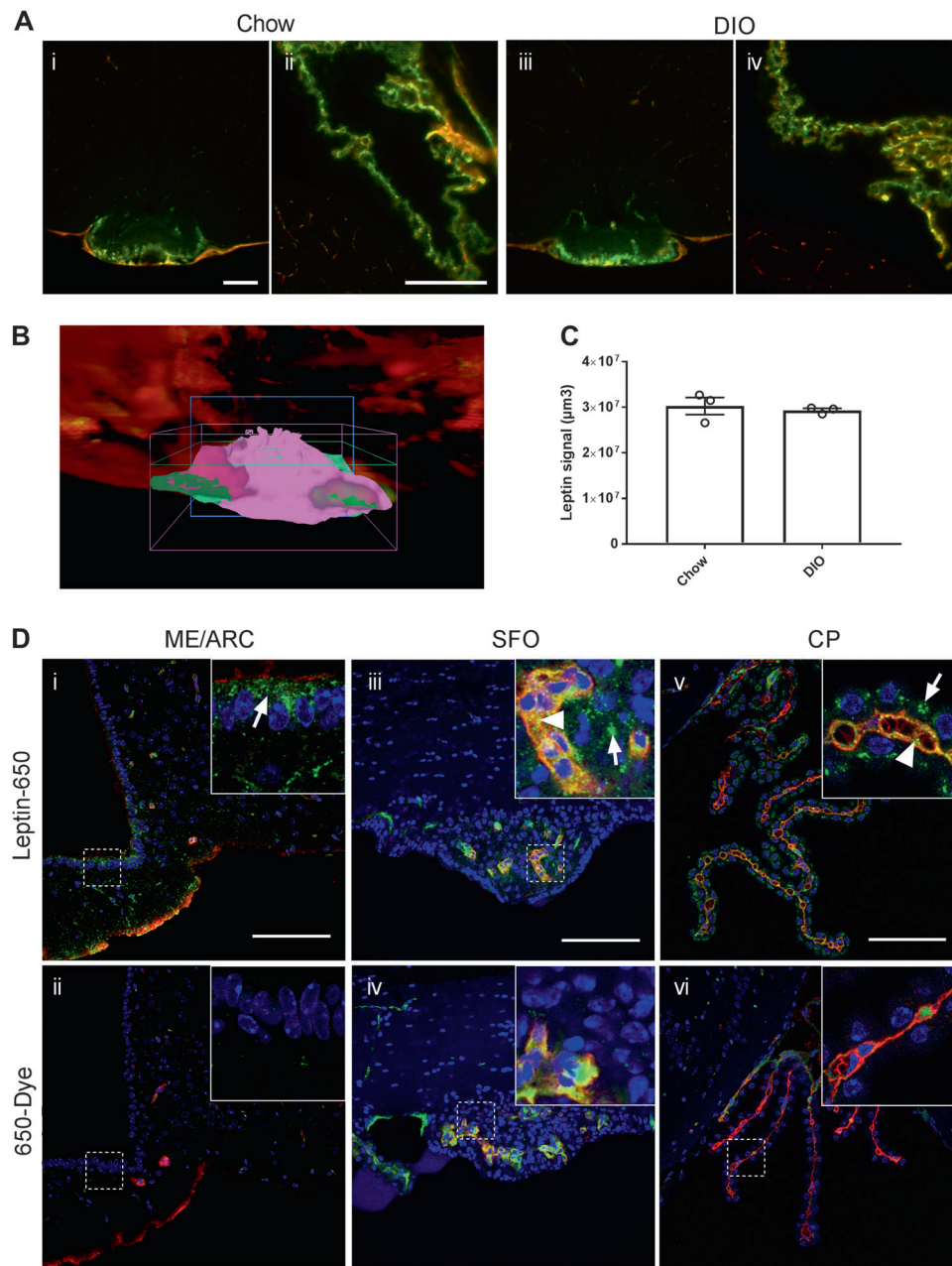


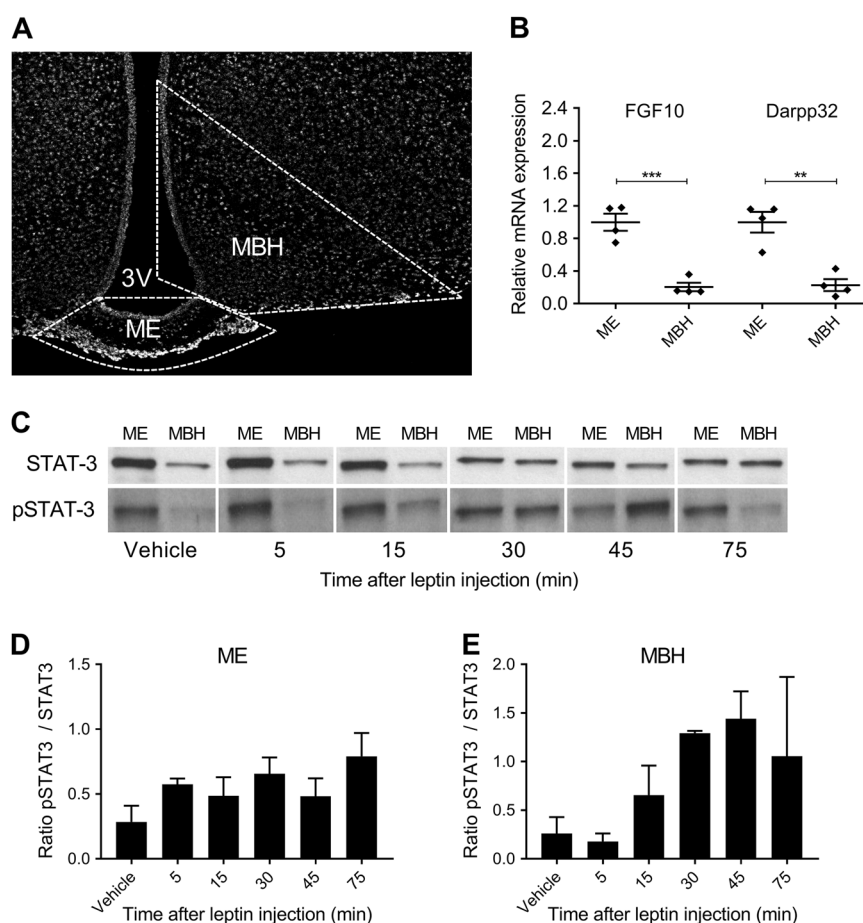
Fig. 2 Accumulation of labeled leptin in circumventricular organs and the choroid plexus of mice. **a** Leptin-CW800 (i.p., 5 mg kg⁻¹) and lectin-647 (i.v., 250 μg) were injected into either DIO or chow control mice, and the brains examined with LSM. (Leptin-CW800 shown in green, lectin-647 shown in red). Leptin-CW800 that has entered the brain parenchyma is seen as green, whereas leptin-CW800 within the blood vessels is visualized as yellow. **a-i** and **a-iii** depict the ME and **a-ii** and **a-iv** depict the CP in the lateral ventricle. **b** Screenshot depicting the leptin volume (pink) and blood vessel volume (turquoise) calculations from the ARIVIS image analysis software package. **c** Quantification of the total leptin volume within the ME for lean chow

fed and DIO mice. **d** To obtain higher resolution of specific regions, leptin-650 (i.p., 5 mg kg⁻¹) or 650-Dye and lectin-488 (i.v., 250 μg) were injected into chow fed mice and examined via confocal microscopy. Arrows indicate leptin-650 in the brain parenchyma, arrowheads indicate leptin-650 within blood vessels. ME median eminence, ARC arcuate nucleus, SFO subfornical organ, CP choroid plexus (lateral ventricle). Scale bars for **a-i** and **ii** are 100 μm , and for **di-vi** 100 μm . Leptin-CW800/leptin-650 are shown in green, lectin-647/lectin488 are shown in red, DAPI is shown in blue. Data in **c** are means \pm SEM for an n of 3. Significance was determined using a two-tailed student's t -test

thereby enabling visualization by confocal microscopy (Fig. 2d). Here, we see that leptin-650 (Fig. 2d-i) but not dye alone (Fig. 2d-ii) is found to accumulate along the

border of the ME to the third ventricle and within the subfornical organ (SFO) (Fig. 2d-iii, iv), which is another circumventricular organ that lacks an intact BBB.

Fig. 3 Leptin signaling in dissected median eminence (ME) and mediobasal hypothalamus (MBH) mouse brain tissue. **a** The ME and MBH were dissected from murine brains as depicted in **a**. **b** A correct dissection was determined using RT-qPCR of specific ME-residing tancyte genes (FGF10 and Darpp32). **c–e** Leptin transport kinetics into the ME and MBH were assessed in mice injected with leptin (i.p., 5 mg kg⁻¹) or vehicle. ME and MBH tissue samples were dissected 5–75 min after leptin/vehicle treatment and subjected to western blot (**c**) and densitometric analyses (**d**, **e**). Data in **b**, **d** and **e** are means \pm SEM. Differences were analyzed by a two-tailed Student's *t*-test. $^{**}p < 0.01$, $^{***}p < 0.001$ between ME and MBH samples. (Each data point consists of samples from 2 animals, which were pooled due to detection limitations. $n = 4$ per group for **b** and $n = 2–3$ for **d**, **e**). ME median eminence, MBH mediobasal hypothalamus. The scale bar in **a** is 200 μ m



Furthermore, leptin-650 appears to be specifically taken up within the ependymal cells of the CP (Fig. 2d–v arrows), when compared to the dye injected alone (Fig. 2d–vi).

Leptin downstream signaling in the MBH peaks 45 min after exogenous leptin administration

Due to the conflicting nature of the literature regarding leptin transport and uptake in obese animals [12, 17, 25, 26], we aimed to confirm our findings using an additional, more quantitative method. A recent study by Balland and colleagues describes a dissection method to separate the ME from the MBH, thus excluding circulating signals and allowing the measurement of proteins found only within the MBH and not within the ME [17]. By adapting this method we were able to isolate the ME and MBH (Fig. 3a) from freshly extracted brains. We confirmed the accuracy and purity of the dissection by analyzing mRNA levels of two ME residing tancyte genes using qPCR (Fig. 3b). Both tancyte genes fibroblast growth factor 10 (FGF10) and dopamine- and cAMP-regulated phosphoprotein (Darpp32) were highly enriched in ME tissue samples and only minimally expressed in MBH samples (Fig. 3b). Having

established MBH dissection, we wished to define the time point at which leptin activity is at its peak within the MBH. We measured pSTAT3 in ME & MBH samples 5, 15, 30, 45 and 75 min after leptin injection (i.p., 5 mg kg⁻¹) in chow fed mice (Fig. 3c). In ME samples there was no change in pSTAT3 levels (Fig. 3d). However, we found a time-dependent increase in pSTAT3 levels in the MBH, which peaked 45 min after leptin injection and began to decrease thereafter (Fig. 3e). For future experiments, we selected the 45 min time point to allow maximum leptin transport into the MBH.

Profound weight loss induces upregulation of LepR in the CP and increased leptin accumulation in the MBH

To gain further insight into how leptin resistance may affect leptin transport, we designed a diet intervention study. Control mice fed chow or HFD maintained their body-weight throughout the study period and the HFD group was significantly heavier (Fig. 4a, b). Additional groups of HFD-fed mice lost weight due to a simple diet switch to chow (HFD > Chow), due to a switch to chow with calorie

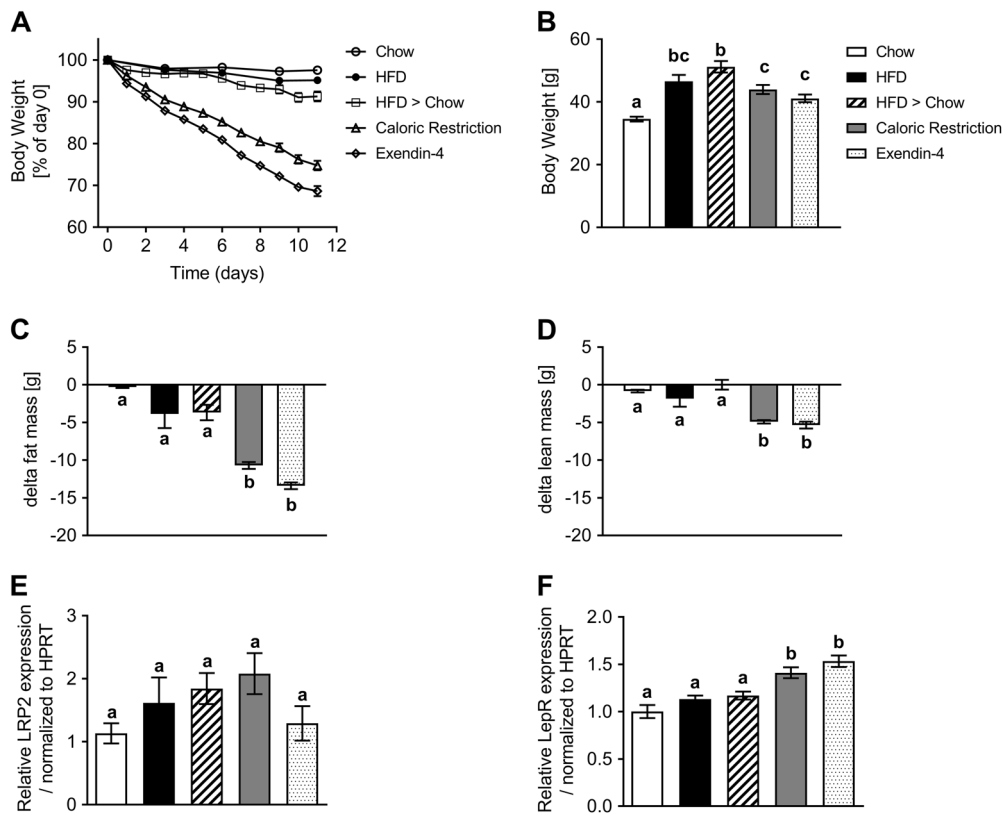


Fig. 4 Weight loss by CR or EX4 treatment drives upregulation of leptin receptor mRNA in the choroid plexus. **a** Effects of obesity and weight loss on the transport of leptin into the MBH were recorded in age-matched mice exposed to at least 20 weeks of chow or HFD (Chow, HFD) and additional groups of age-matched and HFD-fed DIO mice after a diet intervention (HFD>Chow; CR) or pharmacological treatment (EX4). Body weights were recorded daily for all groups (chow and HFD every 3 days) for 11 days during the intervention. **b–d** Final day body weights for all animals (**b**) as well as

changes in fat and lean mass (**c, d**). **e, f** On day 11, the choroid plexus was isolated from all mice and expression levels of LRP2 and LepR were measured. All data are means ± SEM. Groups with the same character indicate groups that are not significantly different from each other. Groups with different characters are significantly different from each other as determined by One-Way or Two-Way ANOVA with Tukey’s post-hoc testing ($n = 11–13$ for **a–d** and $n = 9–10$ for **e, f**. HFD high fat diet, H>C diet switch, CR calorie restriction, EX4 exendin-4)

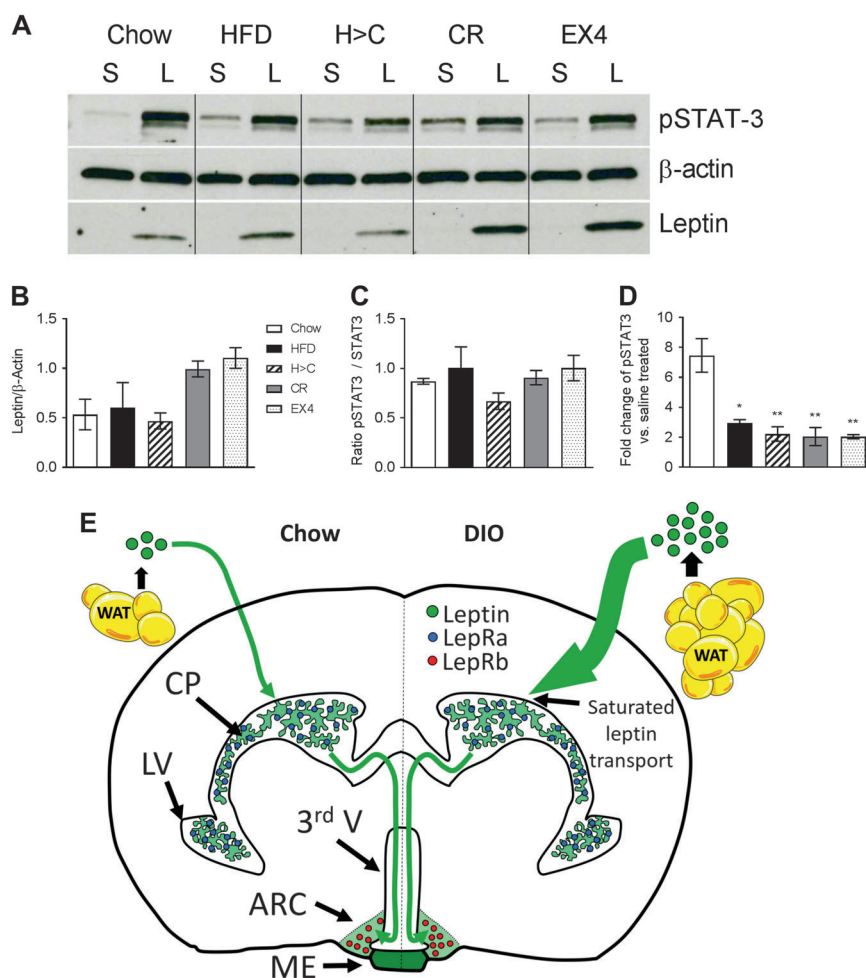
restriction (CR), or due to a switch to chow plus daily treatment with leptin resensitizing glucagon-like peptide 1 (Glp1) agonist exendin-4 (EX4) [22]. The HFD>Chow group lost 9% BW over the 11 day study period (Fig. 4a), similar to that seen by others [27]. Both weight loss intervention groups CR and EX4 lost significant amounts of body weight (Fig. 4b), totaling 26% and 32%, respectively (Fig. 4a). The majority of lost weight derived from a decrease in fat mass (Fig. 4c), accompanied by significant losses in lean mass (Fig. 4d).

Two possible transporters responsible for the movement of leptin from the CP to the CSF are low density lipoprotein-related protein 2 (LRP2) [28] or the short form of the leptin receptor (LepRa) [18, 19]. We extracted the CP from mice in the diet intervention study and examined mRNA levels of LRP2 and LepR (Fig. 4e–f). LRP2 expression levels were much lower when compared to LepR levels (average CP values of 33 for LRP2 vs. 25 for LepR) and unchanged between groups (Fig. 4e). No changes in

LepR expression were seen between chow and HFD groups. Interestingly, LepR was significantly upregulated in both weight loss groups CR and EX4, compared to all groups that did not undergo profound weight loss (Fig. 4f).

We next aimed to assess the impact of weight loss and increased CP LepR expression on the levels of leptin as well as leptin signaling marker pSTAT3 in microdissected MBH tissue (Fig. 5a–d). Western blotting revealed no differences in pSTAT3 or leptin levels in the MBH between chow and HFD animals (Fig. 5a, d), which corroborates the lack of difference observed in our LSFM analyses. Leptin caused a 7 fold increase in pSTAT3 levels, which was significantly reduced in all other diet groups (Fig. 5d). Intriguingly though, we see elevated leptin levels in the MBH of both weight loss intervention groups CR and EX4, when compared to the other 3 groups (Fig. 5a, b), which correlates with the increased LepR expression seen in the CP of these animals (Fig. 4f).

Fig. 5 Profound weight loss is associated with increased leptin transport into the MBH. **a–d** Leptin levels in the MBH 45 min after vehicle (saline, S) or leptin (L) injections (i.p., 5 mg kg⁻¹) in age-matched mice exposed to chow, HFD, H>C, CR or EX4 treatment. Mice were dissected and MBH samples subjected to western blotting (**a**) and densitometric analyses (**b–d**) for leptin or leptin sensitivity marker pSTAT3. **e** Schematic representation of the proposed route of leptin transport to the MBH in chow and DIO mice. Each diet group consists of 6 animals, however samples were pooled due to detection limitations, resulting in $n = 3$ replicates for statistical analyses. All data are means \pm SEM. Significance was determined using one-way ANOVA. HFD high fat diet, H>C diet switch, CR calorie restriction, EX4 exendin-4. Significance is depicted as * $p < 0.05$, ** $p < 0.01$



Discussion

We describe here a novel method of visualizing the transport of leptin across the BBB in mice. By using fluorescently labeled leptin in combination with tissue clearing and light-sheet fluorescence microscopy, we display highest leptin accumulation in the choroid plexus of the ventricular system followed by circumventricular organs such as the ME or SFO. Notably, we found no differences in leptin accumulation between lean and obese mice in the ME, MBH or CP. Comparable leptin protein levels in microdissected ME and MBH tissues of lean and obese mice, quantified via western blotting, corroborated the results of our microscopy analyses. Overall, we found that DIO does not prevent the accumulation of leptin in brain areas important for metabolic control. Moreover, we revealed that weight loss intervention, triggered either by calorie restriction or pharmacological treatment with exendin-4, led to an increase in leptin receptor expression in the CP as well as elevated leptin protein levels in the MBH.

BBB transport of peptides has traditionally been assessed by radioactive tracer studies [12], which combine high sensitivity with excellent quantification capabilities. However, high costs and difficulties in creating the stable peptide tracer conjugates restrict their use to few laboratories specialized in such studies. Our novel method may be a useful tool to complement or even replace radioactive tracer studies. Foremost, our method does not require radiation and the predicaments associated with it. The kit-based chemistry reaction for the coupling of available fluorescent dyes can be readily adapted to specific peptide hormones. Here, by using infrared fluorescent dyes, researchers can ensure that autofluorescence does not impede the imaging. Next, if labeling with the fluorescent dye is successful and the labeled peptide remains bioactive, modern imaging techniques can be applied to visualize the transport route of fluorescent peptides into the brain. Our post mortem imaging approaches were based on LSFM as well as confocal microscopy to combine whole brain 3D imaging with subsequent high resolution imaging in brain slices. It also seems feasible to study the in vivo uptake of fluorescently

labeled peptide into mouse tissues by using alternative biofluorescence imaging techniques. A similar approach, although post mortem, was recently applied to profile the whole body bio-distribution of a fluorescently labeled glucagon-T3 hybrid peptide in mice [29].

Our 3D imaging revealed leptin accumulation predominantly in the CP of the ventricular system, an ependymal secretory organ designed to transfer molecules from the blood to the CSF. The CP has been linked to leptin transport into the brain [5, 18, 21, 30], driven by the short form of the leptin receptor that is highly expressed in the CP [19, 31, 32]. Recent work further revealed diminished delivery of leptin across the BBB and increased DIO when all forms of LepR were partially knocked down in BBB-specific endothelial cells of the CP and related areas of mice [18]. A lack of leptin transport into the MBH was further reported for mice with a genetic mutation in the leptin receptor gene (*db/db*), compared to WT controls [17]. This is however unexpected, as the *db/db* mutation affects only the signal transducing LepRb isoform. *Db/db* mice retain a fully functioning LepRa, and have indeed been reported to transport leptin across the BBB via a saturable mechanism [33].

These reports collectively suggest that LepRa expression in the CP is a critical regulator of BBB transport of leptin. Our data contribute to this concept by showing a clear association between elevated LepR levels in the CP and elevated leptin protein levels in the MBH of mice subjected to profound weight loss via CR or EX4. Notably, we observe very low CP expression levels of Lrp2, a transport protein previously linked with leptin BBB transport in CP epithelium [28]. Overall, our results support a model whereby leptin bio-distribution in the brain is predominantly facilitated by the CP and LepR-driven transfer from blood into the CSF.

The degree and more importantly the type of vasculature present in a particular brain region will play a pivotal part in which blood borne substances are given access to the parenchyma. It has been previously shown that the vasculature of the MBH undergoes vascular remodeling during obesity, which directly influences the accessibility to circulating substances [34, 35]. Langlet and colleagues further showed that during fasting, mice undergo vascular remodeling within the ARC [36]. These changes include an invasion of fenestrated vessels from the ME into the ARC, allowing for an increase in peripheral hormone visibility to the arcuate neurons [36]. Thus in a fasting state, which is exhibited in our CR and EX4 models, it is possible that higher levels of circulating leptin could gain access to the ARC, which may additionally contribute to the increased transport by the CP, which we describe here.

Several recent studies suggest a prominent role of the median eminence and tanycytes in mediating leptin

transport to the MBH [17, 36]. Tanycytes are specialized ependymal cells that form the blood–CSF barrier in circumventricular organs [37]. To avoid free access of blood borne molecules to the rest of the MBH, tanycytes form a border via tight junctions between their processes [38], and wall off the ME from MBH [39]. Modulation of tanycytic tight junctions in the ME was shown to increase leptin transport into the MBH [17]. Moreover, although leptin receptor expression has never been directly shown (largely due to a lacking suitable antibody), leptin receptor mRNA is expressed in tanycytes. Furthermore, isolated tanycytes display phosphorylation of STAT3 upon leptin stimulation, indicating the expression of the leptin receptor. These tanycytes appear to mediate leptin transcytosis to the CSF and from there to the arcuate nucleus [17]. Our LSM revealed comparable leptin-CW800 accumulation in the ME of lean and DIO mice. Confocal microscopy further revealed that CW650-leptin levels are accumulating in the cytosol of β 2 tanycytes, and here predominantly at the ventricular side. Accordingly, our imaging data are in line with these earlier reports. However, future studies are warranted to fully delineate the relative contributions of the ME and the CP in mediating BBB transport of leptin to the MBH and other LepR-positive brain areas.

In our study, we see no differences in the accumulation of leptin in the ME or MBH between lean and DIO mice. These data are discrepant to a previous report that, using essentially the same western blotting methodology, found severely impaired transport of leptin into the MBH of DIO mice compared to lean controls. Nevertheless, both our and the previous study [17] report increased pSTAT3 in the MBH after leptin injection, which suggests sufficient leptin transport to elicit leptin signaling. Leptin resistance, it would appear then, is unlikely to be the result of blunted leptin transport into the MBH. Consistent with that notion, we observed elevated basal pSTAT3 levels in the MBH of vehicle-treated DIO mice, indicating chronically activated leptin signaling due to high endogenous leptin levels. This resonates with a recent study by Ottaway and colleagues who, by using leptin receptor antagonist administration, demonstrated that endogenous leptin is still functional in DIO mice [25]. Earlier studies further reported a complete lack of physiological responses such as weight loss or food intake in DIO mice subjected to intracerebroventricular injections of exogenous leptin, but a low-level preservation of leptin-induced hypothalamic Stat3 activation [13]. Overall, these data highlight the possibility of a non-transport related leptin resistance.

How can we reconcile the apparent discrepancies between our results and previous reports, mostly based on radioactive tracer studies, which suggest diminished leptin BBB transport in a state of obesity [12, 17]? These earlier studies largely focused on assessing the steady-state kinetics

of leptin BBB transport, i.e., the rate of transfer in relation to the concentrations of circulating tracer. Our measurements were made at a fixed point in time when leptin accumulation reached a maximum in the MBH. Accordingly, we did not evaluate the ratio of leptin entering the brain in relation to the levels in circulation. Our data are nonetheless in agreement with a very recent report on unchanged leptin BBB transport kinetics in mice fed chow or two weeks of HFD, which was built upon a novel micro-perfusion technique and the measurement of MBH leptin over a timeframe of 6 h [40].

We acknowledge, as discussed above, that leptin transport appears to be driven by leptin receptor in a saturable manner. Indeed, LepRa expression levels may be the limiting factor for leptin BBB transport rates when endogenous leptin levels are high, or supraphysiological levels of recombinant leptin are administered. However, as shown by our study and outlined in Fig. 5d, even a putative threshold defined by delimited LepRa expression in the CP and impaired leptin BBB transfer kinetics cannot prevent the entry of significant levels of leptin into the CSF and LepR-expressing brain areas such as the MBH.

Here, we demonstrate a novel visualization of leptin distribution in the whole intact mouse brain. The methods described can be readily adapted to accommodate a plethora of other peptide hormones, which may greatly impact the field of hormonal BBB transport. Taken together, we show that despite being leptin resistant, DIO mice retain a functional leptin transport system and display no deficit in leptin accumulation in the MBH or circumventricular organs. Our findings are further solidified by a recent hypothalamic perfusion study, which revealed no changes in leptin transport kinetics [40]. Moreover, emerging evidence suggests persistence of leptin signaling also in DIO mice and obese humans [25, 41]. Lastly, AgRP and POMC neurons in the MBH are also projecting LepR-expressing somato-dendritic processes into the ME, where circulating leptin can induce neuronal leptin signaling without the need of crossing the BBB [42, 43]. Accordingly, in light of recent and our own findings, little evidence points towards impaired leptin BBB transfer as underlying cause for leptin resistance. Future research efforts should thus perhaps be shifted away from leptin transport across the BBB and focused on other possible causes of leptin resistance, which, if corrected has the potential to have a large impact on the treatment of obesity.

Acknowledgements We thank Emily V. Baumgart, Marlene Kilian, Ulrike Buchholz and Claudia-Mareike Pflüger for their skillful technical assistance. The plasmid 426-pCI-HA-mOBRb providing the insert for the plasmid pCAG-2A-H2B Venus_mOBRb-HA was a kind gift from Julie Dam and Ralf Jockers, Institut Cochin, Paris. This work was supported in part by the German Center for Diabetes Research (DZD) (PTP, SCS, LH), by the Deutsche Forschungsgemeinschaft (DFG) within the CRC/Transregio 205/1 “The Adrenal: Central Relay

in Health and Disease” (AW), by the Alexander von Humboldt Foundation (MHT), by an IMF Diabetes Portfolio Grant (ACM) by the Helmholtz Alliance ICEMED-Imaging and Curing Environmental Metabolic Diseases (SCS, MHT), by the Helmholtz-Israel-Cooperation in Personalized Medicine (PP), by the Helmholtz Initiative for Personalized Medicine (iMed; MHT), and through the Initiative and Networking Fund of the Helmholtz Association. Elements of artwork used in Fig. 1 and Fig. 5 were provided by Servier medical art under the creative commons licence 3.0.

Author contributions LH, SCS, PB, KP, and PTP performed *in vivo* experiments in mice. LH conducted immunohistochemical stainings. LH performed qPCRs and Western Blot analyzes. LH performed *in vitro* experiments in HEK293 cells. LH, AF and AW performed LSFM and tissue clearing experiments. LH, EK and ACM designed and performed the anion exchange chromatography. LH, SCS, AF and PTP designed experiments, analyzed and interpreted the results. LH, SCS, AF, AW, MHT and PTP prepared the manuscript. LH, SCS, MHT and PTP developed the conceptual framework of this study.

Compliance with ethical standards

Conflict of interest MHT is a scientific advisor to Novo Nordisk and ERX. The remaining authors declare that they have no conflict of interest.


Open Access This article is licensed under a Creative Commons Attribution 4.0 International License, which permits use, sharing, adaptation, distribution and reproduction in any medium or format, as long as you give appropriate credit to the original author(s) and the source, provide a link to the Creative Commons license, and indicate if changes were made. The images or other third party material in this article are included in the article’s Creative Commons license, unless indicated otherwise in a credit line to the material. If material is not included in the article’s Creative Commons license and your intended use is not permitted by statutory regulation or exceeds the permitted use, you will need to obtain permission directly from the copyright holder. To view a copy of this license, visit <http://creativecommons.org/licenses/by/4.0/>.

References

1. Clemmensen C, Muller TD, Woods SC, Berthoud HR, Seeley RJ, Tschöp MH. Gut-brain cross-talk in metabolic control. *Cell*. 2017;168:758–74.
2. Obermeier B, Daneman R, Ransohoff RM. Development, maintenance and disruption of the blood–brain barrier. *Nat Med*. 2013;19:1584–96.
3. Garcia-Caceres C, Quarta C, Varela L, Gao Y, Gruber T, Legutko B, et al. Astrocytic insulin signaling couples brain glucose uptake with nutrient availability. *Cell*. 2016;166:867–80.
4. Considine RV, Sinha MK, Heiman ML, Kriauciunas A, Stephens TW, Nyce MR, et al. Serum immunoreactive-leptin concentrations in normal-weight and obese humans. *New Engl J Med*. 1996;334:292–5.
5. Karonen S, Koistinen HA, Nikkinen P VAK. Is brain uptake of leptin *in vivo* saturable and reduced by fasting? *Eur J Nucl Med*. 1998;25:607–12.
6. Farooqi IS, Jebb SA, Langmack G, Lawrence E, Cheetham CH, Prentice AM, et al. Effects of recombinant leptin therapy in a child with congenital leptin deficiency. *New Engl J Med*. 1999;341:879–84.

7. Woods SC, Schwartz MW, Baskin DG, Seeley RJ. Food intake and the regulation of body weight. *Annu Rev Psychol.* 2000;51:255–77.
8. Bjørnbæk C, Elmquist JK, Frantz JD, Shoelson SE, Flier JS. Identification of SOCS-3 as a potential mediator. *Mol Cell.* 1998;1:619–25.
9. Chen K, Li F, Li J, Cai H, Strom S, Bisello A, et al. Induction of leptin resistance through direct interaction of C-reactive protein with leptin. *Nat Med.* 2006;12:425–32.
10. Kabra DG, Pfuhlmann K, Garcia-Caceres C, Schriever SC, Casquero Garcia V, Kebede AF, et al. Hypothalamic leptin action is mediated by histone deacetylase 5. *Nat Commun.* 2016;7:10782.
11. Banks WA, Coon Alan B, Nakaoka Ryota, Robinson Sandra M, Morley Aje. Triglycerides induce leptin resistance at the blood–brain barrier. *Diabetes.* 2004;53:1253–60.
12. Banks WAD, Christopher R Farrell, Catherine L. Impaired transport of leptin across the blood–brain barrier in obesity. *Peptides.* 1999;20:1341–5.
13. El-Haschimi K, Pierroz D, Hileman SM, Bjørnbæk C, Flier JS. Two defects contribute to hypothalamic leptin resistance in mice with diet-induced obesity. *J Clin Invest.* 2000;105:1827–32.
14. Rodriguez EM, Blazquez JL, Guerra M. The design of barriers in the hypothalamus allows the median eminence and the arcuate nucleus to enjoy private milieus: the former opens to the portal blood and the latter to the cerebrospinal fluid. *Peptides.* 2010;31:757–76.
15. Knigge KM, Scott DE. Structure and function of the median eminence. *Am J Anat.* 1970;129:223–43.
16. Clarke IJ. Hypothalamus as an endocrine organ. *Comprehensive Physiology.* John Wiley & Sons, Inc.; 2011;5:217–53.
17. Balland E, Dam J, Langlet F, Caron E, Steculorum S, Messina A, et al. Hypothalamic tanycytes are an ERK-gated conduit for leptin into the brain. *Cell Metab.* 2014;19:293–301.
18. Di Spiezio A, Sandin ES, Dore R, Muller-Fielitz H, Storck SE, Bernau M, et al. The LepR-mediated leptin transport across brain barriers controls food reward. *Mol Metab.* 2017;8:13–22.
19. Bjørnbæk C, Elmquist JK, Michl P, Ahima RS, Van Bueren A, Mccall AL, et al. Expression of leptin receptor isoforms in rat brain microvessels. *Endocrinology.* 1998;139:3485–91.
20. Whish S, Dziegielewska KM, Mollgard K, Noor NM, Liddelow SA, Habgood MD, et al. The inner CSF–brain barrier: developmentally controlled access to the brain via intercellular junctions. *Front Neurosci.* 2015;9:16.
21. Berislav VZ, Jovanovic S, Miao W, Samara S, Verma S, Farrell CL. Differential regulation of leptin transport by the choroid plexus and blood–brain barrier and high affinity transport systems for entry into hypothalamus and across the blood–cerebrospinal fluid barrier. *Endocrinology.* 2000;141:1434–41.
22. Müller TD, Sullivan LM, Habegger K, Yi CX, Kabra D, Grant E, et al. Restoration of leptin responsiveness in diet-induced obese mice using an optimized leptin analog in combination with exendin-4 or FGF21. *J Pept Sci.* 2012;18:383–93.
23. Erturk A, Becker K, Jahrling N, Mauch CP, Hojer CD, Egen JG, et al. Three-dimensional imaging of solvent-cleared organs using 3DISCO. *Nat Protoc.* 2012;7:1983–95.
24. Robertson RT, Levine ST, Haynes SM, Gutierrez P, Baratta JL, Tan Z, et al. Use of labeled tomato lectin for imaging vasculature structures. *Histochem Cell Biol.* 2015;143:225–34.
25. Ottaway N, Mahbod P, Rivero B, Norman LA, Gertler A, D'Alessio DA, et al. Diet-induced obese mice retain endogenous leptin action. *Cell Metab.* 2015;21:877–82.
26. Rijnsburger M, Unmehopa UA, Eggels L, Serlie MJ, la Fleur SE. One-week exposure to a free-choice high-fat high-sugar diet does not disrupt blood–brain barrier permeability in fed or overnight fasted rats. *Nutr Neurosci.* 2017:1–10.
27. Fischer IP, Irmiler M, Meyer CW, Sachs SJ, Neff F, Hrabe de Angelis M, et al. A history of obesity leaves an inflammatory fingerprint in liver and adipose tissue. *Int J Obes.* 2017;42:507–17.
28. Dietrich MO, Spuch C, Antequera D, Rodal I, de Yebenes JG, Molina JA, et al. Megalin mediates the transport of leptin across the blood–CSF barrier. *Neurobiol Aging.* 2008;29:902–12.
29. Finan B, Clemmensen C, Zhu Z, Stemmer K, Gauthier K, Muller L, et al. Chemical hybridization of glucagon and thyroid hormone optimizes therapeutic impact for metabolic disease. *Cell.* 2016;167:843–57. e14.
30. Peiser C, McGregor GP, Lang RE. Binding and internalization of leptin by porcine choroid plexus cells. *Neurosci Lett.* 2000;283:209–12.
31. Devos R, Richardst G, Campfield I, Tartaglia L, Guisez Y, Van der heyden J, et al. OB protein binds specifically to the choroid plexus of mice and rats. *Proc Natl Acad Sci.* 1996;93:5668–73.
32. Tartaglia L, Dembski M, Weng X, Deng N, Culpepper J, Devos R, et al. Identification and expression cloning of a leptin receptor, OB-R. *Cell.* 1995;83:1263–71.
33. Maness LM, Banks WA, Kastin AJ. Persistence of blood-to-brain transport of leptin in obese leptin-deficient and leptin receptor-deficient mice. *Brain Res.* 2000;873:165–7.
34. Kalin S, Heppner FL, Bechmann I, Prinz M, Tschop MH, Yi CX. Hypothalamic innate immune reaction in obesity. *Nat Rev Endocrinol.* 2015;11:339–51.
35. Yi CX, Gericke M, Kruger M, Alkemade A, Kabra DG, Hanske S, et al. High calorie diet triggers hypothalamic angiopathy. *Mol Metab.* 2012;1:95–100.
36. Langlet F, Levin BE, Luquet S, Mazzone M, Messina A, Dunn-Meynell AA, et al. Tanycytic VEGF-A boosts blood–hypothalamus barrier plasticity and access of metabolic signals to the arcuate nucleus in response to fasting. *Cell Metab.* 2013;17:607–17.
37. Langlet F, Mullier A, Bouret SG, Prevot V, Dehouck B. Tanycyte-like cells form a blood–cerebrospinal fluid barrier in the circumventricular organs of the mouse brain. *J Comp Neurol.* 2013;521:3389–405.
38. Peruzzo B, Pastor FE, Blázquez JL, Schöbitz K, Peláez B, Amat P, et al. A second look at the barriers of the medial basal hypothalamus. *Exp Brain Res.* 2000;132:10–26.
39. Petrov T, Howarth A, Krukoff T, Stevenson B. Distribution of the tight junction-associated protein ZO-1 in circumventricular organs of the CNS. *Mol Brain Res.* 1994;21:235–46.
40. Kleinert M, Kotzbeck P, Altendorfer-Kroath T, Birngruber T, Tschop MH, Clemmensen C. Time-resolved hypothalamic open flow micro-perfusion reveals normal leptin transport across the blood–brain barrier in leptin resistant mice. *Mol Metab.* 2018;13:77–82.
41. Pan WW, Myers MG Jr.. Leptin and the maintenance of elevated body weight. *Nat Rev Neurosci.* 2018;19:95–105.
42. Djogo T, Robins SC, Schneider S, Kryzskaya D, Liu X, Mingay A, et al. Adult NG2-glia are required for median eminence-mediated leptin sensing and body weight control. *Cell Metab.* 2016;23:797–810.
43. Ha S, Baver S, Huo L, Gata A, Hairston J, Huntoon N, et al. Somato-dendritic localization and signaling by leptin receptors in hypothalamic POMC and AgRP neurons. *PLoS ONE.* 2013;8:e77622.

Affiliations

Luke Harrison^{1,2,3,4} · Sonja C. Schriever^{1,2,3} · Annette Feuchtinger⁵ · Eleni Kyriakou^{6,7} · Peter Baumann^{1,2,3,4} ·
Katrin Pfuhlmann^{2,3,4} · Ana C. Messias^{6,7} · Axel Walch⁵ · Matthias H. Tschöp^{2,3,4} · Paul T. Pfluger^{1,2,3} 

¹ Research Unit Neurobiology of Diabetes, Helmholtz Zentrum München, 85764 Neuherberg, Germany

² Institute for Diabetes and Obesity, Helmholtz Zentrum München, 85764 Neuherberg, Germany

³ German Center for Diabetes Research (DZD), 85764 Neuherberg, Germany

⁴ Division of Metabolic Diseases, Technische Universität München, 80333 Munich, Germany

⁵ Research Unit Analytical Pathology, Helmholtz Zentrum München, 85764 Neuherberg, Germany

⁶ Institute of Structural Biology, Helmholtz Zentrum München, 85764 Neuherberg, Germany

⁷ Biomolecular NMR and Center for Integrated Protein Science Munich at Department Chemistry, Technical University Munich, 85747 Garching, Germany

4.2. Profound weight loss induces reactive astrogliosis in the arcuate nucleus of obese mice

4.2.1. Aim and summary

Recently it was shown that obesity and HFD feeding induces hypothalamic inflammation. Since then, further research has shown variations in the severity and temporal aspect of hypothalamic inflammation and as such the underlying cause for this phenomenon remains not yet fully understood. It seems then that glia, in particular astrocytes and microglia may react to this change in environment by becoming activated in a process known as reactive gliosis. The aim of this project was to examine the effects of chronic obesity and subsequent weight loss on the state of hypothalamic reactive gliosis in astrocytes and microglia. Mice were subjected to long term HFD feeding for 22 weeks after which they were subjected to an 11-day weight loss intervention. Using either a diet-switch to chow for moderate weight loss, and calorie restriction or exendin-4 treatment for profound weight loss, the degree of hypothalamic gliosis was examined. Immunohistochemistry against GFAP or Iba1 in brain sections allowed for visualisation of astrocytes and microglia. Together with a newly devised ordinal ranking score, the extent of reactive astrocytosis and microgliosis was determined. Interestingly, after chronic obesity there was no noticeable difference between the lean and obese mice in regards to RG. Moreover, both the CR and EX4 groups displayed increased RG in astrocytes, but not in microglia. This increase was highly significant when the RG score was correlated to body weight loss, but remained unrelated to absolute bodyweight. Additionally, plasma analysis revealed elevated NEFAs in the two profound weight loss groups.

In summary it was shown chronic obesity does not present with hypothalamic RG. This may be due to adaptation over long term exposure to RG-inducing substances, or due to a basal increase in RG in chow fed mice after ageing. Furthermore, weight loss increased hypothalamic reactive astrocytosis which coincided with elevated NEFAs. NEFAs may be one of the factors that stimulates RG after short term HFD feeding, but this hypothesis requires further testing.

4.2.2. Contribution

The in-vivo studies were performed by Dr. Sonja C. Schriever, Dr. Katrin Pfuhlmann, Dr. Paul T. Pfluger and myself. Moreover, I performed all of the immunohistochemistry experiments and the microscopy. Blood chemistry analysis was carried out by Dr. Sonja C. Schriever. I designed and created the activation scoring system. Additionally, I designed all figures and performed all the statistical analyses of the data. Evaluation of RG was performed by myself and independently by Dr. Sonja C. Schriever and Dr. Katrin Pfuhlmann for confirmation. Finally, I wrote the manuscript with support from Dr. Paul Pfluger. All co-authors were involved in aspects of the scientific discussion, interpretation of the results and reviewed the manuscript.

4.2.3. Publication information

The completed manuscript and data were submitted to the international journal Molecular metabolism on the 11th of March 2019 and was accepted on the 28th of March 2019.

Profound weight loss induces reactive astrogliosis in the arcuate nucleus of obese mice

Luke Harrison, Sonja C. Schriever, Katrin Pfuhlmann and Paul T. Pfluger

<https://doi.org/10.1016/j.molmet.2019.03.009>

Profound weight loss induces reactive astrogliosis in the arcuate nucleus of obese mice

Luke Harrison^{1,2,3,4}, Katrin Pfuhlmann^{1,2,3,4}, Sonja C. Schriever^{1,2,3}, Paul T. Pfluger^{1,2,3,*}

ABSTRACT

Objective: Obesity has been linked to an inflammation like state in the hypothalamus, mainly characterized by reactive gliosis (RG) of astrocytes and microglia. Here, using two diet models or pharmacological treatment, we assessed the effects of mild and drastic weight loss on RG, in the context of high-fat diet (HFD) induced obesity.

Methods: We subjected HFD-induced obese (DIO) male C57BL/6J mice to a weight loss intervention with a switch to standard chow, calorie restriction (CR), or treatment with the Glp1 receptor agonist Exendin-4 (EX4). The severity of RG was estimated by an ordinal scoring system based on fluorescence intensities of glial fibrillary acidic protein, ionized calcium-binding adapter molecule 1 positive (Iba1), cell numbers, and morphological characteristics.

Results: In contrast to previous reports, DIO mice fed chronically with HFD showed no differences in microglial or astrocytic RG, compared to chow controls. Moreover, mild or profound weight loss had no impact on microglial RG. However, astrocyte RG was increased in CR and EX4 groups compared to chow fed animals and strongly correlated to body weight loss. Profound weight loss by either CR or EX4 was further linked to increased levels of circulating non-esterified free fatty acids.

Conclusions: Overall, our data demonstrate that in a chronically obese state, astrocyte and microglial RG is indifferent from that observed in age-matched chow controls. Nonetheless, profound acute weight loss can induce astrocyte RG in the hypothalamic arcuate nucleus, possibly due to increased circulating NEFAs. This suggests that astrocytes may sense acute changes to both the dietary environment and body weight.

© 2019 The Authors. Published by Elsevier GmbH. This is an open access article under the CC BY-NC-ND license (<http://creativecommons.org/licenses/by-nc-nd/4.0/>).

Keywords Reactive gliosis; Obesity; Astrocyte; Weight loss; Hypothalamus; Inflammation

1. INTRODUCTION

The central nervous system plays a major role in the regulation of metabolic balance and energy homeostasis [1]. It modulates the body's supply and demand for energy at a number of different levels ranging from complex behavioral circuits such as reward or motivation [2], to regions governing energy expenditure, food intake [3], and glucose control [4]. The arcuate nucleus of the hypothalamus (ARC) has been shown to be one of the core control centers regulating metabolism and energy expenditure. Here, proopiomelanocortin (POMC) and agouti related neuropeptide (AgRP) neurons respond to signaling cues from the periphery [5,6] such as leptin [5,7], insulin [8], or ghrelin [9]. In obesity, the ARC has been shown to enter an inflammation-like state, disrupting its normal homeostatic function [10]. In this situation, both ARC neurons [11] and glial cells [10,12,13] release and respond to inflammatory signals.

Astrocytes and microglia have important regulatory functions within the central nervous system (CNS), responding to noxious stimuli,

such as physical trauma, neurodegeneration, hypoxia, or cancer [14]. In these situations, astrocytes and microglia become activated in a process known as reactive gliosis (RG). RG is characterized by morphological changes such as increased cell size, enlarged, lengthened processes, and an increase in proliferation [14]. Previously, in mice fed a high-fat diet (HFD) the number of reactive astrocytes and microglia in the ARC was increased [10]. Importantly, astrocytic and microglial RG occurs prior to an increase in body weight [13], suggesting that diet content is one of the main driving factors for RG in obesity. Switching mice from HFD to standard chow results in normalization of body weight and amelioration of associated metabolic disturbances after several weeks [15], including a reversal of RG in the ARC [16]. Pharmacological treatment of diet-induced obese (DIO) mice with gut derived peptides, such as the GLP-1 analog Exendin-4 (EX4), have been successful in transiently reducing body weight [17]. How pharmacologically aided weight loss affects and possibly ameliorates RG has so far not been examined. Here, using a diet switch to chow, calorie restriction (CR) and EX4

¹Research Unit Neurobiology of Diabetes, Helmholtz Zentrum München, 85764, Neuherberg, Germany ²Institute for Diabetes and Obesity, Helmholtz Zentrum München, 85764, Neuherberg, Germany ³German Center for Diabetes Research (DZD), 85764, Neuherberg, Germany ⁴Division of Metabolic Diseases, Technische Universität München, 80333, Munich, Germany

*Corresponding author. Helmholtz Diabetes Center, Ingolstädter Landstraße 1, 85764, Neuherberg, Germany. E-mail: paul.pfluger@helmholtz-muenchen.de (P.T. Pfluger).

Abbreviations: ARC, Arcuate nucleus; POMC, proopiomelanocortin; AgRP, agouti related neuropeptide; RG, reactive gliosis; CNS, central nervous system; DIO, diet-induced obesity; HFD, high-fat diet; EX4, exendin-4; CR, calorie restriction; HC, diet switch; NEFA, non-esterified fatty acid; GFAP, glial fibrillary acidic protein; Iba1, ionized calcium-binding adapter molecule 1; FA, fatty acid

Received March 11, 2019 • Revision received March 27, 2019 • Accepted March 28, 2019 • Available online xxx

<https://doi.org/10.1016/j.molmet.2019.03.009>

treatment, we tested how these mild to drastic weight loss regimes may impact RG after chronic DIO in mice.

2. METHODS

2.1. Animals

Male C57BL/6JRj (Janvier Labs, Le Genest-Saint-Isle, France) were kept under a 12-h light/dark cycle at an ambient temperature of 22 ± 2 °C and with free access to food and water. Mice were fed either a chow (Altromin, #1314) or a 58% high-fat diet (HFD) that is enriched in sucrose (Research Diets, D12331). To induce DIO, mice were ad-libitum fed HFD for 22 weeks. The diet intervention study was performed as described previously [18]. In brief, mice were divided into 5 groups with 8 animals per group: a chow control (chow), a HFD control (HFD), a diet switch group (HC), a calorie restricted group (CR), and an Exendin-4 treated group (EX4). Following 11 days of weight loss, mice were fasted for 6 h and then sacrificed by CO₂ and transcardial perfusion. All studies were based on power analyses to assure adequate sample sizes and approved by the State of Bavaria, Germany.

2.2. Plasma analysis

Plasma was collected from a separate cohort subjected to the same diet intervention (data not shown) [18]. Following a 6 h fast, blood was collected in tubes containing 50 µL EDTA and then centrifuged at $2000 \times g$ and 4 °C for 10 min. Plasma was collected and stored at -80 °C until further testing. Plasma triglycerides and non-esterified fatty acids (NEFA) were measured using the LabAssay™ triglyceride colorimetric assay and the NEFA-HR colorimetric assay, respectively (Fujifilm WAKO chemicals, Neuss, Germany).

2.3. Tissue preparation and immunohistochemistry

Mice were transcardially perfused with 7.5 mL ice-cold phosphate buffered saline (PBS), followed by 7.5 mL of freshly prepared 4% paraformaldehyde (PFA). Brains were harvested and post-fixed in 4% PFA overnight. After rinsing with PBS, brains were placed in a 30% sucrose 0.1 M tris-buffered-saline (TBS) solution for 48 h in preparation for cryo-sectioning. Brains were mounted in OCT compound and 30 µm sections were cut and collected at -20 °C. Sections were then stained using the free-floating approach. Samples were washed with TBS containing 0.1% Tween 20 (TBS-T), blocked for 1 h in a 0.25% gelatin and 0.5% Triton X 100 in 1x TBS buffer. Brain sections were incubated overnight at 4 °C with primary antibodies diluted in blocking buffer. Primary antibodies were: mouse monoclonal α -glial fibrillary acidic protein (GFAP) (Sigma—Aldrich, #G3893) diluted 1:1000 and polyclonal rabbit α -ionized calcium-binding adapter molecule 1 (Iba1) (Synaptic system, #234003) diluted 1:500. Following 3×10 min washing with TBS-T, sections were stained with goat α -mouse Alexa Fluor 568 (Thermo Fisher Scientific, #A11004) and goat α -rabbit Alexa Fluor 488 (Thermo Fisher Scientific, #A11008) diluted 1:1000 in blocking buffer. Following a final 3×10 min wash with TBS-T, sections were mounted with Vectashield® antifade medium containing DAPI (Vectashield, Burlingame, USA).

2.4. Imaging and image analysis

Images were obtained using a Leica TCS SP5 confocal laser scanning microscope (Leica microsystems, Wetzlar, Germany). Fluorophores were excited using 405 diode, 488 argon, and DPSS 561 laser lines. Fluorescence was detected using PMT and hybrid detectors. Identical acquisition settings were used for all images recorded. Fluorescence images were analyzed using the ImageJ based software Fiji (Fiji Is Just ImageJ) [19]. Images were analyzed in a blinded fashion. A total of

eight mice per group were analyzed, averaging two brain sections per mouse. The ARC was defined by drawing a region of interest (ROI) based on the DAPI staining and the known structure of the ARC. Cells were either manually counted, average fluorescence intensity of the ROI was measured, or activation scores were assigned.

2.5. Statistical analyses

Statistical testing and graphing were performed using GraphPad Prism 8.0.2 (GraphPad Software, Inc. La Jolla, USA). One-way ANOVAs with Tukey's post-hoc testing were used to test for differences between treatment groups. The ordinal RG scores were assessed by non-parametric ANOVAs (Kruskal—Wallis) comparing all groups to the chow control. Spearman correlation analyses were used to calculate the association of the activation scores with body weight loss. P-values lower than 0.05 were considered significant. Significances were indicated as follows: * $p < 0.05$, ** $p < 0.01$ or **** $p < 0.0001$. All results are presented as means \pm SEM.

3. RESULTS

3.1. An ordinal scoring system for reactive gliosis

The reactive state of astrocytes and microglia is typically measured by fluorescence intensity of GFAP/Iba1 or by cell number [10,13,16,20]. In an attempt to improve this quantification and to accurately assess the degree of RG in Iba1⁺ microglia and GFAP⁺ astrocytes, we designed a scoring system ranging from 1 (for a resting state) to 5 (fully activated state) [21]. This method, used previously by others [16,22], takes into account both relative amounts of Iba1 and GFAP protein based on staining intensity as well as changes in morphology, which is a key factor in regards to analyzing RG (Figure 1).

3.2. Rapid weight loss increases circulating NEFAs

To understand how weight loss regimes affect reactive gliosis within the ARC, we designed a diet intervention study for mice that had become DIO after 22 weeks of HFD feeding compared to age matched chow controls (Figure 2A). On day 0 of the diet intervention study, the body weight was 49.0 ± 4.7 g for DIO mice and 32.3 ± 1.5 g for the chow controls. Three groups of DIO mice were then switched to chow diet, to exendin-4 treatment (daily, s.c., 0.18 mg·kg⁻¹), or to CR that was matched to the Ex-4 animals. After 11 days of diet intervention, the weight loss groups lost significant amounts of body weight compared to the chow and HFD control groups: HC (-11.7%, $p < 0.0001$), CR (-27.8%, $p < 0.0001$) and EX4 (-30.16%, $p < 0.0001$) (Figure 2B). The body weight before and after the study revealed no significant changes within the chow, HFD and HC groups, however significant decreases within the CR ($p < 0.0001$) and EX4 groups ($p < 0.0001$) (Figure 2C). There were no differences in circulating triglycerides between the diet groups (Figure 2D). Plasma NEFAs were unaltered in the chow, HFD, and HC groups; however, they were significantly increased in EX4 treated mice (chow: $p < 0.0067$, HFD: $p < 0.0180$, HC: $p < 0.0205$) and elevated in CR mice (chow: $p < 0.0572$, HFD: $p < 0.113$, HC: $p < 0.135$) (Figure 2E).

3.3. Chronic HFD feeding and weight loss do not modulate microglial reactivity

To examine the effects of moderate or rapid weight loss on the reactive state of microglia in the ARC, we performed immunofluorescence staining for microglia marker Iba1 in brain sections of mice undergoing weight loss interventions (Figure 3A). Interestingly, we could not detect an increase in microglia RG between chow fed mice and any of the other study groups (Figure 3B). This was consistent with either

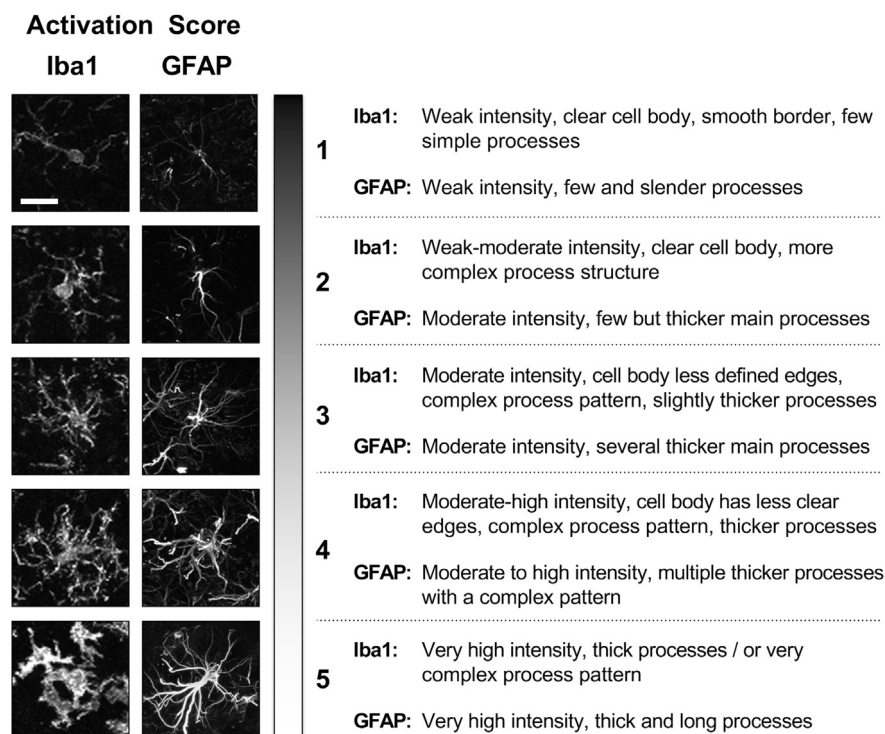


Figure 1: An ordinal activation score allows for a precise evaluation of reactive gliosis in microglia and astrocytes. Iba1+ microglia and GFAP + astrocytes were analyzed according to their staining intensity, cell body form, and process complexity and thickness. The resulting descriptions were ranked from 1 (resting) to 5 (severe reactive gliosis). Representative microscopy images for each assigned activation score are depicted. Scale bar: 20 μ m.

measuring Iba1 fluorescence intensity (Figure 3C) or number of microglia (Figure 3D). Weight loss did also not impact the reactive state of microglia in the ARC (Figure 3B–D). There was also no correlation between body weight loss and RG of microglia (Figure 3E).

3.4. Rapid weight loss induces RG in astrocytes but not in microglia

The degree of astrocyte RG following a diet intervention in DIO mice was measured by analyzing brain sections stained for GFAP (Figure 4A). Astrocytic RG was significantly increased in mice that had shown a drastic weight loss due to treatment with EX4 ($p < 0.0253$) or CR ($p < 0.0383$) compared to the chow controls (Figure 4B). The HC group also displayed increased astrocytic RG, however this did not reach significance ($p < 0.334$) (Figure 4B). GFAP expression as measured by GFAP signal intensity showed no significant differences between all groups (Figure 4C). Interestingly, when we matched the astrocyte RG score to the body weight loss of the animal, we saw a significant positive correlation between body weight lost and RG ($p < 0.0045$) (Figure 4D). This correlation was specific to body weight loss as we could not detect any correlation of RG to absolute body weight (Figure 4E).

4. DISCUSSION

In the current study, we investigated how weight loss regimes with either a simple diet switch from HFD to chow, CR, or pharmacological treatment with EX4 could affect RG within the ARC. Overall, we show that after chronic feeding of HFD for 22 weeks, mice do not show an increased RG in microglia or astrocytes compared to chow fed controls. Similar to Baufeld et al., who report unperturbed astrocytosis in the

hypothalamus of human individuals with BMI <25 vs. BMI >30 , we found no correlation for GFAP fluorescence intensities or GFAP scores with body weight [23]. However, when chronically DIO mice undergo profound weight loss, astrocytes display an increase in RG which is not seen in microglia. This finding coincides with an increase in circulating NEFAs seen in the weight loss groups. This is in line with a study in which cultured astrocytes exposed to saturated fatty acids (FA) such as palmitic acid, lauric acid and stearic acid were shown to directly trigger the release of inflammatory cytokines [24]. Consistent with our findings, they also revealed that this effect was independent of microglia [24]. Lipolysis due to CR and subsequent increase in circulating NEFAs is well understood and has been shown in mice [25]; however, a direct link to RG remains to be tested. The possibility that circulating NEFAs may induce RG in astrocytes is supported by a number of factors. NEFAs may easily cross the blood-brain-barrier and gain access to metabolically relevant hypothalamic centers [26,27]. Furthermore, when administered peripherally, NEFAs were shown to accumulate in astrocytes localized close to blood-brain-barrier borders [28]. However, it must be stated that although the evidence is indicative, this mechanism remains speculative. CR is known to induce hormonal and metabolic changes that include decreased leptin [29] or IGF-1 levels [30], increased adiponectin [31] or FGF21 levels [32] or increased insulin sensitivity [33]. Next to increased NEFA levels, RG after an acute CR could in theory be influenced by any of these factors. Future studies should delineate the impact of NEFA and CR-linked hormonal and metabolic changes on RG. Ideally, such studies should include additional CR models, for example a lean, never obese group, which is then subjected to CR.

When mice suffering from DIO are subjected to CR, they lose significant amounts of fat mass and are able to normalize their body weight within

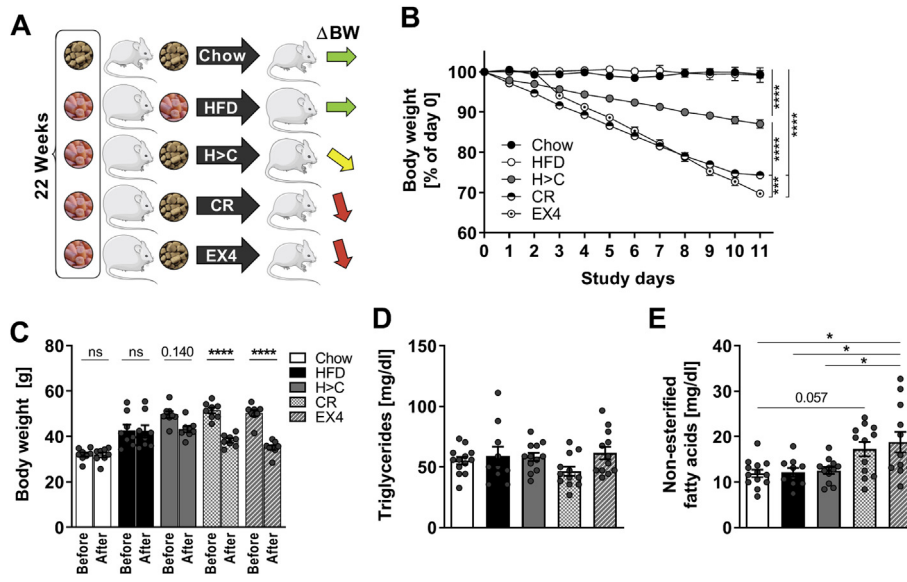


Figure 2: Weight loss by CR or EX4 results in increased circulating NEFAs. Mice were subjected to chow or HFD feeding for 22 weeks (A). Groups of obese HFD-fed mice were then switched to chow diet and either fed ad libitum (HC), treated daily with EX4 (s.c., 0.18 mg kg⁻¹) or calorie restricted to the average food intake of the EX4 group (A). Colored arrows indicate the change in body weight. Body weight change in %, n = 8 mice per group (B). Average body weights of the groups before and after the intervention (C). Fasting triglycerides (D) and non-esterified fatty acids (E) were measured at the end of the treatments in an additional cohort of mice, consisting of n = 10–13 mice per group. Statistical test: One-way ANOVA with Tukey's post-hoc test. *p < 0.05, ***p < 0.001, ****p < 0.0001 or specific p values displayed.

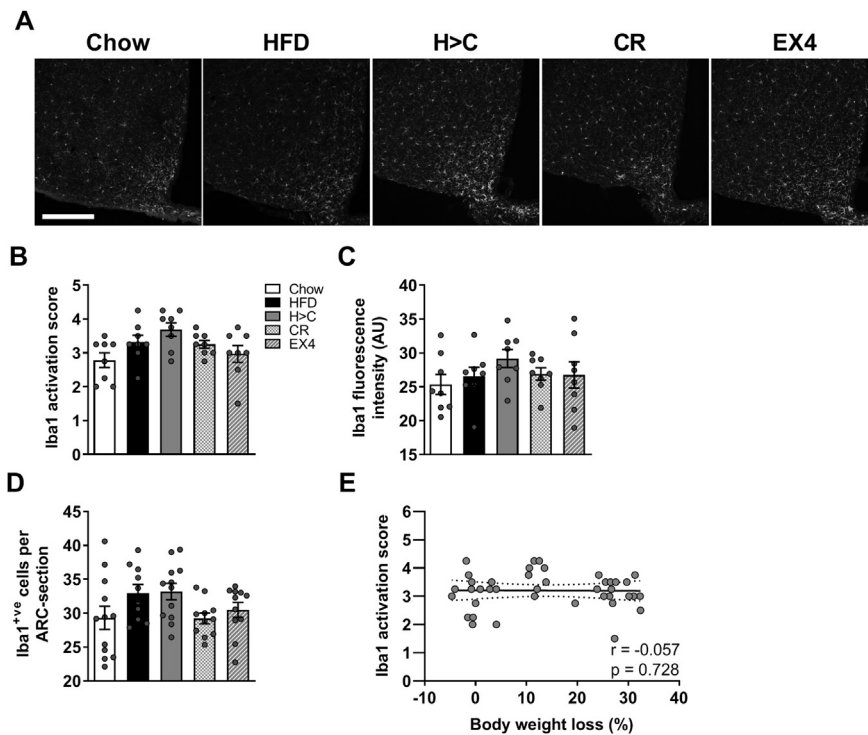


Figure 3: Microglial RG is unchanged in chronic obesity and after profound weight loss. Brain sections of mice after diet intervention were stained for Iba1 and examined using confocal microscopy. Scale bar: 200 μm (A). Brain sections were assigned a microglia activation score as defined in Figure 1, n = 8 (B). The average Iba1 fluorescence intensity was measured in the ARC (C). Iba1⁺ cells were manually counted within the ARC (D). The microglial activation score was correlated to body weight loss in a linear correlation (E). Statistical test for B–D: One-way ANOVA with Tukey's post-hoc test. Statistical test for E: Spearman correlation. r = correlation coefficient.

several weeks [34]. However, when mice are then allowed to feed ad libitum, they regain the weight lost, regardless if they consume HFD or chow [34]. This indicates that CR, although providing acute metabolic benefits, prevents a long term reduction in body weight, which is

achieved by a diet switch to chow alone [15]. We reveal that CR, resulting in profound body weight loss, leads to an increase in astrocyte RG in the ARC. Whether or not increased astroglia can functionally contribute to the increased susceptibility for weight regain

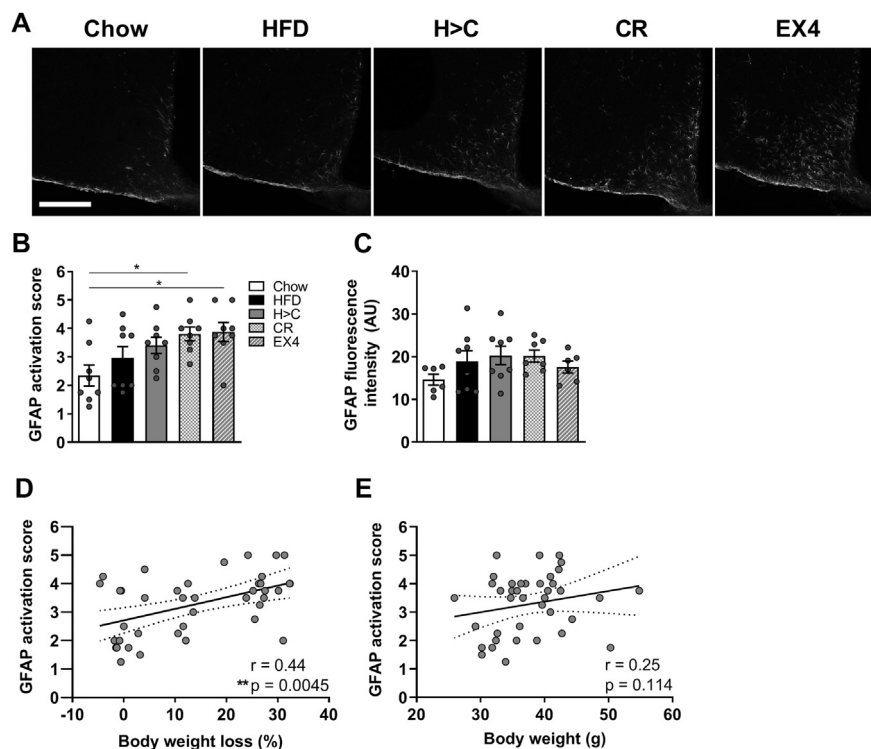


Figure 4: Weight loss is correlated to increased astrocyte RG. Brain sections of mice after diet intervention were stained for GFAP and examined using confocal microscopy. Scale bar: 200 μ m (A). Brain sections were assigned an astrocyte activation score as defined in Figure 1, $n = 8$ (B). The average GFAP fluorescence intensity was measured in the ARC (C). Astrocyte activation scores based on GFAP staining showed a positive correlation to body weight loss (D). Astrocyte activation scores showed no correlation to absolute body weight. Statistical test for B–C: One-way ANOVA with Tukey’s post-hoc test. Statistical test for D–E: Spearman correlation. r = correlation coefficient.

of previously obese mice remains to be tested. Indeed, we did not examine if the observed RG after CR would be reverted if mice were refed a HFD or normal chow and allowed to regain the lost body weight. We would assume, however, that acute refeeding of HFD would induce RG in the ARC, as reported previously [10,16,20].

A further trait of obesity is the inability of exogenously administered leptin to decrease food intake and body weight, known as leptin resistance. An inflammation like state in the ARC has been linked to leptin resistance on numerous occasions (reviewed by [35]). Using EX4 treatment, which has been shown to induce leptin re-sensitization [17], we found increased RG after significant weight loss. This indicates that although a general inflammation state in the ARC is linked to leptin resistance, RG does not seem to be responsible for this resistance. This is in line with recent work by Balland and colleagues who showed that despite an increase in RG after 10 days of HFD feeding, mice retained leptin sensitivity [20].

Astrocyte and microglial RG in the ARC has typically been assessed in an acute to sub-chronic situation, in which animals have been exposed to HFD for time spans of a 1–10 days [10,20,36], up to several weeks [10,16]. In our case, mice were subjected to chronic HFD feeding for over 22 weeks. Consistent with our findings, Baufeld et al. report a subdued microglia phenotype in the hypothalamus of mice chronically exposed to HFD, which may serve as protective mechanism to preserve neuronal homeostasis [23]. We were unable to reproduce the finding that HFD feeding induces RG in the ARC of mice. Our results differ from those of Thaler and colleagues who found that after 8 months of HFD feeding, mice showed an increased detection of GFAP in the ARC [10]. Although this seems to be in direct contradiction to our findings, there are differences between these

studies in respect to the types of chow or HFD used. Thaler et al. fed their mice a 60% HFD (D12492; Research Diets) with 90% of the fat content coming from lard (i.e. 40% saturated FAs, 60% unsaturated FAs). The carbohydrate component made up 20% of total calories and consisted of 63% maltodextrin and 37% sucrose. We fed a 58% HFD (D12331; Research Diets) in which 90% of the fat was derived from coconut oil, which consists mainly of saturated FAs. 25% of the calories in the 58% HFD were from carbohydrates, with 52% sucrose and 48% maltodextrin. The overall composition of the chow diets used in our (Altromin #1314) and the study of Thaler et al. (PMI Nutrition International; 3.34 kcal/g) appeared to be similar. Nonetheless, slight differences in fat or carbohydrate composition were present, and these may contribute to changes in RG after chronic diet feeding. Overall, we observed comparable RG in astrocytes in our chow and HFD groups. This may point toward a relative lack of effect of our 58% HFD on astrocytes even after 22 weeks of exposure. On the other hand, we may also observe a more pronounced effect of our chow-diet on astrocyte RG as compared to the earlier studies by Thaler and colleagues [10].

Reactive gliosis is a complex process induced by inflammatory cytokines such as interleukin 1, interleukin-6 and tumor necrosis factor alpha [37]. Both astrocyte and microglial RG are characterized by morphological changes such as thickening of cellular processes, cell body size increase and upregulation of certain proteins such as GFAP in astrocytes or Iba1 in microglia [38,39]. It has been previously described that analyses not taking these multiple aspects into account may result in misleading results [16]. The authors revealed that despite not seeing differences in counting of microglia between lean and DIO mice, when they incorporated multiple RG features into the analysis by

the use of a scoring system, differences became apparent. Our work is in agreement with these previous findings, as although no difference was seen in GFAP intensity, we could detect differences when using an activation scoring system (Figure 4A,B). Our scoring system was designed according to established ordinal scoring requirements, such as using 4–5 score levels, which are optimal in terms of sensitivity and reliability [21].

5. CONCLUSION

Taken together, our findings suggest that mice which are chronically obese after 22 weeks of HFD feeding display RG levels in the ARC comparable to levels seen in age-matched chow fed mice. Furthermore, profound weight loss by CR or EX4 treatment results in an increase in ARC related astrocytic RG, which coincides with an increased concentration of circulating NEFAs. The role of hypothalamic glia in regulating metabolism and sensing hormonal and nutrient cues is clearly established [40]. However, whether or not reactive gliosis plays a role in chronic obesity and its comorbidities, or rather in the acute adaptation to the dietary environment, remains to be fully understood.

AUTHOR CONTRIBUTIONS

LH, KP, SCS, and PTP designed and performed the experiments, analyzed and interpreted data. LH and PTP drafted the manuscript. LH, KP, SCS, and PTP co-conceptualized the project, and reviewed the manuscript.

ACKNOWLEDGMENTS

We thank Emily Baumgart for her technical assistance. This work was supported in part by the German Center for Diabetes Research (DZD), by the Helmholtz Alliance ICEMED-Imaging and Curing Environmental Metabolic Diseases and by the Helmholtz-Israel-Cooperation in Personalized Medicine. Elements of artwork used in the table of contents image and Figure 2 were provided by Servier Medical Art under the Creative Commons license 3.0.

CONFLICT OF INTEREST

None declared.

REFERENCES

- [1] Brobeck, J.R., 1946. Mechanism of the development of obesity in animals with hypothalamic lesions. *Physiology Reviews* 4:541–559.
- [2] Simon, J.J., Wetzal, A., Sinno, M.H., Skunde, M., Bendszus, M., Preissl, H., et al., 2017. Integration of homeostatic signaling and food reward processing in the human brain. *JCI Insight* 15. <https://doi.org/10.1172/jci.insight.92970>.
- [3] Woods, S.C., Lotter, E.C., McKay, L.D., Porte, D., 1979. Chronic intracerebroventricular infusion of insulin reduces food intake and body weight of baboons. *Nature* 5738:503–505.
- [4] Schwartz, M.W., Seeley, R.J., Tschöp, M.H., Woods, S.C., Morton, G.J., Myers, M.G., et al., 2013. Cooperation between brain and islet in glucose homeostasis and diabetes. *Nature*, 59–66.
- [5] Cowley, M.A., Smart, J.L., Rubinstein, M., Cerdán, M.G., Diano, S., Horvath, T.L., et al., 2001. Leptin activates anorexigenic POMC neurons through a neural network in the arcuate nucleus. *Nature*, 480–484.
- [6] Fan, W., Boston, B.A., Kesterson, R.A., Hruby, V.J., Cone, R.D., 1997. Role of melanocortinergic neurons in feeding and the agouti obesity syndrome. *Nature* 6612:165–168.

- [7] Faouzi, M., Leshan, R., Bjornholm, M., Hennessey, T., Jones, J., Munzberg, H., 2007. Differential accessibility of circulating leptin to individual hypothalamic sites. *Endocrinology* 11:5414–5423.
- [8] Belgardt, B.F., Brüning, J.C., 2010. CNS leptin and insulin action in the control of energy homeostasis. *Annals of the New York Academy of Sciences* 1:97–113.
- [9] Cowley, M.A., Smith, R.G., Diano, S., Tschöp, M., Pronchuk, N., Grove, K.L., et al., 2003. The distribution and mechanism of action of ghrelin in the CNS demonstrates a novel hypothalamic circuit regulating energy homeostasis. *Neuron* 4:649–661.
- [10] Thaler, J.P., Yi, C.X., Schur, E.A., Guyenet, S.J., Hwang, B.H., Dietrich, M.O., et al., 2012. Obesity is associated with hypothalamic injury in rodents and humans. *Journal of Clinical Investigation* 1:153–162.
- [11] De Souza CuT, Araujo, E.P., MrJA, Saad, Zollner, R.L., Ashimine, R., LcA, Velloso, et al., 2005. Consumption of a fat-rich diet activates a proinflammatory response and induces insulin resistance in the hypothalamus. *Endocrinology* 10:4192–4199.
- [12] Schur, E.A., Melhorn, S.J., Oh, S.K., Lacy, J.M., Berkseth, K.E., Guyenet, S.J., et al., 2015. Radiologic evidence that hypothalamic gliosis is associated with obesity and insulin resistance in humans. *Obesity (Silver Spring)* 11:2142–2148.
- [13] Valdearcos, M., Douglass, J.D., Robblee, M.M., Dorfman, M.D., Stifler, D.R., Bennett, M.L., et al., 2017. Microglial inflammatory signaling orchestrates the hypothalamic immune response to dietary excess and mediates obesity susceptibility. *Cell Metabolism* 1:185–197.
- [14] Ridet, J.L., Privat, A., Malhotra, S.K., Gage, F.H., 1997. Reactive astrocytes: cellular and molecular cues to biological function. *Trends in Neurosciences* 12: 570–577.
- [15] Fischer, I.P., Irmeler, M., Meyer, C.W., Sachs, S.J., Neff, F., Hrabec de Angelis, M., et al., 2017. A history of obesity leaves an inflammatory fingerprint in liver and adipose tissue. *International Journal of Obesity*. <https://doi.org/10.1038/ijo.2017.224>.
- [16] Berkseth, K.E., Guyenet, S.J., Melhorn, S.J., Lee, D., Thaler, J.P., Schur, E.A., et al., 2014. Hypothalamic gliosis associated with high-fat diet feeding is reversible in mice: a combined immunohistochemical and magnetic resonance imaging study. *Endocrinology* 8:2858–2867.
- [17] Müller, T.D., Sullivan, L.M., Habegger, K., Yi, C.X., Kabra, D., Grant, E., et al., 2012. Restoration of leptin responsiveness in diet-induced obese mice using an optimized leptin analog in combination with exendin-4 or FGF21. *Journal of Peptide Science* 6:383–393.
- [18] Harrison, L., Schriever, S.C., Feuchtinger, A., Kyriakou, E., Baumann, P., Pfuhlmann, K., et al., 2018. Fluorescent blood–brain barrier tracing shows intact leptin transport in obese mice. *International Journal of Obesity (Lond)*. <https://doi.org/10.1038/s41366-018-0221-z>.
- [19] Schindelin, J., Arganda-Carreras, I., Frise, E., Kaynig, V., Longair, M., Pietzsch, T., et al., 2012. Fiji: an open-source platform for biological-image analysis. *Nature Methods*, 676–682.
- [20] Balland, E., Cowley, M.A., 2017. Short-term high-fat diet increases the presence of astrocytes in the hypothalamus of C57BL6 mice without altering leptin sensitivity. *Journal of Neuroendocrinology* 10. <https://doi.org/10.1111/jne.12504>.
- [21] Gibson-Corley, K.N., Olivier, A.K., Meyerholz, D.K., 2013. Principles for valid histopathologic scoring in research. *Veterinary pathology* 6:1007–1015.
- [22] Lemstra, A.W., Groen in't Woud, J.C.M., Hoozemans, J.J.M., van Haastert, E.S., Rozemuller, A.J.M., Eikelenboom, P., et al., 2007. Microglia activation in sepsis: a case-control study. *Journal of Neuroinflammation*. <https://doi.org/10.1186/742-2094-4-4>.
- [23] Baufeld, C., Osterloh, A., Prokop, S., Miller, K.R., Heppner, F.L., 2016. High-fat diet-induced brain region-specific phenotypic spectrum of CNS resident microglia. *Acta Neuropathologica* 3:361–375.
- [24] Gupta, S., Knight, A.G., Gupta, S., Keller, J.N., Bruce-Keller, A.J., 2012. Saturated long-chain fatty acids activate inflammatory signaling in astrocytes. *Journal of Neurochemistry* 6:1060–1071.

- [25] Bruss, M.D., Khambatta, C.F., Ruby, M.A., Aggarwal, I., Hellerstein, M.K., 2009. Calorie restriction increases fatty acid synthesis and whole body fat oxidation rates. *American Journal of Physiology. Endocrinology and Metabolism* 1:108–116.
- [26] Dhopeswarkar, G.A., Mead, J.F., 1973. Uptake and transport of fatty acids into the brain and the role of the blood–brain barrier system. In: Paoletti, R., Kritchevsky, D. (Eds.), *Adv lipid res.* Elsevier. p. 109–42.
- [27] Smith, Q.R., Nagura, H., 2001. Fatty acid uptake and incorporation in brain. *Journal of Molecular Neuroscience* 2:167–172.
- [28] Bernoud, N., Fenart, L., Bénistant, C., Pageaux, J.F., Dehouck, M.P., Molière, P., et al., 1998. Astrocytes are mainly responsible for the polyunsaturated fatty acid enrichment in blood–brain barrier endothelial cells in vitro. *The Journal of Lipid Research* 9:1816–1824.
- [29] Lecoultrre, V., Ravussin, E., Redman, L.M., 2011. The fall in leptin concentration is a major determinant of the metabolic adaptation induced by caloric restriction independently of the changes in leptin circadian rhythms. *The Journal of Clinical Endocrinology and Metabolism* 9:1512–1516.
- [30] Berrigan, D., Lavigne, J.A., Perkins, S.N., Nagy, T.R., Barrett, J.C., Hursting, S.D., 2005. Phenotypic effects of calorie restriction and insulin-like growth factor-1 treatment on body composition and bone mineral density of C57BL/6 mice: implications for cancer prevention. *In Vivo* 4: 667–673.
- [31] Ding, Q., Ash, C., Mracek, T., Merry, B., Bing, C., 2012. Caloric restriction increases adiponectin expression by adipose tissue and prevents the inhibitory effect of insulin on circulating adiponectin in rats. *The Journal of Nutritional Biochemistry* 8:867–874.
- [32] Thompson, A.C.S., Bruss, M.D., Nag, N., Kharitonov, A., Adams, A.C., Hellerstein, M.K., 2014. Fibroblast growth factor 21 is not required for the reductions in circulating insulin-like growth factor-1 or global cell proliferation rates in response to moderate calorie restriction in adult mice. *PLoS One* 11. <https://doi.org/10.1371/journal.pone.0111418>.
- [33] Johnson, M.L., Distelmaier, K., Lanza, I.R., Irving, B.A., Robinson, M.M., Konopka, A.R., et al., 2016. Mechanism by which caloric restriction improves insulin sensitivity in sedentary obese adults. *Diabetes* 1:74–84.
- [34] Kirchner, H., Hofmann, S.M., Fischer-Rosinsky, A., Hembree, J., Abplanalp, W., Ottaway, N., et al., 2012. Caloric restriction chronically impairs metabolic programming in mice. *Diabetes* 11:2734–2742.
- [35] de Git, K.C.G., Adan, R.A.H., 2015. Leptin resistance in diet-induced obesity: the role of hypothalamic inflammation. *Obesity Reviews* 3:207–224.
- [36] Buckman, L.B., Thompson, M.M., Lippert, R.N., Blackwell, T.S., Yull, F.E., Ellacott, K.L.J., 2015. Evidence for a novel functional role of astrocytes in the acute homeostatic response to high-fat diet intake in mice. *Mol Metab* 1:58–63.
- [37] Johns, P., 2014. Chapter 8 - cellular mechanisms of neurological disease. In: Johns, P. (Ed.), *Clin neurosci.* Churchill Livingstone. p. 91–103.
- [38] Robel, S., Berninger, B., Götz, M., 2011. The stem cell potential of glia: lessons from reactive gliosis. *Nature Reviews Neuroscience*, 88–104.
- [39] Pekny, M., Nilsson, M., 2005. Astrocyte activation and reactive gliosis. *Glia* 4: 427–434.
- [40] Garcia-Caceres, C., Bolland, E., Prevot, V., Luquet, S., Woods, S.C., Koch, M., et al., 2019. Role of astrocytes, microglia, and tanycytes in brain control of systemic metabolism. *Nature Neuroscience* 1:7–14.

4.3. Low-medium dosed cranial irradiation in young mice induces sex specific metabolic disturbances later in life

4.3.1. Aim and summary

Childhood CrI has been indicated as a risk factor for developing the MetS. The aim of this study was to assess the risk of low to moderate doses of CrI, targeted primarily at the hypothalamus, in developing metabolic abnormalities such as glucose intolerance, insulin resistance, weight gain and dyslipidaemia. Overall it was shown that 2 Gy of radiation resulted in an acute astrocytosis in male mice 1 week after treatment. Using in-depth metabolic phenotyping via indirect calorimetry, it was revealed that 2 Gy irradiated female mice had become leptin resistant 2 months' post radiation. Apart from this deficit, none of the treatment doses influenced energy homeostasis after 2 months. However, 40 weeks after treatment, latent effects started to appear. Female mice that received 2 Gy doses gained significantly more body weight in the form of fat mass compared to sham and 0.5 Gy groups. Moreover, glucose tolerance was impaired in male mice (2 Gy) after 18 months. This coincided with an increase in V-LDL and decreased HDL in both male and female 2 Gy groups.

To summarise, these findings provide novel insights into the possible mechanisms involved in latent MetS following childhood irradiation, and suggest a causative role of the hypothalamus. However, higher doses and more precise irradiation methodology will be required to potentiate the effects seen in the current study, perhaps highlighting disease processes and revealing the cell populations involved.

4.3.2. Contribution

I performed the in-vivo studies with support from Peter Baumann, Dr. Sonja C. Schriever, Raian Contreras, Dr. Michael Rosemann and Dr. Paul T. Pfluger. Moreover, I performed all of the immunohistochemistry experiments, microscopy, blood chemistry analysis, apart from the FPLC and cholesterol measurements which were performed by Sebastian Cucuruz (Institute of diabetes and regeneration research, Hofmann group). Additionally, I designed all figures and performed all the statistical analyses of the data. Finally, Dr. Paul

Pfluger and I wrote the manuscript. All co-authors were involved in aspects of the scientific discussion, interpretation of the results and reviewed the manuscript.

4.3.3. Publication information

The completed manuscript and data are ready for submission.

Low-medium dosed cranial irradiation in young mice induces sex specific metabolic disturbances later in life

Luke Harrison, Peter Baumann, Sonja C. Schriever, Raian Contreras, Susanna Hofmann
Michael Rosemann and Paul T. Pfluger

Title: Low-medium dosed cranial irradiation in young mice induces sex specific metabolic disturbances later in life

Authors: Luke Harrison^{1,2,3,4}, Peter Baumann^{1,2,3,4}, Sonja C. Schriever^{1,2,3}, Raian Contreras^{1,2,3,4}, Susanna Hofmann⁵, Michael Rosemann⁶ and Paul T. Pfluger^{1,2,3}

1 Research Unit Neurobiology of Diabetes, Helmholtz Zentrum München, 85764 Neuherberg, Germany.

2 Institute for Diabetes and Obesity, Helmholtz Zentrum München, 85764 Neuherberg, Germany.

3 German Centre for Diabetes Research (DZD), 85764 Neuherberg, Germany.

4 Division of Metabolic Diseases, Technische Universität München, 80333 Munich, Germany.

5 Institute for Diabetes and Regeneration, Helmholtz Zentrum München, 85764 Neuherberg, Germany.

6 Institute of Radiation Biology, Helmholtz Zentrum München, 85764 Neuherberg, Germany.

Corresponding author:

Paul T. Pfluger, paul.pfluger@helmholtz-muenchen.de

Telephone + 49 (0) 89 3187 2104

Helmholtz Diabetes Centre

Ingolstädter Landstraße 1

85764 Neuherberg

Number of figures: 7 (+2 supplemental)

Word count abstract: 270

Word count main text: 4100

Acknowledgments: We thank Emily Baumgart, Laura Seherer and Sebastian Cucuruz for their technical assistance. This work was supported in part by the German Center for Diabetes Research (DZD), by the Helmholtz Alliance ICEMED-Imaging and Curing Environmental Metabolic Diseases and by the Helmholtz-Israel-Cooperation in Personalized Medicine. Elements of artwork used in the table of contents image and figures 5 & 6 were provided by Servier Medical Art under the Creative Commons license 3.0.

Abstract

Survivors of childhood cancers who received high doses (40-60 Gy) of cranial irradiation have an increased risk to develop obesity, type 2 diabetes and other features of the metabolic syndrome (MetS). The responsible brain region and mechanism are currently unknown, as well as the risk when exposed to far lower doses. The hypothalamus is known as a main centre in the brain for metabolic control and is a likely candidate for the cranial irradiation related MetS risk. Here, three cohorts of 6-week old male and female C57BL/6 mice were subjected to either sham treatment (0 Gy), low (0.5 Gy) or moderate (2 Gy) doses of cranial irradiation aimed towards the hypothalamus. Subsequently, we assessed the acute (1-week), sub-chronic (3-month) and chronic (2-year) effects of cranial irradiation on biochemical, morphological and physiological parameters of metabolic control. One week following 2 Gy irradiation, male mice displayed an increase in hypothalamic astrocytosis, but not microglial reactive gliosis. Indirect calorimetry 2 months' post irradiation showed no changes between all groups, yet long-term monitoring of the chronic cohort revealed weight gain in the 2 Gy female group, due to increased fat mass, 10 months after treatment. Furthermore, 2 Gy irradiated male mice became glucose intolerant after 18 months. At this time point insulin sensitivity, plasma insulin and triglycerides remained unaltered, however male and female 2 Gy groups revealed elevated V-LDL and lowered HDL levels. Overall mortality remained unaffected by all doses of radiation treatment. The data presented here, and that by others, strongly suggest a significant risk to developing MetS following low to moderate doses of cranial irradiation, in particular when the hypothalamus is targeted.

Introduction

Overconsumption of energy-dense food and a concomitant reduction in physical activity promote a cluster of conditions that are summarized as metabolic syndrome (MetS), including: obesity, increased fasting glucose levels, dyslipidaemia (e.g. increased fasting triglyceride and decreased HDL-cholesterol levels) and high blood pressure. Each component of the MetS may be associated with impaired quality of life. In combination, these MetS components can greatly exacerbate the development of comorbidities such as T2DM and cardiovascular disease (Laaksonen, Lakka et al. 2002).

An exogenous risk factor for the development of the MetS is childhood exposure to high doses (40-60 Gy) of cranial irradiation. In a study comparing the prevalence of T2DM in childhood cancer survivors and their siblings, an increased risk for T2DM was detected among cancer survivors (Meacham, Sklar et al. 2009). In a follow-up study of young patients who received radiation therapy to the head (to treat leukaemia, lymphoma and solid cancers), a persistent increase of cholesterol, triglycerides and LDL cholesterol was found compared to their healthy control siblings (Miller, Lipsitz et al. 2010). Similarly, the MetS was more frequently diagnosed in cranially irradiated survivors compared with non-irradiated survivors (van Waas, Neggers et al. 2013). Notably, an increased risk for obesity also became apparent after exposure to lower doses (10-19 Gy) of irradiation and a longer observation period (Garmey, Liu et al. 2008).

Radiation as a diagnostic tool and as a therapy modality is an important component of modern medicine. High dose cranial irradiation (e.g. of 60Gy s), remains a standard therapy for a variety of cancers. Although exposure is directed towards the tumour, surrounding regions are within the radiation pathways, often resulting in low to moderate doses delivered to off-target areas (Lax 1993, Halasz and Rockhill 2013). These off-target effects can have unknown consequences and latent complications often arise (Fetcko, Lukas et al. 2017). Advances in clinical practice led to a dramatic surge in the number of long-term cancer survivors that may be at risk for late-arising radiation side effects. Moreover, there is a growing discussion on the association between early exposure to diagnostic procedures, mainly X-ray computed tomography (CT), and cancer (Brenner, Elliston et al. 2001, Pearce, Salotti et al. 2012). Diagnostic CT scans of the head can expose the hypothalamus with a single dose of 10-20mGy, and higher doses following multiple CTs. This technology is considered to be the main source for exposure to radiation in

medicine nowadays. In 2007, more than 69 million CT exams were performed in the United States and that number has increased nearly 10% annually. It is estimated that CT examinations contribute up to 70% of the total radiation dose to the population. This has led to increasing public health concern regarding the potential cancer risks associated with CT use (Hess, Haas et al. 2014).

The possibility that much lower doses of cranial irradiation have detrimental health effects has yet to be fully explored. A recent study in by Xu and colleagues subjected 11 day old female rats to a moderate dose of 6 Gy whole brain irradiation and discovered increased body weight from 15 weeks onwards, as well as further metabolic abnormalities (Xu, Sun et al. 2018). These findings are promising in regards to unravelling the molecular mechanisms involved, yet a low-dose long term study, which includes both sexes, would highlight risks presented to a far higher number of subjects. Additionally, the responsible brain region remains to be revealed.

The hypothalamus is recognised as one of the main brain regions involved in regulating energy homeostasis (Woods, Schwartz et al. 2000). It does so by responding to signalling cues from the periphery, thus regulating food intake, energy expenditure and glucose metabolism (Timper and Bruning 2017). We suspected that brain irradiation related MetS may be due to damage specifically in the hypothalamus. Here, we subjected 3 separate cohorts of young 6-week old male and female mice to low and moderate doses (sham, 0.5 Gy, 2 Gy) cranial irradiation targeted towards the hypothalamus to investigate the risk of developing the MetS at acute, sub-chronic and chronic time points.

Methods

Animal experiments

All experiments were performed in C57BL/6JRj wild type mice that were kept under a 12h light : 12h dark cycle, at 22 ± 2 °C, fed a normal rodent chow diet ad libitum except were specified otherwise. Mice were purchased from Janvier Labs (Saint-Berthevin, Cedex, France). All animal studies were based on power analyses to assure adequate sample sizes, and approved by the state of upper Bavaria.

Dosimetry calibration

Thermoluminescent dosimeters (TLD) were used to detect radiation dosage. TLDs were irradiated with a Buchler gamma-calibrator OB 20 at specific doses between 0.1 Gy and 5 Gy. These were then analysed using a thermoluminescence-reader. These values were used to generate a standard curve for the TLDs. For the internal dosimetry a 1 mm³ LiF TLD MicroCube (Thermo Fischer Scientific, USA) was wrapped in 12 µm Mylar foil and placed in the cadavers of 6 mice (2 month of age) at the site of the hypothalamus, the sublingual salivary gland and the thyroid gland. Mice were placed under a 50 mm thick lead shield house with a 4 mm diameter bore hole focusing on the hypothalamus. Gamma irradiation was done using a ⁶⁰Co therapy machine (ELDORADO, AEC, Canada) with a 270mm distance between table surface and the lower filter holder, yielding a dose rate (in air) of 0.38 Gy/min (according to ionization chamber measurements). Read-out of the LiF TLDs was done within 1 hour after irradiation using a programmed, heated luminescence photometer with internal beta-calibration. The measurements were done twice on each mouse. The individual values were plotted according to the standard curve derived from the calibrated irradiation values (Data not shown).

Cranial Irradiation

Six week old male and female mice were subjected to cranial irradiation of either 0.5 Gy, 2 Gy or a sham treatment. Mice were anaesthetised using isoflurane for the duration of the irradiation. Sham treated mice received only anaesthesia for the same duration as the 2 Gy treated mice. A custom built sterile irradiation chamber was used to fix the mice to avoid movement of the head during the irradiation. A camera was used to monitor the health of the mice whilst irradiation was ongoing and it was not possible to enter the facility. A total of 3 study cohorts were generated. The acute cohort consisted of 18 male mice divided up into 6 mice per condition (Sham, 0.5 Gy, 2 Gy). These mice were sacrificed 7 days' post irradiation to look for signs of hypothalamic inflammation. The sub-chronic cohort consisted of 36 male and 36 female mice with 12 mice per condition. Two months' post irradiation the mice were subjected to body composition measurement, indirect calorimetry and a leptin sensitivity test. Three months after irradiation the mice were sacrificed for organ collection. The chronic cohort was composed of 36 male and 36 female mice with 12 mice per treatment group. This cohort was subjected to body

composition and glucose tolerance tests at specific time intervals (3, 6, 12, 18 and 24 months' post irradiation).

Body composition

Body composition (fat and lean mass) was analysed non-invasively via nuclear magnetic resonance (NMR) with an EchoMRI device (Houston, TX, USA).

Indirect calorimetry

Energy expenditure, respiratory exchange quotient (RER), food intake and locomotor activity were measured as previously described (Pfuhlmann, Schriever et al. 2018) using a combined indirect calorimetry system (TSE System, Bad Homburg, Germany). Mice were single housed and groups were distributed randomly to avoid technical bias between TSE cabinets. Mice were in the system for 24 h prior to data collection for acclimatisation purposes. Data collection was performed for 72 h under a 12 h light / 12 h dark cycle at 23 °C.

Leptin challenge

Leptin (R&D Systems, USA) was dissolved in 20 mM Tris-HCl, pH 8.0 to 5 mg/ml, then diluted in saline (0.9 % NaCl) to a concentration of 1 mg/ml. Saline or 5 mg/kg leptin was injected shortly before the beginning of the dark phase. Food intake was measured in the combined indirect calorimetry system for 24 h.

Glucose tolerance test

To assess glucose tolerance, mice were subjected to a glucose tolerance test (GTT). At the onset of the light phase, mice were fasted for 6 h after which a basal glucose value was measured from the punctured tail vein with a handheld glucometer. Following this, mice were injected intraperitoneally (i.p.) with 2 g/kg glucose solution and blood glucose was measured 15, 30, 60 and 120 min post injection.

Sacrifice and organ withdrawal

Mice were always sacrificed by cervical dislocation, unless cardiac perfusion of the mouse was performed, in which case the mice were sacrificed using CO₂. Organs were removed immediately post sacrifice and frozen on dry ice or liquid nitrogen and stored at -80 °C. Following perfusions, the brains were post-fixed in 4 % paraformaldehyde overnight,

then placed in a 20 % sucrose solution for 48 h. Brains were then mounted for cryo-sectioning and sliced into 30 μm sections.

Plasma insulin, triglycerides, NEFA, HOMA-IR measurements

Mice were fasted for 6 h and blood was collected in tubes containing 50 μL EDTA during the sacrifice or from bleeding via the tail vein. The blood was centrifuged at 4 $^{\circ}\text{C}$ for 10 min at 2000 x g to allow separation. Plasma was collected and either frozen at -80 $^{\circ}\text{C}$ or directly processed for lipid fractionation using fast protein liquid chromatography (FPLC) as described previously (Hofmann, Perez-Tilve et al. 2008). An ultra-sensitive insulin ELISA was performed using an ELISA kit (Alpco Diagnostics, USA). Basal glucose values were measured as described above. Insulin resistance was calculated using the homeostatic model of insulin resistance (HOMA-IR), i.e. fasting blood glucose (mmol/l) was multiplied by the fasting plasma insulin levels (mIU/l) and then divided by a factor of 22.5. Plasma triglyceride content was measured using a colorimetric triglyceride detection kit (Wako Chemicals, Germany). Non-esterified fatty acids (NEFA) were measured using a commercially available kit (Wako Chemicals, Germany).

Immunohistochemistry

Free floating brain sections were placed in a blocking buffer consisting of 0.25 % gelatine and 0.5 % triton X-100 in a 1 x tris-buffered saline solution for 1 h at room temperature. The primary antibodies mouse glial fibrillary acidic protein (GFAP) (Sigma Aldrich, #G3893) at a dilution of 1:1000 and rabbit ionized calcium-binding adapter molecule 1 (Iba1) (Synaptic system, #234003) at a dilution of 1:500 were incubated with the brain sections overnight at 4 $^{\circ}\text{C}$. Following 3 washing steps with TBS-tween, sections were incubated with the secondary antibodies goat a-mouse Alexa Fluor 568 (Thermo Fisher Scientific, #A11004) or goat a-rabbit Alexa Fluor 488 (Thermo Fisher Scientific, #A11008), both diluted 1:1000. After a further 3 washing steps, sections were incubated with DAPI and then mounted using Vectashield antifade (Vectashield, Burlingame, USA).

Image and statistical analysis

16-bit images were captured using a Leica TCS SP5. Images were analysed using the Fiji software (v. 1.52i, NIH, USA (Schindelin, Arganda-Carreras et al. 2012)). The ME was defined using a drawn region of interest (ROI) and the average signal intensity for Iba1 and GFAP staining was measured. Furthermore, the number of Iba1 positive microglia

was manually counted within each ROI. All statistical analyses were conducted using the Prism 8 software (GraphPad Software, Inc. La Jolla, CA, USA). Two-tailed t-tests, One-way or Two-way ANOVAs with Tukey's post hoc tests were performed to test for statistical differences between treatment groups. P-values lower than 0.05 were considered significant. Significances were indicated as follows: * $p < 0.05$, ** $p < 0.01$, *** $p < 0.001$ or **** $p < 0.0001$. All results are presented as means \pm SEM.

Results

Cranial irradiation increases hypothalamic GFAP protein levels in male mice

Obesity was recently linked with increases in microglia and astrocyte activation, commonly referred to as microgliosis and astrocytosis (Thaler, Yi et al. 2012). Accordingly, we first tested whether an acute exposure to irradiation can cause a state of neuroinflammation similar as HFD-induced obesity. We found an increase in staining intensities for astrocyte marker GFAP in hypothalamic of male mice irradiated with 2 Gy compared to mice receiving 0.5 Gy ($p=0.016$) or Sham-treatment ($p=0.13$) (Fig. 1A, B). In

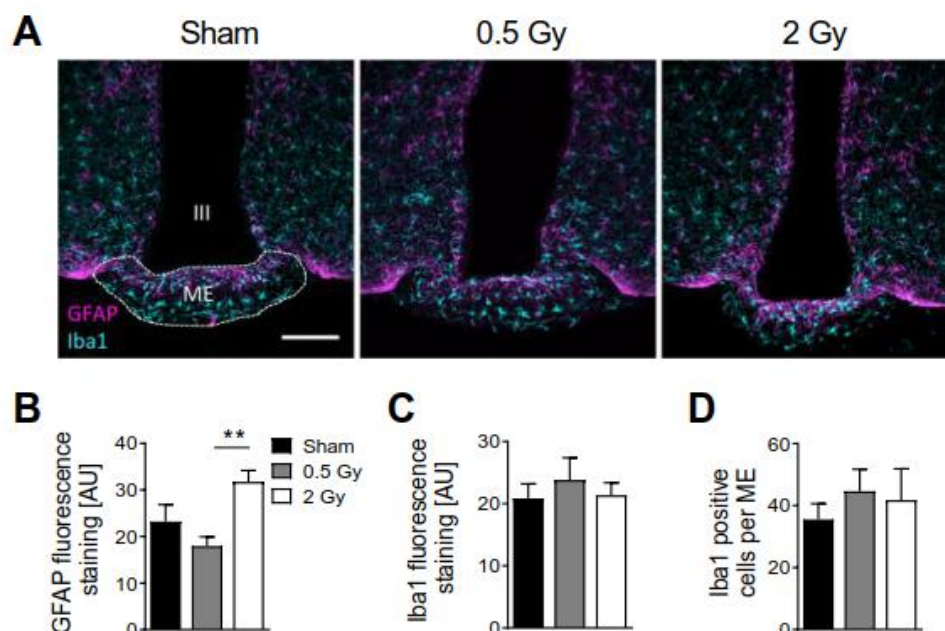


Figure 1: Immunohistochemical staining (A) for astrocytosis marker GFAP and microgliosis marker Iba1 in 7-week-old male and chow-fed C57Bl/6J mice one week after cranial irradiation with 0 (sham), 0.5 Gy or 2 Gy. (B) depicts fluorescence intensities for GFAP, (C) depicts fluorescence intensities for Iba1, (D) depicts the number of Iba1 positive cells. Means \pm SEM. One-Way ANOVA with Tukey post-hoc tests. * $p < 0.05$. Scale bar = 30 μ m.

contrast, we could not detect any alterations in staining intensities for Iba1 (Fig. 1A, C), or in Iba1-positive microglia cell numbers between groups (Fig. 1A, D).

Unperturbed metabolic homeostasis 10 weeks after cranial irradiation in male and female mice

We next aimed to interrogate the sub-chronic effects of childhood cranial irradiation at 0 (Sham), 0.5 or 2 Gy on body weight and energy metabolism in male chow-fed C57Bl/6J mice. Eight weeks after their irradiation at 6 weeks of age, we found unchanged body weight and body composition (Fig. 2 A, B). Moreover, indirect calorimetry revealed unperturbed food intake, nutrient preference and utilization, energy expenditure and locomotor activity between groups (Fig. 2C-F). Similarly, 8 weeks after female chow-fed C57Bl/6J mice received sham treatment or cranial irradiation at 6 weeks of age, we found unchanged body weights and body composition (Fig. 3A, B) and unperturbed food intake, respiratory quotients, energy expenditure, and locomotor activity (Fig. 3C-F) compared to sham controls.

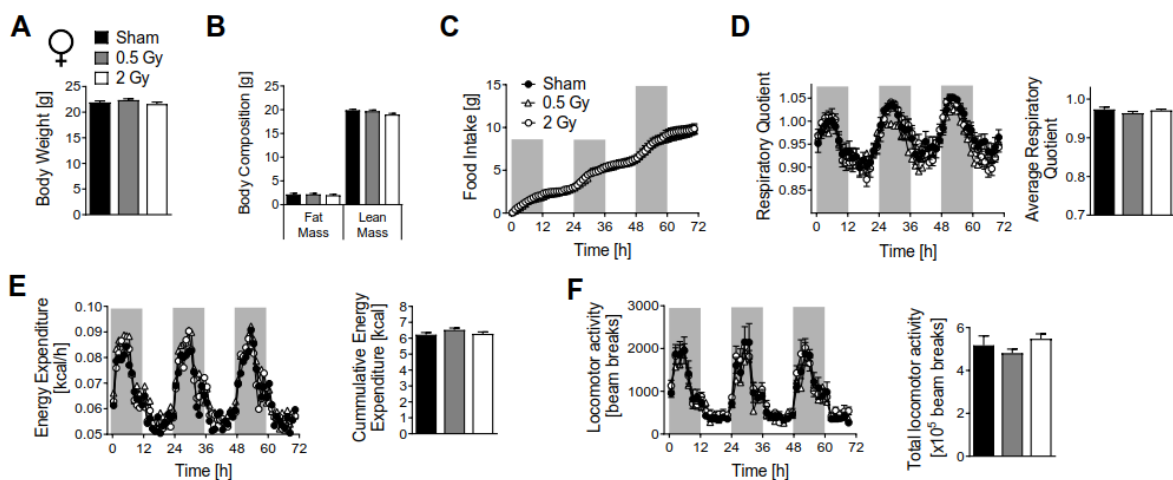


Figure 3: Metabolic phenotyping of 14-week-old female chow-fed C57Bl/6J mice that received 0 (sham), 0.5 or 2 Gy cranial irradiation at 6 weeks of age. Body weight (A), fat and lean mass (B), food intake (C), the respiratory quotient (D), energy expenditure (E) and locomotor activity (F) were unaffected by cranial irradiation. Means \pm SEM. N = 12 per group. A,B and right panels D,E,F: One-Way ANOVA with Tukey post-hoc tests. C and left panels D,E,F: Two-Way Repeated Measures ANOVA with Sidak's multiple comparison testing.

Cranial irradiation impairs leptin sensitivity in female mice

Prompted by a recent study that revealed hypothalamic leptin resistance after cranial irradiation with 60 Gy (14), we next subjected male and female mice to an additional leptin challenge test. In sham-treated female but not male mice, we revealed a clear

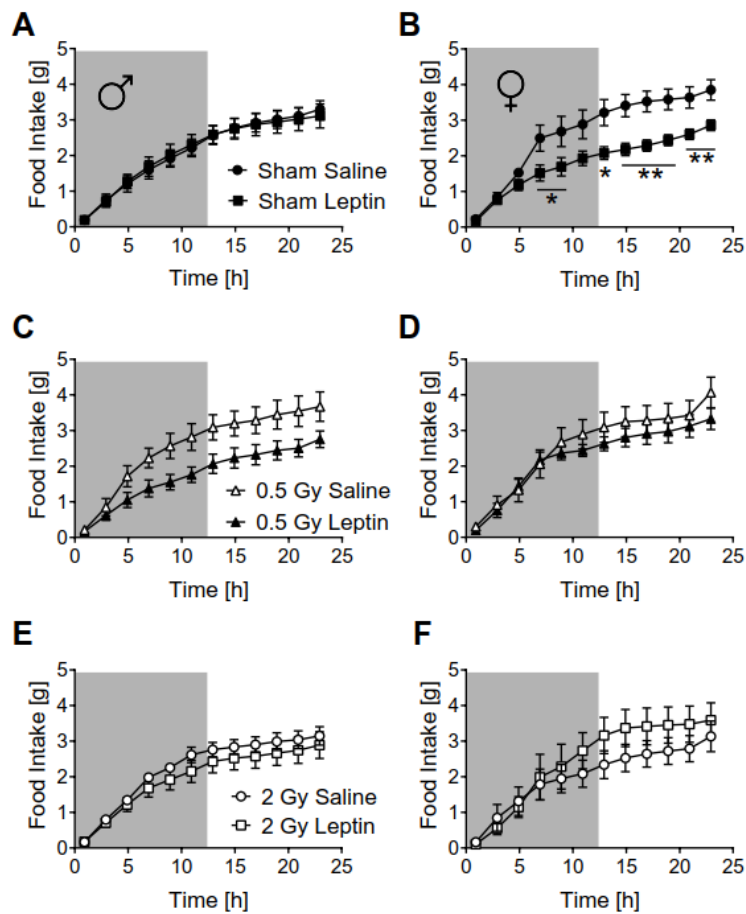


Figure 4: Leptin sensitivity test in 15-week-old male (A,C,E) and female (B,D,F) chow-fed C57Bl/6J mice 9 weeks after cranial irradiation with 0 (A,B; sham), 0.5 (C,D) or 2 (E,F) Gy. Mice received either vehicle or 3mg/kg leptin by a single intraperitoneal injection at the beginning of the dark phase, followed by a 24-hour-measurement of food intake. Means \pm SEM. N=5-6. Two-Way Repeated Measures ANOVA with Sidak's multiple comparison testing. * $p < 0.05$, ** $p < 0.01$.

reduction of food intake by leptin compared to saline controls (2-way ANOVA $F(1, 9) = 9.61$, $p = 0.012$) (Fig. 4A, B). However, after irradiation with 0.5 or 2 Gy, neither male (0.5 Gy: $F(1, 8) = 4.49$, $p = 0.066$ / 2 Gy: $F(1, 9) = 0.68$, $p = 0.428$) nor female (0.5 Gy: $F(1, 8) = 0.55$, $p = 0.477$ / 2 Gy: $F(1, 9) = 0.58$, $p = 0.463$) mice had significantly reduced food intake after injection of 5 mg/kg leptin, compared to vehicle controls (Fig. 4C-F). Overall, these data indicate leptin resistance in male mice regardless of irradiation. In contrast, sham-treated female mice are leptin sensitive, which is impaired after cranial irradiation.

Medium doses of cranial irradiation increase body adiposity in female mice

After revealing impaired leptin sensitivity in female mice 9 weeks after undergoing 2 Gy of cranial irradiation, we next aimed to reveal long-term metabolic consequences of low-to-moderate-dose cranial irradiation on body adiposity and glucose tolerance. A 2-year study cohort served as the basis for this study, with metabolic sampling points carried out at 3, 6, 12, 18 and 24 months' post irradiation, as depicted in the experimental paradigm (Fig. 5A). In the male mice, we did not observe differences in body weight (Fig. 5B) or mortality (Fig. 5C) between. Similarly, we observed no differences in fat or lean mass and glucose tolerance, displayed as glucose excursions (left panel) and area under the curve values (AUC) (right panel), in male mice 3, 6, 12 and 24 months after cranial irradiation or sham treatment (Fig. S1A-D & Fig. 5D,E,F,H,I). However, 18 months' post irradiation, 2 Gy irradiated males presented with a significant glucose intolerance (Fig. 5G). Following a further 6 months the glucose tolerance became less severe, however the AUC still indicated a mild intolerance ($p = 0.08$) (Fig 5I).

In female mice undergoing the chronic 2-year study paradigm (Fig. 6A), we observed an increase in body weight in 2 Gy treated mice compared to sham controls or mice receiving 0.5 Gy which reached significance 40 weeks after cranial irradiation (Fig. 6B). Shortly after the 12-month time point, the female mice further began to show increased mortality rates (Fig. 6C); although not reaching statistical significance, 67 % of the 2 Gy irradiated females had died by the 22-month time point compared to 42 % and 25 % in the sham or 0.5 Gy groups, respectively. Notably, while body composition and glucose tolerance remained unaffected 3 months after cranial irradiation (Fig. S2A), we observed increased fat mass in 2 Gy treated mice 6 months after cranial irradiation, compared to sham or 0.5 Gy treated mice (Fig. 6D). Glucose tolerance 6 months after the cranial irradiation was normal in all mice tested (Fig. 6E). Increases in fat mass after 2 Gy cranial irradiation and unperturbed glucose tolerance were further observed 12 months after cranial irradiation (Fig. S2C,D). Glucose tolerance and body composition was unchanged between groups 18 and 22 months' post irradiation (Fig. 6F-I). Moreover, 18 months after irradiation, the

female mice had unchanged fasting insulin and triglyceride levels, and no signs of insulin resistance (Fig. 7F-H).

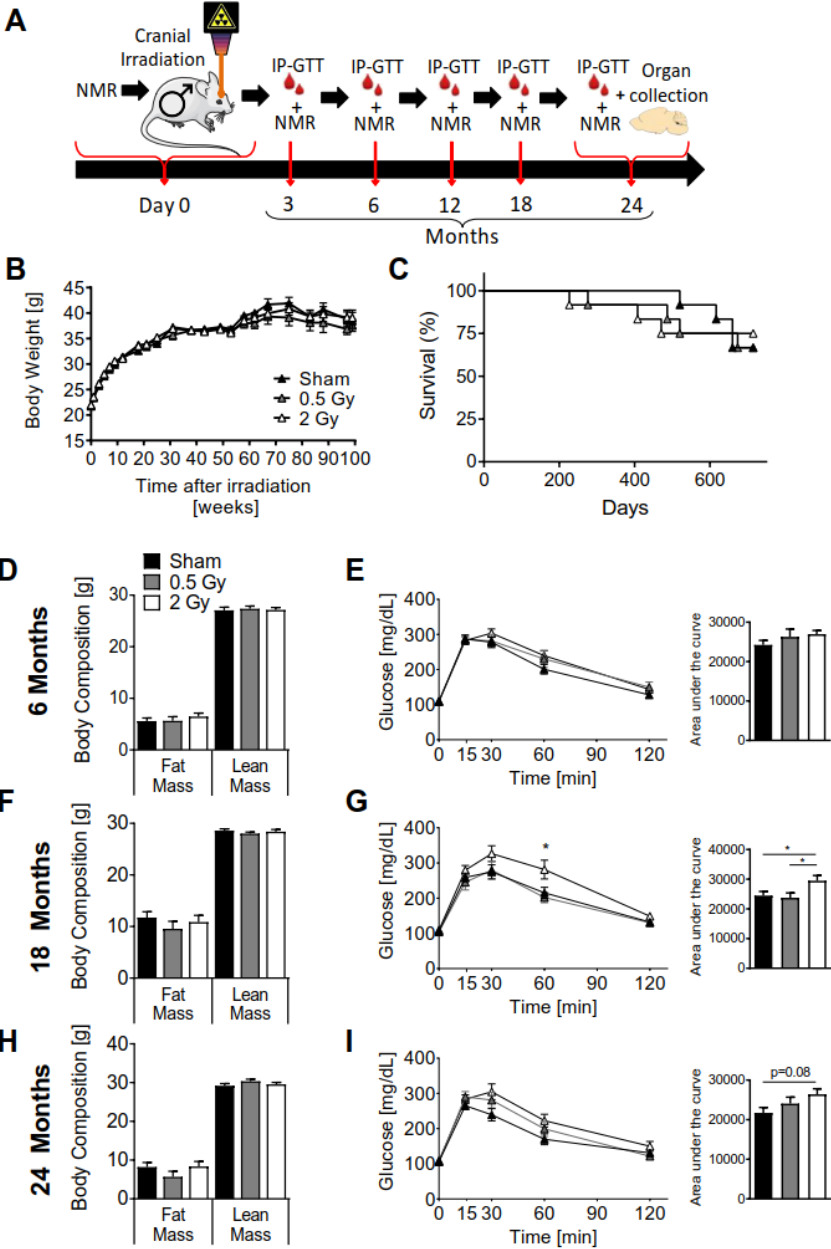


Figure 5: Long-term effects on body adiposity and glucose tolerance in male chow-fed C57Bl/6J mice undergoing 0 (sham), 0.5 or 2 Gy of cranial irradiation at 6 weeks of age. (A) depicts the experimental paradigm of the 2-year-study, (B) displays results on body weight. (C) Survival depicted as Kaplan-Meier plots. NMR-based body composition analyses and intraperitoneal glucose tolerance tests (2g glucose per kg body weight) were conducted 6 (D,E), 18 (F,G) and 24 (H,I) months after cranial irradiation. Means \pm SEM. N=9-12. B and left panels in E,G,I: Two-Way Repeated Measures ANOVA with Sidak's multiple comparison testing; D,F,H and right panels E,G,I: One-Way ANOVA with Tukey post-hoc tests. * $p < 0.05$.

Cranial irradiation induces age-onset perturbations of lipid metabolism

The liver is known to receive autonomic input from the hypothalamus, regulating lipid metabolism (Bruinstroop, Fliers et al. 2014). Indeed, impaired lipid metabolism is a major hallmark of high body adiposity. As cranial irradiation may induce damage to the

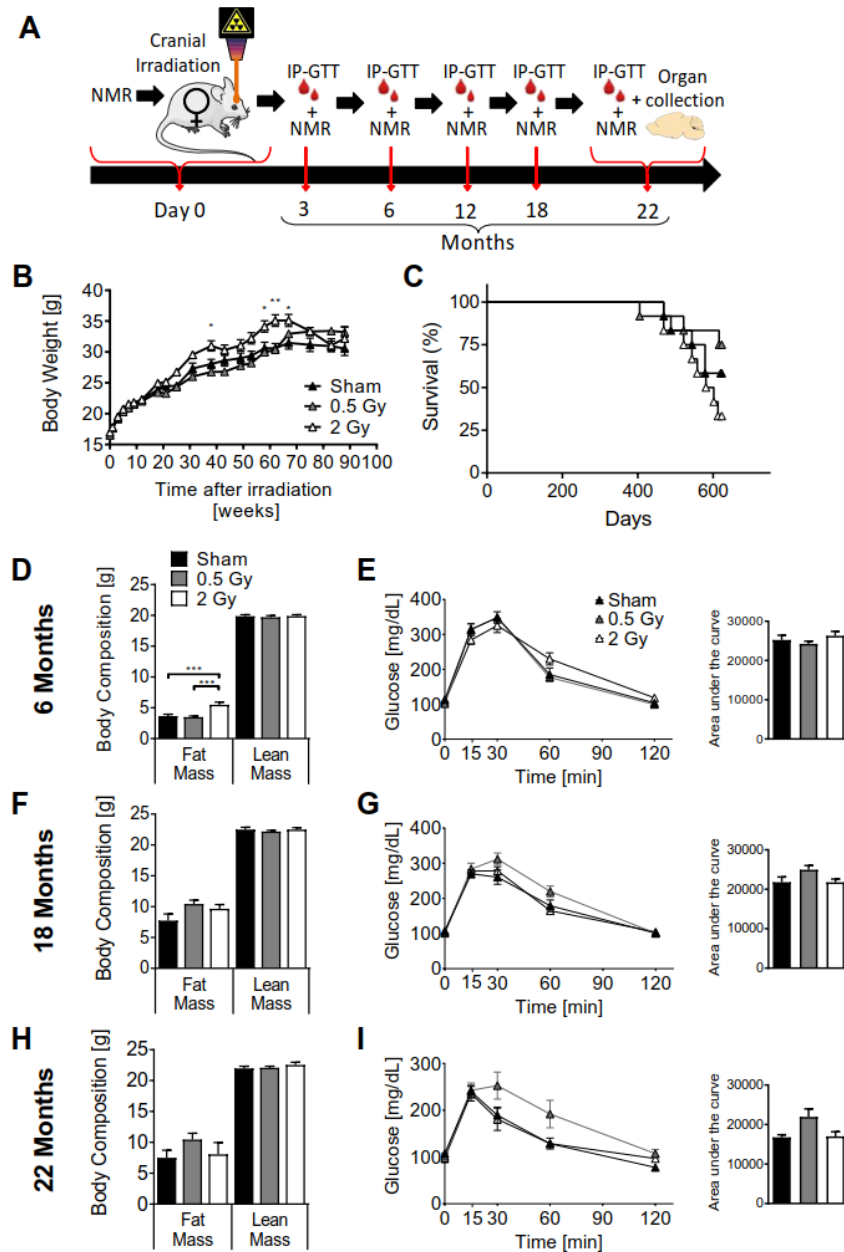


Figure 6: Long-term effects on body adiposity and glucose tolerance in female chow-fed C57Bl/6J mice undergoing 0 (sham), 0.5 or 2 Gy of cranial irradiation at 6 weeks of age. (A) depicts the experimental paradigm of the 2-year-study, (B) displays results on body weight. (C) Survival depicted as Kaplan-Meier plots. NMR-based body composition analyses and intraperitoneal glucose tolerance tests (2g glucose per kg body weight) were conducted 6 (D,E), 18 (F,G) and 24 (H,I) months after cranial irradiation. Means \pm SEM. N=9-12. B and left panels in E,G,I: Two-Way Repeated Measures ANOVA with Sidak's multiple comparison testing; D,F,H and right panels E,G,I: One-Way ANOVA with Tukey post-hoc tests. * p <0.05.

hypothalamus, thus impacting lipid distribution, we measured plasma V-LDL, LDL and HDL 18 months after irradiation. Lipid fractionation at this time point revealed increased V-LDL and decreased HDL in the 2 Gy group compared to the sham treated male and female mice (Fig. 7A,E). Furthermore, plasma analysis detected no differences in fasting triglycerides, insulin or insulin resistance as measured by HOMA-IR (Fig. 7B-D, F-H).

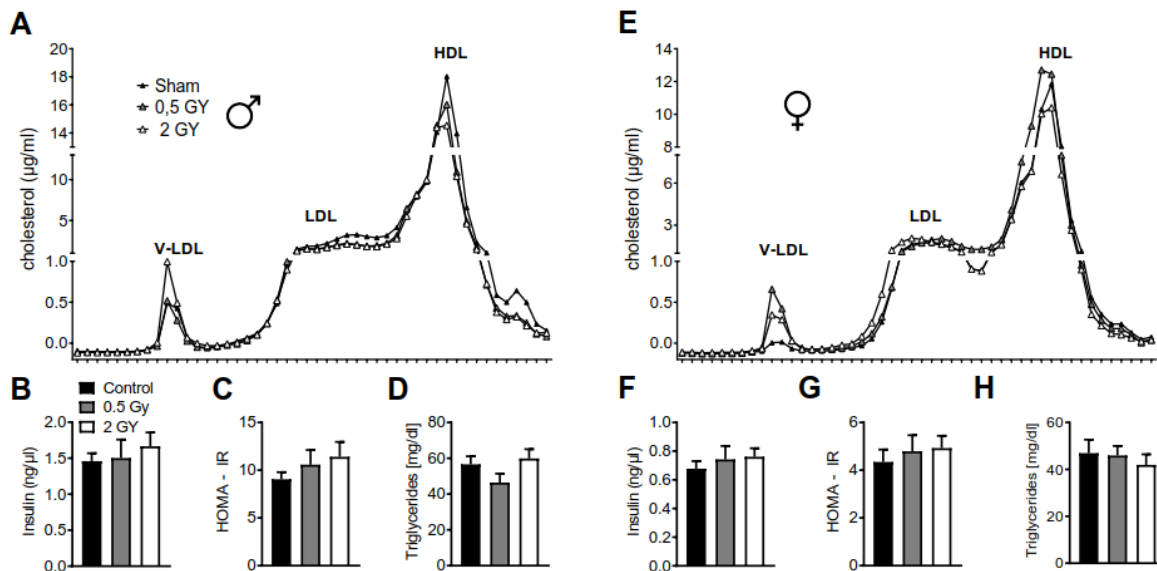


Figure 7: Plasma analysis performed 18 months' post irradiation treatment of either 0 (Sham), 0.5 or 2 Gy. (A,E) display lipid fractionation by FPLC and subsequent cholesterol measurement. Fractions are denoted as either V-LDL, LDL or HDL fractions. Fasting plasma analyses of insulin, triglycerides and HOMA-IR calculation are shown in (B,F), (D,H) and (C,G) respectively. N = 7-10. (A,E depict the FPLC of pooled sample sets. B-D and F-H: One-Way ANOVA with Tukey post-hoc tests. N = 7-10. Means \pm SEM.

Discussion

Childhood cancer survivors are at risk of becoming obese and developing the MetS (Meacham, Sklar et al. 2009, Pearce, Salotti et al. 2012). This may be due to the high doses of cranial irradiation they received as part of the cancer treatment, however the underlying evidence is lacking. Importantly, it is also currently unknown whether or not more moderate doses may result in a similar effect. To find out more, we subjected mice to moderate (2 Gy) and low (0.5 Gy) doses of cranial irradiation and performed a long term metabolic analysis. Overall we found increased hypothalamic astrocytosis, glucose

intolerance and altered V-LDL and HDL levels in male mice. Female mice developed leptin resistance as well as an increase in body weight.

In the present study, we found evidence of increased hypothalamic astrocytosis in male mice subjected to 2 Gy cranial irradiation directed towards the hypothalamus. The activation of astrocytes and microglia in the hypothalamus has previously been demonstrated in diet induced obesity (DIO) (Thaler, Yi et al. 2012, Berkseth, Guyenet et al. 2014, Baufeld, Osterloh et al. 2016) and in response to weight loss (Harrison, Pfuhlmann et al. 2019). Although we did not note increased body weight in male mice following 2 Gy irradiation, our findings of astrocytosis are in agreement with the literature. A single 8 Gy dose of cranial irradiation in 14 day old male C57BL/6 mice was sufficient to induce microglial activation in the corpus callosum 4 months post treatment (Roughton, Boström et al. 2013). Accordingly, acute effects only 6 h after a dose of 6 Gy cranial irradiation resulted in increased microglial activation in the hypothalamus of 11 day old female rats (Xu, Sun et al. 2018). In the same study the authors showed that hypothalamic astrocytes were also activated compared to sham controls (Xu, Sun et al. 2018). Thus, we can conclude that even moderate doses of cranial irradiation are sufficient to induce astrocytosis in the hypothalamus, whereas microglial RG may require slightly higher doses of at least 6 Gy. However, the implications of irradiation induced RG in terms of metabolic control remain unanswered.

Childhood cancer survivors are at risk to develop obesity later in life as a result of high dosed cranial irradiation (Garmey, Liu et al. 2008). Our findings using low-moderate dosed cranial irradiation could partially recapitulate this, as we noted similar effects in female, but not male mice. The sex-dependent effects revealed here share similarities to other previous rodent based irradiation studies (both of which treated mice with a single dose of 6 Gy), which also could not find increased body weight in males (Zhou, Bostrom et al. 2017), but could in females (Xu, Sun et al. 2018). It appears that following cranial irradiation, a certain time period is required for weight gain to develop. In our study, we could detect a significant weight increase only after 10 months. Despite higher doses of cranial irradiation (8 Gy), others were not able to induce weight gain within 4 months (Roughton, Boström et al. 2013), suggesting that the latency period is not dependent on radiation dose. This is in line with our observation, that within 2 months following radiation treatment, no metabolic changes could be detected.

Moreover, total body irradiation studies differ in their outcomes compared to cranial irradiation. Total body irradiation of young (7 week old) female mice using a dose of 5 Gy was not able to induce body weight changes after 12 months of monitoring (Zhang, Yang et al. 2017). Furthermore, in agreement with our data, applying 0.5 Gy total body irradiation to adolescent (10 week old) female mice did not induce changes in body weight following 2 years of measurements (Dalke, Neff et al. 2018).

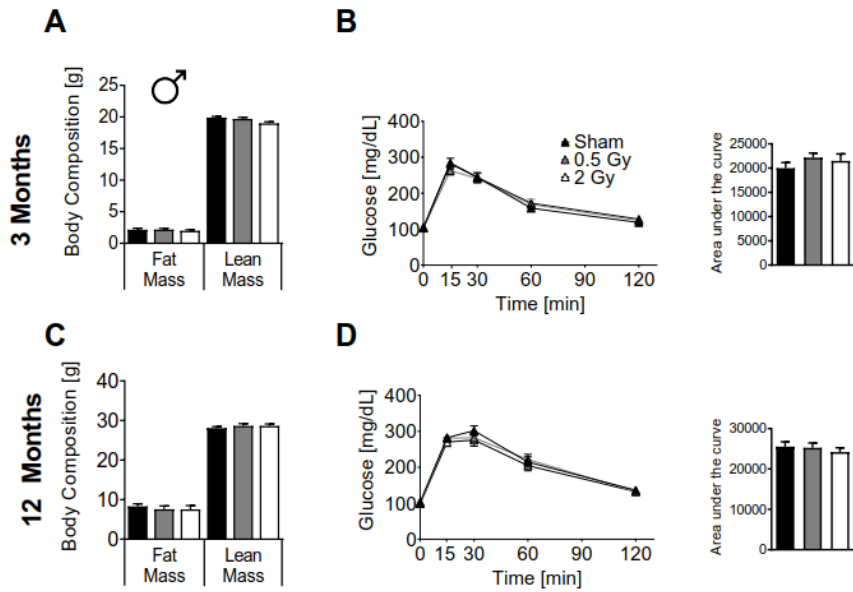
In contrast, a study that included over 700 female mice and 4 different doses of total body irradiation (0 (sham), 3, 4 and 5 Gy) revealed that all irradiated mice were significantly heavier, already 50 days after treatment (Babbitt, Kharazi et al. 2001), significantly faster than in other studies. One explanation for this may be the irradiation scheme used in the study, which did not consist of a single dose, as in the previous studies, but rather was administered in 4 separate equal fractions over the period of 4 weeks. Fractionated irradiation is often used to treat tumours more effectively as the relative biological effect is higher, but with lower irradiation doses (Kim, Cho et al. 2011).

Taken together, it would seem that total body irradiation studies differ in their outcomes compared to those directing the irradiation directly to the brain. Nonetheless, several studies support our findings of increased body weight in females following low-moderate doses of irradiation (Babbitt, Kharazi et al. 2001, Nakamura, Tanaka et al. 2010, Xu, Sun et al. 2018).

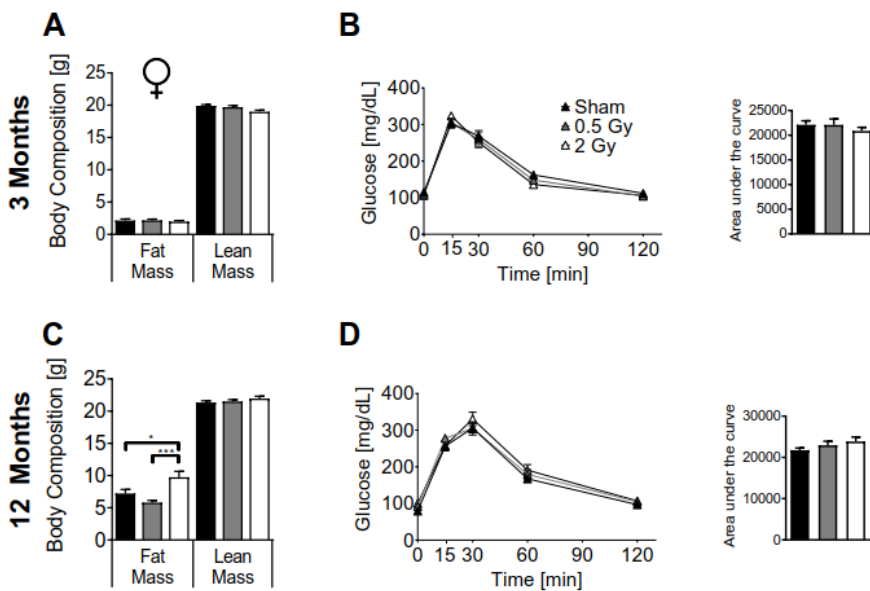
Studies reporting the effects of moderate dose irradiation on more specific metabolic parameters such as insulin sensitivity, glucose tolerance and blood lipid profiles are limited to a single study. The authors showed that 20 weeks after 6 Gy of radiation to the brain female rats developed glucose intolerance, increased fasting insulin, insulin resistance (HOMA-IR), decreased insulin receptor expression, increased leptin levels and increased plasma triglycerides (Xu, Sun et al. 2018). In the present work, we measured glucose tolerance over a period of 2 years following low-moderate doses of cranial irradiation. Interestingly, although only the female mice gained weight, it was in the male mice that we noted a decrease in glucose tolerance. When treated with a higher dose (6 Gy) of cranial irradiation, female rats developed glucose intolerance after 20 weeks (Xu, Sun et al. 2018). Indeed, further traits of the MetS, such as increased fasting insulin, insulin resistance, hyperleptinemia and increased triglycerides were also visible in these rats. Plasma cholesterol, HDL and LDL levels remained unchanged (Xu, Sun et al. 2018). This

differs to our findings, as we see unaltered plasma insulin and triglycerides, as well as normal insulin sensitivity. Also differing from Xu et. al., we show increased V-LDL and decreased HDL in both male and female 2 Gy irradiated groups, suggesting a dysregulation in lipid metabolism. As the hypothalamus is known to modulate hepatic glucose and lipid metabolism, damage to this region may be the underlying cause for shifts in lipid balance. When activated, neuropeptide Y (NPY) neurons in the arcuate nucleus of the hypothalamus (ARC) signal to second order neurons, and ultimately to the liver, increasing hepatic V-LDL secretion (Stafford, Yu et al. 2008). Indeed, damage to the hypothalamus or modulation of NPY neuron signalling could explain the imbalance in circulating lipids, which is an indication of insulin resistance and a developing type 2 diabetes (Bitzur, Cohen et al. 2009). It would seem then that although there are notable discrepancies between the studies, the higher dose of 6 Gy results in more prominent metabolic irregularities.

Overall, there is evidence to show that low to moderate doses of cranial irradiation may be a risk factor for developing the MetS. Although the hypothalamus remains a prime suspect for the responsible brain region, further studies are required to verify this claim. Ideally these would make use of modern irradiation equipment such as the small animal radiation research platform (SARRP), which would allow for a precise irradiation of the hypothalamus without the surrounding regions receiving significant doses. These studies could provide as important information for the risk-management of those patients receiving even low doses of irradiation to the brain.



Supplementary Figure 1: Long-term effects on body adiposity and glucose tolerance in male chow-fed C57Bl/6J mice undergoing 0 (sham), 0.5 or 2 Gy of cranial irradiation at 6 weeks of age. NMR-based body composition analyses and intraperitoneal glucose tolerance tests (2g glucose per kg body weight) were conducted 3 (A,B) and 12 (C,D) months after cranial irradiation. Means \pm SEM. N=9-12. B and D: Two-Way Repeated Measures ANOVA with Sidak's multiple comparison testing; A, C and right panels B and D: One-Way ANOVA with Tukey post-hoc tests.



Supplementary Figure 2: Long-term effects on body adiposity and glucose tolerance in female chow-fed C57Bl/6J mice undergoing 0 (sham), 0.5 or 2 Gy of cranial irradiation at 6 weeks of age. NMR-based body composition analyses and intraperitoneal glucose tolerance tests (2g glucose per kg body weight) were conducted 3 (A,B) and 12 (C,D) months after cranial irradiation. Means \pm SEM. N=9-12. B and D: Two-Way Repeated Measures ANOVA with Sidak's multiple comparison testing; A, C and right panels B and D: One-Way ANOVA with Tukey post-hoc tests. * $p < 0.05$, *** $p < 0.001$.

References

- Babbitt, J. T., A. I. Kharazi, J. M. G. Taylor, C. B. Bonds, D. Zhuang, S. G. Mirell, E. Frumkin and T. J. Hahn (2001). "Increased body weight in C57BL/6 female mice after exposure to ionizing radiation or 60Hz magnetic fields." International Journal of Radiation Biology **77**(8): 875-882.
- Baufeld, C., A. Osterloh, S. Prokop, K. R. Miller and F. L. Heppner (2016). "High-fat diet-induced brain region-specific phenotypic spectrum of CNS resident microglia." Acta Neuropathologica **132**(3): 361-375.
- Berkseth, K. E., S. J. Guyenet, S. J. Melhorn, D. Lee, J. P. Thaler, E. A. Schur and M. W. Schwartz (2014). "Hypothalamic gliosis associated with high-fat diet feeding is reversible in mice: a combined immunohistochemical and magnetic resonance imaging study." Endocrinology **155**(8): 2858-2867.
- Bitzur, R., H. Cohen, Y. Kamari, A. Shaish and D. Harats (2009). "Triglycerides and HDL Cholesterol." Stars or second leads in diabetes? **32**(suppl 2): S373-S377.
- Brenner, D., C. Elliston, E. Hall and W. Berdon (2001). "Estimated risks of radiation-induced fatal cancer from pediatric CT." AJR Am J Roentgenol **176**(2): 289-296.
- Bruinstroop, E., E. Fliers and A. Kalsbeek (2014). "Hypothalamic control of hepatic lipid metabolism via the autonomic nervous system." Best Practice & Research Clinical Endocrinology & Metabolism **28**(5): 673-684.
- Dalke, C., F. Neff, S. K. Bains, S. Bright, D. Lord, P. Reitmeir, U. Rößler, D. Samaga, K. Unger, H. Braselmann, F. Wagner, M. Greiter, M. Gomolka, S. Hornhardt, S. Kunze, S. J. Kempf, L. Garrett, S. M. Hölter, W. Wurst, M. Rosemann, O. Azimzadeh, S. Tapio, M. Aubele, F. Theis, C. Hoeschen, P. Slijepcevic, M. Kadhim, M. Atkinson, H. Zitzelsberger, U. Kulka and J. Graw (2018). "Lifetime study in mice after acute low-dose ionizing radiation: a multifactorial study with special focus on cataract risk." Radiation and Environmental Biophysics **57**(2): 99-113.
- Fetcko, K., R. V. Lukas, G. A. Watson, L. Zhang and M. Dey (2017). "Survival and complications of stereotactic radiosurgery: A systematic review of stereotactic radiosurgery for newly diagnosed and recurrent high-grade gliomas." Medicine **96**(43): e8293-e8293.
- Garmey, E. G., Q. Liu, C. A. Sklar, L. R. Meacham, A. C. Mertens, M. A. Stovall, Y. Yasui, L. L. Robison and K. C. Oeffinger (2008). "Longitudinal changes in obesity and body mass index among adult survivors of childhood acute lymphoblastic leukemia: a report from the Childhood Cancer Survivor Study." J Clin Oncol **26**(28): 4639-4645.
- Halasz, L. M. and J. K. Rockhill (2013). "Stereotactic radiosurgery and stereotactic radiotherapy for brain metastases." Surgical neurology international **4**(Suppl 4): S185-S191.
- Harrison, L., K. Pfuhlmann, S. C. Schriever and P. T. Pfluger (2019). "Profound weight loss induces reactive astrogliosis in the arcuate nucleus of obese mice." Molecular Metabolism.

Hess, E. P., L. R. Haas, N. D. Shah, R. J. Stroebel, C. R. Denham and S. J. Swensen (2014). "Trends in computed tomography utilization rates: a longitudinal practice-based study." J Patient Saf **10**(1): 52-58.

Hofmann, S. M., D. Perez-Tilve, T. M. Greer, B. A. Coburn, E. Grant, J. E. Basford, M. H. Tschöp and D. Y. Hui (2008). "Defective lipid delivery modulates glucose tolerance and metabolic response to diet in apolipoprotein E-deficient mice." Diabetes **57**(1): 5-12.

Kim, Y. J., K. H. Cho, J. Y. Kim, Y. K. Lim, H. S. Min, S. H. Lee, H. J. Kim, H. S. Gwak, H. Yoo and S. H. Lee (2011). "Single-dose versus fractionated stereotactic radiotherapy for brain metastases." Int J Radiat Oncol Biol Phys **81**(2): 483-489.

Laaksonen, D. E., H. M. Lakka, L. K. Niskanen, G. A. Kaplan, J. T. Salonen and T. A. Lakka (2002). "Metabolic syndrome and development of diabetes mellitus: application and validation of recently suggested definitions of the metabolic syndrome in a prospective cohort study." Am J Epidemiol **156**(11): 1070-1077.

Lax, I. (1993). "Target Dose Versus Extratarget Dose in Stereotactic Radiosurgery." Acta Oncologica **32**(4): 453-457.

Meacham, L. R., C. A. Sklar, S. Li, Q. Liu, N. Gimpel, Y. Yasui, J. A. Whitton, M. Stovall, L. L. Robison and K. C. Oeffinger (2009). "Diabetes mellitus in long-term survivors of childhood cancer. Increased risk associated with radiation therapy: a report for the childhood cancer survivor study." Arch Intern Med **169**(15): 1381-1388.

Miller, T. L., S. R. Lipsitz, G. Lopez-Mitnik, A. S. Hinkle, L. S. Constine, M. J. Adams, C. French, C. Proukou, A. Rovitelli and S. E. Lipshultz (2010). "Characteristics and determinants of adiposity in pediatric cancer survivors." Cancer Epidemiol Biomarkers Prev **19**(8): 2013-2022.

Nakamura, S., I. B. Tanaka, 3rd, S. Tanaka, K. Nakaya, N. Sakata and Y. Oghiso (2010). "Adiposity in female B6C3F1 mice continuously irradiated with low-dose-rate gamma rays." Radiat Res **173**(3): 333-341.

Pearce, M. S., J. A. Salotti, M. P. Little, K. McHugh, C. Lee, K. P. Kim, N. L. Howe, C. M. Ronckers, P. Rajaraman, A. W. Sir Craft, L. Parker and A. Berrington de González (2012). "Radiation exposure from CT scans in childhood and subsequent risk of leukaemia and brain tumours: a retrospective cohort study." Lancet (London, England) **380**(9840): 499-505.

Pfuhmann, K., S. C. Schriever, P. Baumann, D. G. Kabra, L. Harrison, S. E. Mazibuko-Mbeje, R. E. Contreras, E. Kyriakou, S. E. Simonds, T. Tiganis, M. A. Cowley, S. C. Woods, M. Jastroch, C. Clemmensen, M. De Angelis, K. W. Schramm, M. Sattler, A. C. Messias, M. H. Tschöp and P. T. Pfluger (2018). "Celastrol-Induced Weight Loss Is Driven by Hypophagia and Independent From UCP1." Diabetes **67**(11): 2456-2465.

Roughton, K., M. Boström, M. Kalm and K. Blomgren (2013). "Irradiation to the young mouse brain impaired white matter growth more in females than in males." Cell Death & Disease **4**: e897.

Schindelin, J., I. Arganda-Carreras, E. Frise, V. Kaynig, M. Longair, T. Pietzsch, S. Preibisch, C. Rueden, S. Saalfeld, B. Schmid, J.-Y. Tinevez, D. J. White, V. Hartenstein, K. Eliceiri, P.

Tomancak and A. Cardona (2012). "Fiji: an open-source platform for biological-image analysis." Nat Meth **9**: 676-682.

Stafford, J. M., F. Yu, R. Printz, A. H. Hasty, L. L. Swift and K. D. Niswender (2008). "Central Nervous System Neuropeptide Y Signaling Modulates VLDL Triglyceride Secretion." Diabetes **57**(6): 1482-1490.

Thaler, J. P., C. X. Yi, E. A. Schur, S. J. Guyenet, B. H. Hwang, M. O. Dietrich, X. Zhao, D. A. Sarruf, V. Izgur, K. R. Maravilla, H. T. Nguyen, J. D. Fischer, M. E. Matsen, B. E. Wisse, G. J. Morton, T. L. Horvath, D. G. Baskin, M. H. Tschoop and M. W. Schwartz (2012). "Obesity is associated with hypothalamic injury in rodents and humans." J Clin Invest **122**(1): 153-162.

Timper, K. and J. C. Bruning (2017). "Hypothalamic circuits regulating appetite and energy homeostasis: pathways to obesity." Dis Model Mech **10**(6): 679-689.

van Waas, M., S. J. Neggers, A. G. Uitterlinden, K. Blijdorp, I. M. van der Geest, R. Pieters and M. M. van den Heuvel-Eibrink (2013). "Treatment factors rather than genetic variation determine metabolic syndrome in childhood cancer survivors." Eur J Cancer **49**(3): 668-675.

Woods, S. C., M. W. Schwartz, D. G. Baskin and R. J. Seeley (2000). "Food Intake and the Regulation of Body Weight." Annual Review of Psychology **51**(1): 255-277.

Xu, Y., Y. Sun, K. Zhou, T. Li, C. Xie, Y. Zhang, J. Rodriguez, Y. Wu, M. Hu, L. R. Shao, X. Wang and C. Zhu (2018). "Cranial Irradiation Induces Hypothalamic Injury and Late-Onset Metabolic Disturbances in Juvenile Female Rats." Dev Neurosci **40**(2): 120-133.

Zhang, S. B., S. Yang, Z. Zhang, A. Zhang, M. Zhang, L. Yin, K. Casey-Sawicki, S. Swarts, S. Vidyasagar, L. Zhang and P. Okunieff (2017). "Thoracic gamma irradiation-induced obesity in C57BL/6 female mice." International Journal of Radiation Biology **93**(12): 1334-1342.

Zhou, K., M. Bostrom, C. J. Ek, T. Li, C. Xie, Y. Xu, Y. Sun, K. Blomgren and C. Zhu (2017). "Radiation induces progenitor cell death, microglia activation, and blood-brain barrier damage in the juvenile rat cerebellum." Sci Rep **7**: 46181.

5. Summary of key findings

The overall aim of this thesis was to deepen our understanding of the phenomenon known as leptin resistance. The cause of leptin resistance remains unknown, but several hypotheses exist in the literature.

In the first part of this thesis, the theory that leptin resistance is caused by a defect in leptin transport across the BBB was tested. Overall, it was shown that although leptin transport is a dynamic process that can be regulated, it does not appear to be defective in leptin resistant mice, and thus is most unlikely as an underlying cause of leptin resistance.

Second, it was evaluated how chronic obesity and weight loss regimes may impact reactive gliosis, which is a further possible contributor to leptin resistance. Here, the results revealed that in chronic obesity due to HFD feeding, RG is no longer increased. Furthermore, the act of acute, extensive weight loss resulted in an increase of hypothalamic astrogliosis in the ARC.

Finally, this thesis aimed to investigate the effects of low-to-medium dosed cranial irradiation as a risk factor for the metabolic syndrome, including leptin sensitivity and reactive gliosis. The findings revealed that moderately-dosed CrI resulted in a late-onset weight gain and failure to respond to leptin, that was limited to females. Additionally, male mice presented with an acute astrogliosis following 2 Gy irradiation and glucose intolerance 18 months after the irradiation. Overall mortality remained largely unaltered.

6. Discussion and future perspectives

Obesity and being overweight has developed into a global health issue that affects over close to 2 billion people (WHO 2018). Losing excess weight is a process that is difficult and in most cases treatment comes in the form of life style interventions such as diet management combined with physical activity (Wirth et al. 2014). These interventions are however often unsuccessful due to a plethora of potential reasons ranging from underlying genetic causes (Yeo et al. 1998) to social interaction and behavioural aspects (Patel and Schlundt 2001). Understanding the underlying causes of obesity is then of utmost importance as the search for cures and remedies for this disease remain scarce. For over 25 years, leptin resistance has been suggested as an underlying cause for obesity, yet our understanding of leptin resistance and the molecular underpinnings of the syndrome as such remain unclear. This piece of work has explored several physiological situations that are either related to, or may themselves be the underlying cause of leptin resistance. In addition to the individual discussions presented in the research articles, this section will further consider how the presented findings may be interpreted, integrated and compared to the existing literature.

6.1. Leptin transport across the BBB and our understanding of leptin resistance

The discovery that the leptin receptor is highly expressed in various regions of the brain (Couce et al. 1997), including those that were known to play key roles in energy homeostasis (Brobeck 1946) provided the first evidence that the brain is one of leptin's targets in the body. To reach these regions however, leptin needs to cross the BBB. Leptin, being 16 kDa in size cannot achieve this passively and thus must be actively transported via a specific transporter. The first indication that leptin transport may be defective in a state of leptin resistance came from the Banks lab in 1999. With the use of radio-labelled leptin they showed that brain/serum ratio was declined in DIO male CD-1 mice (Banks et al. 1999). This was supported by the fact that previous studies in obese humans had revealed a decreased CSF/serum leptin ratio. Further studies from the Banks lab built on these initial findings to show that triglycerides were able to induce a reduction in leptin transport, again as measured by brain/serum concentrations (Banks et al. 2004). An

aspect that is critical to these studies however is that a decreasing brain/serum ratio would only indicate a decrease in leptin transport if the transport system would increase linearly with increasing serum levels. There is no evidence at present that would suggest that this is the case. Moreover, it is perhaps conceivable that an upper limit to leptin transport may indeed be beneficial as unregulated leptin accumulation in the CSF may prove detrimental. For example, increased insulin CSF concentrations were associated with a decreased cognition and an increased risk for Alzheimer's disease (Geijselaers et al. 2017). A further limitation of the Banks studies is the method of leptin detection. As leptin is detected in the whole brain, there is no exclusivity to the leptin responsive brain regions. Thus, detection of leptin in unresponsive regions may not support findings in regard to leptin resistance.

More recently a further study once again presented data supporting the hypothesis that leptin transport was reduced in obesity. Here the authors used microdissections of the brain to then detect leptin protein, which was significantly reduced in the MBH of DIO mice (Balland et al. 2014). In particular, it is these most recent results that were surprising as they are in direct contradiction with the results presented in this thesis, which suggest that leptin transport is unaltered in obesity. This is even more so as the dissection and protein detection methods used were indeed very similar (Harrison et al. 2018). Using fluorescently labelled leptin offered a further, as yet undescribed method, which supported the findings by the current work (Harrison et al. 2018). The discrepancy between these studies may be due to subtle experimental design differences such as period of HFD feeding, age of the mice or washing and handling of the dissected tissue prior to analysis. One could claim that in the present study, samples may be contaminated and thus show identical leptin amounts for both lean and DIO mice. However, as the CR and EX4 weight loss groups showed an increase in leptin accumulation in the MBH, it is unlikely that a contamination is the cause. The fact that the increase in accumulation seen in these groups correlated with LepR expression in the choroid plexus suggest that the dynamic leptin accumulation observed is genuine. A study published around the time of the present work provided vital new information to the hypothesis in question. Kleinert and colleagues made use of a novel micro-perfusion technique, which allowed for the direct sampling of interstitial fluid from the MBH at various time points (Kleinert et al. 2018). This new method provided a further way by which leptin transport had been measured, but included a kinetic aspect which was lacking in previous models.

Interestingly, the researchers could show that the leptin transport kinetics were identical for lean and DIO mice (Kleinert et al. 2018), which is in line with findings presented here (Harrison et al. 2018).

Intranasal administration of peptide hormones has been used previously in humans as an alternative method when peripheral applications have remained unsuccessful or when systemic effects were undesirable (Benedict et al. 2004, Jauch-Chara et al. 2012, Heni et al. 2014). Studies with intranasal leptin have unveiled interesting results regarding leptin transport across the BBB. The first study to appear revealed that when lean and obese rats were treated with intranasal leptin, in contrast to peripheral leptin administration, it caused the animals to reduce their food intake and lose weight (Schulz et al. 2012). The authors also showed that this was not due to peripheral leakage of leptin, as plasma concentrations were the same as those treated with saline (Schulz et al. 2012). This year a second study was published that treated DIO mice with intranasal leptin and could replicate the findings by Schulz and colleagues. Although the study was not directly targeted towards metabolism, rather obesity related airway obstruction, the authors also checked the hypothalamus and medulla for leptin signalling and could clearly show an increase in pSTAT3 induction via intranasal treatment, but not peripheral (Berger et al. 2019). Similar to the previous study, the leptin plasma concentrations were unaffected by intranasal leptin. Together these studies suggest that intranasal leptin treatment is capable of circumventing the typical lack of response seen in peripherally treated DIO animals.

Although it is currently thought that leptin is transported via the LepR in the choroid plexus (Devos et al. 1996, Couce et al. 1997, Berislav et al. 2000, Peiser et al. 2000, Harrison et al. 2018) and tanycytes of the third ventricle (Balland et al. 2014), the latter has been questioned by a recent study (Yoo et al. 2019). Yoo and colleagues used single molecule fluorescent *in situ* hybridisation to reveal that hypothalamic tanycytes do not express LepR. Furthermore, the specific LepR deletion in tanycytes did not affect leptin mediated pSTAT3 signalling in the hypothalamus, regardless of whether it was administered intraperitoneal or ICV (Yoo et al. 2019). Thus, tanycyte involvement remains questionable and further studies are called for in this regard.

Despite a large effort from the scientific community it appears that whether or not leptin transport plays a role in leptin resistance cannot be confidently answered with a “yes” or

“no”. The fact that leptin resistant DIO mice appear to show no difference in leptin accumulation (Harrison et al. 2018) or dynamics (Kleinert et al. 2018) would suggest that leptin transport is not an underlying cause for leptin resistance. However when leptin is administered intranasally, which circumvents the BBB, leptin signalling is robustly activated (Schulz et al. 2012, Berger et al. 2019). An important piece of information regarding the definition of leptin resistance may shed some light on this confusing situation.

Leptin resistance is often defined as the inability of high circulating, or exogenously administered leptin to decrease food intake, or induce pSTAT3 in the ARC (Myers et al. 2010). However, the levels of pSTAT3 are often represented in the form of a fold increase after leptin injection, compared to saline injected levels. Critically, DIO mice already present a basal increase in pSTAT3 due to the elevated circulating leptin concentrations and thus will naturally tend towards a lower fold increase after exogenous leptin. This can be nicely seen in the current study (Harrison et al. 2018) in figure 5A, where HFD mice show increased endogenous pSTAT3 when compared to the chow group, but has also been shown by others (Martin et al. 2006, Ottaway et al. 2015). A key study revealed that endogenous leptin was indeed fully functional in DIO leptin resistant mice (Ottaway et al. 2015). Utilising a leptin receptor antagonist, the authors showed how leptin signalling inhibition in DIO mice results in weight gain (Ottaway et al. 2015). This clearly illustrates that endogenous leptin signalling is functional in leptin resistant mice.

Taken together, it would seem then that endogenous leptin is fully functional, yet not sufficient to reduce food intake or drive weight loss during obesity. It is perhaps then unsurprising that additional peripherally administered leptin also fails to do so. Intranasal leptin is however capable of doing just this. It is plausible that intranasal leptin acts not just on the hypothalamus to drive down food intake, but also in additional brain regions, which have yet to be examined in this context. Nevertheless, the term leptin resistance is perhaps not suitable to describe the phenomenon, as it suggests a lack in response, which has been shown not to be the case.

6.2. Reactive gliosis in obesity

Glia cells are the most numerous cell type within the brain. They were once described as being only simplistic non-functional cells that act as the glue for more complex cell types

such as neurons. Years of research have now clearly demonstrated that glia perform critical tasks that are vital to the maintenance of tissue homeostasis and normal brain function (Jäkel and Dimou 2017). Their role in energy homeostasis first became apparent when they were shown to sense glucose and as a result modulate systemic glucose production (Chari et al. 2011). Since then the glial cells role in metabolic control has been further solidified by a number of key publications examining sensitivity towards other signals such as insulin (Garcia-Caceres et al. 2016), leptin (Cheunsuang and Morris 2005), ghrelin (Fuente-Martin et al. 2016), insulin-like growth factor 1 (Cardona-Gomez et al. 2000) and thyroid hormones (Dezonne et al. 2015). When glial cells such as astrocytes and microglia sense inflammatory or pro-inflammatory signals they become activated in the form of RG. Previously, it has been shown that this process occurs in response to HFD feeding and DIO (Thaler et al. 2012, Valdearcos et al. 2017). This thesis has examined the effects of chronic obesity and weight loss on RG in astrocytes and microglia (Harrison et al. 2019).

The finding that chronic obesity did not reveal signs of reactive astrocytosis indicates that this may be a dynamic process with several phases. Certain studies have shown that even after very short periods of HFD feeding as low as 24 h, signs of astrocytosis are present (Buckman et al. 2015). In this particular study the authors measured levels of GFAP protein in the MBH after 24 h of HFD feeding. Whilst GFAP labels astrocytes and is also upregulated when astrocytes become activated, it is questionable as to whether this method alone is sufficient to suggest reactive astrocytosis. As described in section 1.7.1, RG is a complex response involving cell migration, transcriptional changes (such as GFAP for astrocytes or Iba1 in microglia), cell proliferation and stark morphological changes (Ridet et al. 1997). For a full appreciation of RG, several, if not all of these variables should be taken into consideration, which is often not the case in the literature. Other studies, including the landmark study revealing RG in obesity (Thaler et al. 2012) have employed immunohistochemistry approaches by staining for GFAP or Iba1 in rat brain slices, which revealed morphological changes. Microglia appear to increase in number and size just 3 days after HFD feeding, and continue to remain elevated until 14 days. In the same study astrocytes were detected in mice brain sections, which were elevated 1 week after HFD feeding, but reverted to chow fed levels after only 3 weeks (Thaler et al. 2012). Conversely these levels are elevated again after 8 months of HFD feeding. This is in contrast to the results presented in the current work, as here, no changes were seen after 22 weeks of

HFD feeding (Harrison et al. 2019). One possible cause for the discrepancies in the literature could be the age of the mice. In particular, although it was not noted in the original article, the GFAP staining images provided by Thaler and colleagues reveal a clear increase in GFAP immunoreactivity in mice fed chow for 8 months compared to 1 weeks. This indicates that as the mice aged, the amount of activated astrocytes increased. It is then plausible that in aged mice, the elevated basal astrocytosis masks an otherwise present increase after HFD feeding. Alternatively, the chronic exposure of inflammatory dietary components may desensitize the responsiveness of astrocytes and thus lead to a normalised morphology and GFAP expression.

The finding that profound weight loss increased astrocytosis points further towards RG being a highly dynamic process, which may be modulated by diet and endogenous energy metabolism. Evidence from the literature supports this theory, however contradicts the findings in this thesis. Berkseth et al. subjected mice to a HFD for 16 weeks to induce RG in both astrocytes and microglia (Berkseth et al. 2014). Then switching the mice to a chow diet for 4 weeks resulted in a complete reversal of gliosis back to control levels (Berkseth et al. 2014). There are then clear differences between this study and the one described here. A possible explanation for this contrast is the duration and rate of weight loss. In the current study CR and EX4 groups lost 30 % body weight in a period of 11 days and the diet-switch group lost 12 %, whereas in the study by Berkseth et al. mice lost 20 % body weight in 4 weeks. Calorie restriction and subsequent rapid weight loss is known to induce a wide range of metabolic adaptations from mitochondrial energy metabolism in many tissues, to increased stress response and dampened immune pathways (Lamming and Rozalyn 2014). Indeed, any number of these aspect may impact RG, possibly explaining the observed differences. Nonetheless, a dynamic shift of gliosis is supported by a large body of evidence. The discrepancies between the literature create an uncertainty as to the translational value of this line of work. Accordingly, human data comparing the GFAP immunoreactivity of hypothalami from patients with a BMI < 25 vs. BMI > 30 shown no significant difference (Baufeld et al. 2016). Thus, although peripheral inflammation is a clear and well described phenomenon of obesity (Lumeng and Saltiel 2011), obesity related hypothalamic RG seems less convincing and data, particularly in human subjects, is lacking in clarity. Future studies should aim to reveal whether or not this cellular response is maintained in chronic obesity, potentially hindering sustainable

weight loss, or rather is a temporary adjustment to changes in nutrient content and body weight.

6.3. Moderate doses of cranial irradiation result in disturbed metabolic regulation

Brain irradiation remains the most effective treatment against most brain cancers, as well as metastases in the brain (Schimmel et al. 2018). Radiotherapy often results in irreversible side-effects such as cognitive impairment, visual defects and memory loss (Habets et al. 2015). Furthermore, when performed early in life, CrI has also been shown to increase the risk of developing a range of maladies such as obesity, dyslipidaemia and disrupted glucose control, collectively also described as MetS (Oeffinger et al. 2006, Gunn et al. 2015). The underlying cause for this has yet to be revealed, however recent work using rodent models, as well as that presented in this thesis, has made some headway in our understanding of this phenomenon (Xu et al. 2018). Overall, the findings in this thesis show a moderately increased risk for developing MetS following 2 Gy CrI focused towards the hypothalamus. Xu and colleagues revealed more prominent effects using a higher dose of 6 Gy whole brain irradiation indicating a possible dose-dependency. Although the irradiation was targeted to the entire brain, the authors also focused their attention on the hypothalamus revealing increased cell death, decreased proliferation and increased RG (Xu et al. 2018). However, other brain regions were unfortunately not analysed, so it remains unclear if these findings were specific to the hypothalamus or a general response in the whole brain. Delayed onset brain inflammation following CrI has been reported before with increases in inflammatory markers such as TNF- α , intercellular adhesion molecule 1 and CC-chemokine ligand 2 (Moravan et al. 2011). These markers were increased after 1 day, following which they decrease, only to increase again after 180 days (Moravan et al. 2011). This discovery indicates similarities to the findings presented here, in such that an extended period of time is required for radiation induced effects to appear. Indeed, the latent onset observation has been described in the literature (Hopewell 1979) and the underlying causes remains a current topic of debate to this date (De Ruyscher et al. 2019).

It was recently shown that very high doses of irradiation (60 Gy) to the hypothalamus caused a significant reduction in ME residing microglia (Djogo et al. 2016). These neuron-

glia antigen 2 (NG2) glia, also referred to as oligodendrocyte progenitor cells, are an important source of oligodendrocytes that provide axonal support as well as myelination of axons (Dimou and Gallo 2015). Ablation of NG2-glia in the ME resulted in disrupted axonal structure of LepR positive processes within the ME and a loss of functional signalling from ARC neurons. It is possible that, if NG2-glia are particularly sensitive to radiation damage, more moderate doses of irradiation may result in similar effects, partially explaining the metabolic phenotype we and others have noted.

To elucidate the precise role of the hypothalamus in the late onset development of MetS after moderate doses of CrI it would be beneficial to exclusively irradiate this region. Although this was attempted in the current work, regions above the hypothalamus such as the thalamus, cortex and hippocampus were included in the beam path. More modern techniques such as stereotactic radiotherapy would allow for an exclusive irradiation of the hypothalamus and will be an interesting option for future studies. Overall, the data currently available indicate that moderate doses do show signs of metabolic disturbances localised to the hypothalamus, however further work is required to elucidate the responsible mechanisms involved and more importantly, the potential MetS risk to those receiving CrI during childhood.

In conclusion, this thesis has explored various aspects of leptin resistance, hypothalamic gliosis and CrI in regards to obesity and the MetS. Obesity is a disease that influences the lives of billions of people. Research in this field has transformed our views that being overweight is synonymous with laziness, lack of willpower and insufficient discipline. Yet despite this, obesity remains one of the few diseases with a strong social stigma. The findings described in detail here will support our efforts in further understanding this complex and multifactorial disease, possibly aiding in the development of therapeutic strategies to improve treatment and prevention options.

7. References

- American Diabetes Association (2015). "(7) Approaches to glycemic treatment." Diabetes Care **38**(Suppl): 41-48.
- Andermann, M. L. and B. B. Lowell (2017). "Toward a Wiring Diagram Understanding of Appetite Control." Neuron **95**(4): 757-778.
- Antl-Weiser, W. (2000). "Die Auffindung der Venus von Willendorf: eine unendliche Geschichte." Mitteilungen der Anthropologischen Gesellschaft in Wien **130**: 39-57.
- Ash, C., M. Dubec, K. Donne and T. Bashford (2017). "Effect of wavelength and beam width on penetration in light-tissue interaction using computational methods." Lasers in medical science **32**(8): 1909-1918.
- Balland, E., Dam, J., Langlet, F., Caron, E., Steculorum, S., A. Messina, S. Rasika, A. Falluel-Morel, Y. Anouar, B. Dehouck, E. Trinquet, R. Jockers, S. G. Bouret and V. Prevot (2014). "Hypothalamic tanycytes are an ERK-gated conduit for leptin into the brain." Cell Metab **19**(2): 293-301.
- Banati, R. B., J. Gehrmann, P. Schubert and G. W. Kreutzberg (1993). "Cytotoxicity of microglia." Glia **7**(1): 111-118.
- Banks, A. S., S. M. Davis, S. H. Bates and M. G. Myers (2000). "Activation of Downstream Signals by the Long Form of the Leptin Receptor." Journal of Biological Chemistry **275**(19): 14563-14572.
- Banks, W. A., Alan B. Coon, Ryota Nakaoke, Sandra M. Robinson and a. J. E. Morley (2004). "Triglycerides Induce Leptin Resistance at the Blood-Brain Barrier." Diabetes **53**: 1253-1260.
- Banks, W. A., Christopher R DiPalma and C. L. Farrell. (1999). "Impaired transport of leptin across the blood-brain barrier in obesity." Peptides **20**: 1341-1345.
- Bates, S. H., W. H. Stearns, T. A. Dundon, M. Schubert, A. W. K. Tso, Y. Wang, A. S. Banks, H. J. Lavery, A. K. Haq, E. Maratos-Flier, B. G. Neel, M. W. Schwartz and M. G. Myers (2003). "STAT3 signalling is required for leptin regulation of energy balance but not reproduction." Nature **421**(6925): 856-859.
- Bauer, H.-C., I. A. Krizbai, H. Bauer and A. Traweger (2014). ""You Shall Not Pass"-tight junctions of the blood brain barrier." Frontiers in neuroscience **8**: 392-392.
- Baufeld, C., A. Osterloh, S. Prokop, K. R. Miller and F. L. Heppner (2016). "High-fat diet-induced brain region-specific phenotypic spectrum of CNS resident microglia." Acta Neuropathologica **132**(3): 361-375.
- Baumann, H., K. K. Morella, D. W. White, M. Dembski, P. S. Bailon, H. Kim, C. F. Lai and L. A. Tartaglia (1996). "The full-length leptin receptor has signaling capabilities of interleukin 6-type cytokine receptors." Proceedings of the National Academy of Sciences **93**(16): 8374.

- Bence, K. K., M. Delibegovic, B. Xue, C. Z. Gorgun, G. S. Hotamisligil, B. G. Neel and B. B. Kahn (2006). "Neuronal PTP1B regulates body weight, adiposity and leptin action." Nature Medicine **12**: 917.
- Benedict, C., M. Hallschmid, A. Hatke, B. Schultes, H. L. Fehm, J. Born and W. Kern (2004). "Intranasal insulin improves memory in humans." Psychoneuroendocrinology **29**(10): 1326-1334.
- Berbesque, J. C., F. W. Marlowe, P. Shaw and P. Thompson (2014). "Hunter-gatherers have less famine than agriculturalists." Biol Lett **10**(1): 20130853.
- Berger, S., H. Pho, T. Fleury-Curado, S. Bevans-Fonti, H. Younas, M.-K. Shin, J. C. Jun, F. Anokye-Danso, R. S. Ahima, L. W. Enquist, D. Mendelowitz, A. R. Schwartz and V. Y. Polotsky (2019). "Intranasal Leptin Relieves Sleep-disordered Breathing in Mice with Diet-induced Obesity." American Journal of Respiratory and Critical Care Medicine **199**(6): 773-783.
- Berislav, V. Z., S. Jovanovic, W. Miao, S. Samara, S. Verma and C. L. Farrell (2000). "Differential regulation of leptin transport by the choroid plexus and blood-brain barrier and high affinity transport systems for entry into hypothalamus and across the blood-cerebrospinal fluid barrier." Endocrinology **141**(4): 1434-1441.
- Berkseth, K. E., S. J. Guyenet, S. J. Melhorn, D. Lee, J. P. Thaler, E. A. Schur and M. W. Schwartz (2014). "Hypothalamic gliosis associated with high-fat diet feeding is reversible in mice: a combined immunohistochemical and magnetic resonance imaging study." Endocrinology **155**(8): 2858-2867.
- Bjørnbæk, C., J. K. Elmquist, J. D. Frantz, S. E. Shoelson and J. S. Flier (1998). "Identification of SOCS-3 as a Potential Mediator of Central Leptin Resistance." Molecular Cell **1**(4): 619-625.
- Bolborea, M. and N. Dale (2013). "Hypothalamic tanycytes: potential roles in the control of feeding and energy balance." Trends in Neurosciences **36**(2): 91-100.
- Brobeck, J. R. (1946). "Mechanism of the development of obesity in animals with hypothalamic lesions." Physiology Reviews **26**(4): 541-559.
- Buckman, L. B., A. H. Hasty, D. K. Flaherty, C. T. Buckman, M. M. Thompson, B. K. Matlock, K. Weller and K. L. J. Ellacott (2014). "Obesity induced by a high-fat diet is associated with increased immune cell entry into the central nervous system." Brain, behavior, and immunity **35**: 33-42.
- Buckman, L. B., M. M. Thompson, R. N. Lippert, T. S. Blackwell, F. E. Yull and K. L. J. Ellacott (2015). "Evidence for a novel functional role of astrocytes in the acute homeostatic response to high-fat diet intake in mice." Mol Metab **4**(1): 58-63.
- Bugge, K., S. Seo, V. C. Sheffield, D.-F. Guo, D. A. Morgan and K. Rahmouni (2009). "Requirement of Bardet-Biedl syndrome proteins for leptin receptor signaling." Human Molecular Genetics **18**(7): 1323-1331.
- Burda, J. E. and M. V. Sofroniew (2014). "Reactive gliosis and the multicellular response to CNS damage and disease." Neuron **81**(2): 229-248.

- Bushong, E. A., M. E. Martone and M. H. Ellisman (2004). "Maturation of astrocyte morphology and the establishment of astrocyte domains during postnatal hippocampal development." International Journal of Developmental Neuroscience **22**(2): 73-86.
- Calle, E. E., C. Rodriguez, K. Walker-Thurmond and M. J. Thun (2003). "Overweight, Obesity, and Mortality from Cancer in a Prospectively Studied Cohort of U.S. Adults." New England Journal of Medicine **348**(17): 1625-1638.
- Cardona-Gomez, G. P., L. DonCarlos and L. M. Garcia-Segura (2000). "Insulin-like growth factor I receptors and estrogen receptors colocalize in female rat brain." Neuroscience **99**(4): 751-760.
- Chalfie, M., Y. Tu, G. Euskirchen, W. W. Ward and D. C. Prasher (1994). "Green fluorescent protein as a marker for gene expression." Science **263**(5148): 802-805.
- Chari, M., C. S. Yang, C. K. Lam, K. Lee, P. Mighiu, A. Kokorovic, G. W. Cheung, T. Y. Lai, P. Y. Wang and T. K. Lam (2011). "Glucose transporter-1 in the hypothalamic glial cells mediates glucose sensing to regulate glucose production in vivo." Diabetes **60**(7): 1901-1906.
- Cheunsuang, O. and R. Morris (2005). "Astrocytes in the arcuate nucleus and median eminence that take up a fluorescent dye from the circulation express leptin receptors and neuropeptide Y Y1 receptors." Glia **52**(3): 228-233.
- Coleman, D. L. (1973). "Effects of parabiosis of obese with diabetes and normal mice." Diabetologia **9**(4): 294-298.
- Coleman, D. L. (2010). "A historical perspective on leptin." Nature Medicine **16**: 1097.
- Coleman, D. L. and K. P. Hummel (1969). "Effects of parabiosis of normal with genetically diabetic mice." American Journal of Physiology-Legacy Content **217**(5): 1298-1304.
- Considine, R. V., M. K. Sinha, M. L. Heiman, A. Kriauciunas, T. W. Stephens, M. R. Nyce, J. P. Ohannesian, C. C. Marco, L. J. McKee, T. L. Bauer and J. F. Caro (1996). "Serum Immunoreactive-Leptin Concentrations in Normal-Weight and Obese Humans." New England Journal of Medicine **334**(5): 292-295.
- Couce, M. E., B. Burguera, J. E. Parisi, M. D. Jensen and R. V. Lloyd (1997). "Localization of leptin receptor in the human brain." Neuroendocrinology **66**(3): 145-150.
- Cox, R. D., D. Sellayah and F. R. Cagampang (2014). "On the Evolutionary Origins of Obesity: A New Hypothesis." Endocrinology **155**(5): 1573-1588.
- Daneman, R. and A. Prat (2015). "The blood-brain barrier." Cold Spring Harbor perspectives in biology **7**(1): DOI: 10.1101/cshperspect.a020412.
- De Ruyscher, D., G. Niedermann, N. G. Burnet, S. Siva, A. W. M. Lee and F. Hegi-Johnson (2019). "Radiotherapy toxicity." Nature Reviews Disease Primers **5**(1): 13.
- De Souza, C. u. T., E. P. Araujo, M. r. J. A. Saad, R. L. Zollner, R. Ashimine, L. c. A. Velloso, A. C. Boschero and S. Bordin (2005). "Consumption of a Fat-Rich Diet Activates a Proinflammatory Response and Induces Insulin Resistance in the Hypothalamus." Endocrinology **146**(10): 4192-4199.

- Deng, H., C. W. Kennedy, E. Armour, E. Tryggestad, E. Ford, T. McNutt, L. Jiang and J. Wong (2007). "The small-animal radiation research platform (SARRP): dosimetry of a focused lens system." Physics in Medicine and Biology **52**(10): 2729-2740.
- Deren, K. E., M. Packer, J. Forsyth, B. Milash, O. M. Abdullah, E. W. Hsu and J. P. McAllister (2010). "Reactive astrocytosis, microgliosis and inflammation in rats with neonatal hydrocephalus." Experimental Neurology **226**(1): 110-119.
- Devos, R., G. Richardst, I. Campfieldt, L. Tartaglia, Y. Guisez, J. Van der heyden, J. Tavernier, G. Plaetinck and P. Burn (1996). "OB protein binds specifically to the choroid plexus of mice and rats." Proc. Natl. Acad. Sci. **93**: 5668-5673.
- Dezonne, R. S., F. R. Lima, A. G. Trentin and F. C. Gomes (2015). "Thyroid hormone and astroglia: endocrine control of the neural environment." J Neuroendocrinol **27**(6): 435-445.
- Diano, S., S. P. Kalra and T. L. Horvath (1998). "Leptin Receptor Immunoreactivity is Associated with the Golgi Apparatus of Hypothalamic Neurones and Glial Cells." Journal of Neuroendocrinology **10**(9): 647-650.
- Dimou, L. and V. Gallo (2015). "NG2-glia and their functions in the central nervous system." Glia **63**(8): 1429-1451.
- Dinarello, C. A. (2011). "Interleukin-1 in the pathogenesis and treatment of inflammatory diseases." Blood **117**(14): 3720-3732.
- Djogo, T., S. C. Robins, S. Schneider, D. Kryzskaya, X. Liu, A. Mingay, C. J. Gillon, J. H. Kim, K. F. Storch, U. Boehm, C. W. Bourque, T. Stroh, L. Dimou and M. V. Kokoeva (2016). "Adult NG2-Glia Are Required for Median Eminence-Mediated Leptin Sensing and Body Weight Control." Cell Metab **23**(5): 797-810.
- Dodt, H.-U., U. Leischner, A. Schierloh, N. Jährling, C. P. Mauch, K. Deininger, J. M. Deussing, M. Eder, W. Zieglgänsberger and K. Becker (2007). "Ultramicroscopy: three-dimensional visualization of neuronal networks in the whole mouse brain." Nature Methods **4**: 331.
- Dong, Y. and E. N. Benveniste (2001). "Immune function of astrocytes." Glia **36**(2): 180-190.
- El-Haschimi, K., D. Pierroz, S. M. Hileman, C. Bjørnbæk and J. S. Flier (2000). "Two defects contribute to hypothalamic leptin resistance in mice with diet-induced obesity." J. Clin. Invest **105**(12): 1827-1832.
- Emdin, C. A., A. V. Khera, P. Natarajan, D. Klarin, S. M. Zekavat, A. J. Hsiao and S. Kathiresan (2017). "Genetic Association of Waist-to-Hip Ratio With Cardiometabolic Traits, Type 2 Diabetes, and Coronary Heart Disease WHR and Cardiometabolic Traits, Type 2 Diabetes, and CHD WHR and Cardiometabolic Traits, Type 2 Diabetes, and CHD." JAMA **317**(6): 626-634.
- FAO, IFAD, UNICEF, WFP and WHO (2017). "Food security and nutrition around the world in 2017."

- Farooqi, I. S., J. M. Keogh, G. S. H. Yeo, E. J. Lank, T. Cheetham and S. O'Rahilly (2003). "Clinical Spectrum of Obesity and Mutations in the Melanocortin 4 Receptor Gene." New England Journal of Medicine **348**(12): 1085-1095.
- Fei, H., H. J. Okano, C. Li, G.-H. Lee, C. Zhao, R. Darnell and J. M. Friedman (1997). "Anatomic localization of alternatively spliced leptin receptors (Ob-R) in mouse brain and other tissues." Proceedings of the National Academy of Sciences **94**(13): 7001.
- Feng, X., D. Guan, T. Auen, J. W. Choi, M. A. Salazar Hernández, J. Lee, H. Chun, F. Faruk, E. Kaplun, Z. Herbert, K. D. Copps and U. Ozcan (2019). "IL1R1 is required for celestrol's leptin-sensitization and antiobesity effects." Nature Medicine **25**(4): 575-582.
- Findeisen, H. M., F. Gizard, Y. Zhao, H. Qing, K. L. Jones, D. Cohn, E. B. Heywood and D. Bruemmer (2011). "Glutathione depletion prevents diet-induced obesity and enhances insulin sensitivity." Obesity (Silver Spring) **19**(12): 2429-2432.
- Fitch, M. T. and J. Silver (2008). "CNS injury, glial scars, and inflammation: Inhibitory extracellular matrices and regeneration failure." Experimental Neurology **209**(2): 294-301.
- Fothergill, E., J. Guo, L. Howard, J. C. Kerns, N. D. Knuth, R. Brychta, K. Y. Chen, M. C. Skarulis, M. Walter, P. J. Walter and K. D. Hall (2016). "Persistent metabolic adaptation 6 years after "The Biggest Loser" competition." Obesity (Silver Spring) **24**(8): 1612-1619.
- Freeman, M. R. (2010). "Specification and Morphogenesis of Astrocytes." Science **330**(6005): 774-778.
- Frier, B. M., G. Schernthaner and S. R. Heller (2011). "Hypoglycemia and Cardiovascular Risks." Diabetes Care **34**(Supplement 2): S132-S137.
- Fu, R., Q. Shen, P. Xu, J. J. Luo and Y. Tang (2014). "Phagocytosis of Microglia in the Central Nervous System Diseases." Molecular Neurobiology **49**(3): 1422-1434.
- Fuente-Martin, E., C. Garcia-Caceres, P. Argente-Arizon, F. Diaz, M. Granado, A. Freire-Regatillo, D. Castro-Gonzalez, M. L. Ceballos, L. M. Frago, S. L. Dickson, J. Argente and J. A. Chowen (2016). "Ghrelin Regulates Glucose and Glutamate Transporters in Hypothalamic Astrocytes." Sci Rep **6**: 23673.
- Gao, S., D. Chen, Q. Li, J. Ye, H. Jiang, C. Amatore and X. Wang (2014). "Near-infrared fluorescence imaging of cancer cells and tumors through specific biosynthesis of silver nanoclusters." Scientific Reports **4**: 4384.
- Garcia-Caceres, C., E. Balland, V. Prevot, S. Luquet, S. C. Woods, M. Koch, T. L. Horvath, C. X. Yi, J. A. Chowen, A. Verkhratsky, A. Araque, I. Bechmann and M. H. Tschop (2019). "Role of astrocytes, microglia, and tanycytes in brain control of systemic metabolism." Nat Neurosci **22**(1): 7-14.
- García-Cáceres, C., E. Fuente-Martín, J. Argente and J. A. Chowen (2012). "Emerging role of glial cells in the control of body weight." Molecular Metabolism **1**(1): 37-46.
- Garcia-Caceres, C., C. Quarta, L. Varela, Y. Gao, T. Gruber, B. Legutko, M. Jastroch, P. Johansson, J. Ninkovic, C. X. Yi, O. Le Thuc, K. Szigeti-Buck, W. Cai, C. W. Meyer, P. T. Pfluger, A. M. Fernandez, S. Luquet, S. C. Woods, I. Torres-Aleman, C. R. Kahn, M. Gotz, T. L. Horvath

and M. H. Tschop (2016). "Astrocytic Insulin Signaling Couples Brain Glucose Uptake with Nutrient Availability." Cell **166**(4): 867-880.

García, M. C., I. Wernstedt, A. Berndtsson, M. Enge, M. Bell, O. Hultgren, M. Horn, B. Ahrén, S. Enerback, C. Ohlsson, V. Wallenius and J.-O. Jansson (2006). "Mature-Onset Obesity in Interleukin-1 Receptor I Knockout Mice." Diabetes **55**(5): 1205.

Garmey, E. G., Q. Liu, C. A. Sklar, L. R. Meacham, A. C. Mertens, M. A. Stovall, Y. Yasui, L. L. Robison and K. C. Oeffinger (2008). "Longitudinal changes in obesity and body mass index among adult survivors of childhood acute lymphoblastic leukemia: a report from the Childhood Cancer Survivor Study." J Clin Oncol **26**(28): 4639-4645.

Geijselaers, S. L. C., P. Aalten, I. H. G. B. Ramakers, P. P. De Deyn, A. C. Heijboer, H. L. Koek, M. G. M. OldeRikkert, J. M. Papma, F. E. Reesink, L. L. Smits, C. D. A. Stehouwer, C. E. Teunissen, F. R. J. Verhey, W. M. van der Flier, G. J. Biessels and g. Parelsnoer Institute Neurodegenerative Diseases study (2017). "Association of Cerebrospinal Fluid (CSF) Insulin with Cognitive Performance and CSF Biomarkers of Alzheimer's Disease." Journal of Alzheimer's disease : JAD **61**(1): 309-320.

Gregor, M. F. and G. S. Hotamisligil (2011). "Inflammatory Mechanisms in Obesity." Annual Review of Immunology **29**(1): 415-445.

Groop, L. (2000). "Pathogenesis of type 2 diabetes: the relative contribution of insulin resistance and impaired insulin secretion." Int J Clin Pract Suppl(113): 3-13.

Gunn, H. M., H. Emilsson, M. Gabriel, A. M. Maguire and K. S. Steinbeck (2015). "Metabolic Health in Childhood Cancer Survivors: A Longitudinal Study in a Long-Term Follow-Up Clinic." Journal of Adolescent and Young Adult Oncology **5**(1): 24-30.

Gurney, J. G., K. K. Ness, M. Stovall, S. Wolden, J. A. Punyko, J. P. Neglia, A. C. Mertens, R. J. Packer, L. L. Robison and C. A. Sklar (2003). "Final height and body mass index among adult survivors of childhood brain cancer: childhood cancer survivor study." J Clin Endocrinol Metab **88**(10): 4731-4739.

Habets, E. J. J., L. Dirven, R. G. Wiggeraad, A. Verbeek-de Kanter, G. J. Lycklama à Nijeholt, H. Zwinkels, M. Klein and M. J. B. Taphoorn (2015). "Neurocognitive functioning and health-related quality of life in patients treated with stereotactic radiotherapy for brain metastases: a prospective study." Neuro-Oncology **18**(3): 435-444.

Hales, C. N. and D. J. P. Barker (1992). "Type 2 (non-insulin-dependent) diabetes mellitus: the thrifty phenotype hypothesis." Diabetologia **35**(7): 595-601.

Harrison, L., K. Pfuhlmann, S. C. Schriever and P. T. Pfluger (2019). "Profound weight loss induces reactive astrogliosis in the arcuate nucleus of obese mice." Molecular Metabolism.

Harrison, L., S. C. Schriever, A. Feuchtinger, E. Kyriakou, P. Baumann, K. Pfuhlmann, A. C. Messias, A. Walch, M. H. Tschöp and P. T. Pfluger (2018). "Fluorescent blood-brain barrier tracing shows intact leptin transport in obese mice." Int J Obes (Lond): DOI: 10.1038/s41366-41018-40221-z.

Havrankova, J., J. Roth and M. Brownstein (1978). "Insulin receptors are widely distributed in the central nervous system of the rat." Nature **272**(5656): 827-829.

Head, G. A. (2015). "Cardiovascular and metabolic consequences of obesity." Frontiers in physiology **6**: 32-32.

Heni, M., R. Wagner, S. Kullmann, R. Veit, H. Mat Husin, K. Linder, C. Benkendorff, A. Peter, N. Stefan, H.-U. Häring, H. Preissl and A. Fritsche (2014). "Central Insulin Administration Improves Whole-Body Insulin Sensitivity via Hypothalamus and Parasympathetic Outputs in Men." Diabetes **63**(12): 4083-4088.

Hervey, G. R. (1959). "The effects of lesions in the hypothalamus in parabiotic rats." The Journal of Physiology **145**(2): 336-352.

Heymsfield, S. B., A. S. Greenberg, K. Fujioka, R. M. Dixon, R. Kushner, T. Hunt, J. A. Lubina, J. Patane, B. Self, P. Hunt and M. McCamish (1999). "Recombinant Leptin for Weight Loss in Obese and Lean Adults: A Randomized, Controlled, Dose-Escalation Trial." JAMA **282**(16): 1568-1575.

Hileman, S. M., C. Bjørnbæk, D. D. Pierroz, H. Masuzaki, K. El-Haschimi, J. S. Flier and W. A. Banks (2002). "Characterization of Short Isoforms of the Leptin Receptor in Rat Cerebral Microvessels and of Brain Uptake of Leptin in Mouse Models of Obesity." Endocrinology **143**(3): 775-783.

Hirosumi, J., G. Tuncman, L. Chang, C. Z. Görgün, K. T. Uysal, K. Maeda, M. Karin and G. S. Hotamisligil (2002). "A central role for JNK in obesity and insulin resistance." Nature **420**(6913): 333-336.

Hopewell, J. W. (1979). "LATE RADIATION DAMAGE TO THE CENTRAL NERVOUS SYSTEM: A RADIOBIOLOGICAL INTERPRETATION." Neuropathology and Applied Neurobiology **5**(5): 329-343.

Horvath, T. L., F. Naftolin, S. P. Kalra and C. Leranth (1992). "Neuropeptide-Y innervation of beta-endorphin-containing cells in the rat mediobasal hypothalamus: a light and electron microscopic double immunostaining analysis." Endocrinology **131**(5): 2461-2467.

Hotamisligil, G. S. (2006). "Inflammation and metabolic disorders." Nature **444**(7121): 860-867.

Howard, J. K., B. J. Cave, L. J. Oksanen, I. Tzamelis, C. Bjørnbæk and J. S. Flier (2004). "Enhanced leptin sensitivity and attenuation of diet-induced obesity in mice with haploinsufficiency of Socs3." Nature Medicine **10**: 734.

Hummel, K. P., M. M. Dickie and D. L. Coleman (1966). "Diabetes, a new mutation in the mouse." Science **153**(3740): 1127-1128.

Huxley, R., S. Mendis, E. Zheleznyakov, S. Reddy and J. Chan (2009). "Body mass index, waist circumference and waist:hip ratio as predictors of cardiovascular risk—a review of the literature." European Journal Of Clinical Nutrition **64**: 16.

Ingalls, A. M., M. M. Dickie and G. D. Snell (1950). "Obese, a new mutation in the house mouse." J Hered **41**(12): 317-318.

Jäkel, S. and L. Dimou (2017). "Glial Cells and Their Function in the Adult Brain: A Journey through the History of Their Ablation." Frontiers in Cellular Neuroscience **11**(24).

- Jauch-Chara, K., A. Friedrich, M. Rezmer, U. H. Melchert, H. G. Scholand-Engler, M. Hallschmid and K. M. Oltmanns (2012). "Intranasal Insulin Suppresses Food Intake via Enhancement of Brain Energy Levels in Humans." Diabetes **61**(9): 2261-2268.
- Johnson, M. L., K. Distelmaier, I. R. Lanza, B. A. Irving, M. M. Robinson, A. R. Konopka, G. I. Shulman and K. S. Nair (2016). "Mechanism by Which Caloric Restriction Improves Insulin Sensitivity in Sedentary Obese Adults." Diabetes **65**(1): 74-84.
- Johnstone, M., A. J. H. Gearing and K. M. Miller (1999). "A central role for astrocytes in the inflammatory response to β -amyloid; chemokines, cytokines and reactive oxygen species are produced." Journal of Neuroimmunology **93**(1): 182-193.
- Kastin, A. J., W. Pan, L. M. Maness, R. J. Koletsky and P. Ernsberger (1999). "Decreased transport of leptin across the blood-brain barrier in rats lacking the short form of the leptin receptor." Peptides **20**(12): 1449-1453.
- Kaszubska, W., H. D. Falls, V. G. Schaefer, D. Haasch, L. Frost, P. Hessler, P. E. Kroeger, D. W. White, M. R. Jirousek and J. M. Trevillyan (2002). "Protein tyrosine phosphatase 1B negatively regulates leptin signaling in a hypothalamic cell line." Molecular and Cellular Endocrinology **195**(1): 109-118.
- Kaufman, R. J. (1999). "Stress signaling from the lumen of the endoplasmic reticulum: coordination of gene transcriptional and translational controls." Genes & Development **13**(10): 1211-1233.
- Keeseey, R. E. and M. D. Hirvonen (1997). "Body weight set-points: determination and adjustment." J Nutr **127**(9): 1875s-1883s.
- Keller, P. J. and H.-U. Dodt (2012). "Light sheet microscopy of living or cleared specimens." Current Opinion in Neurobiology **22**(1): 138-143.
- Khaodhiar, L., K. C. McCowen and G. L. Blackburn (1999). "Obesity and its comorbid conditions." Clinical Cornerstone **2**(3): 17-31.
- Kimple, M. E., A. L. Brill and R. L. Pasker (2013). "Overview of affinity tags for protein purification." Current protocols in protein science **73**: Unit-9.9.
- Kiss, J. Z., E. Mezey, M. D. Cassell, T. H. Williams, G. P. Mueller, T. L. O'Donohue and M. Palkovits (1985). "Topographical distribution of pro-opiomelanocortin-derived peptides (ACTH/ β -END/ α -MSH) in the rat median eminence." Brain Research **329**(1): 169-176.
- Kleinert, M., P. Kotzbeck, T. Altendorfer-Kroath, T. Birngruber, M. H. Tschop and C. Clemmensen (2018). "Time-resolved hypothalamic open flow micro-perfusion reveals normal leptin transport across the blood-brain barrier in leptin resistant mice." Mol Metab **13**: 77-82.
- Kleinridders, A., H. A. Ferris, W. Cai and C. R. Kahn (2014). "Insulin action in brain regulates systemic metabolism and brain function." Diabetes **63**(7): 2232-2243.
- Knigge, K. M. and D. E. Scott (1970). "Structure and function of the median eminence." American Journal of Anatomy **129**(2): 223-243.

- Knott, C., G. Stern and G. P. Wilkin (2000). "Inflammatory Regulators in Parkinson's Disease: iNOS, Lipocortin-1, and Cyclooxygenases-1 and -2." Molecular and Cellular Neuroscience **16**(6): 724-739.
- Kreutzberg, G. W. (1996). "Microglia: a sensor for pathological events in the CNS." Trends Neurosci **19**(8): 312-318.
- Kusnezow, W. and J. D. Hoheisel (2002). "Antibody microarrays: promises and problems." Biotechniques Suppl: 14-23.
- Lambadiari, V., K. Triantafyllou and G. D. Dimitriadis (2015). "Insulin action in muscle and adipose tissue in type 2 diabetes: The significance of blood flow." World journal of diabetes **6**(4): 626-633.
- Lamming, D. W. and M. A. Rozalyn (2014). *Metabolic Effects of Caloric Restriction*. eLS. L. E. John Wiley & Sons.
- Langlet, F., A. Mullier, S. G. Bouret, V. Prevot and B. Dehouck (2013). "Tanycyte-like cells form a blood-cerebrospinal fluid barrier in the circumventricular organs of the mouse brain." J Comp Neurol **521**(15): 3389-3405.
- Lannering, B., S. Rutkowski, F. Doz, B. Pizer, G. Gustafsson, A. Navajas, M. Massimino, R. Reddingius, M. Benesch, C. Carrie, R. Taylor, L. Gandola, T. Björk-Eriksson, J. Giralt, F. Oldenburger, T. Pietsch, D. Figarella-Branger, K. Robson, M. Forni, S. C. Clifford, M. Warmuth-Metz, K. von Hoff, A. Faldum, V. Mosseri and R. Kortmann (2012). "Hyperfractionated Versus Conventional Radiotherapy Followed by Chemotherapy in Standard-Risk Medulloblastoma: Results From the Randomized Multicenter HIT-SIOP PNET 4 Trial." Journal of Clinical Oncology **30**(26): 3187-3193.
- Lehrke, M. and M. A. Lazar (2004). "Inflamed about obesity." Nature Medicine **10**(2): 126-127.
- Liao, G.-Y., J. J. An, K. Gharami, E. G. Waterhouse, F. Vanevski, K. R. Jones and B. Xu (2012). "Dendritically targeted Bdnf mRNA is essential for energy balance and response to leptin." Nature Medicine **18**: 564.
- Liu, J., J. Lee, Mario A. Salazar Hernandez, R. Mazitschek and U. Ozcan (2015). "Treatment of Obesity with Celastrol." Cell **161**(5): 999-1011.
- Liu, M.-M., Q.-J. Liu, J. Wen, M. Wang, L.-Y. Wu, M.-L. Qu, M. Li, M.-X. Shen and J. Wu (2018). "Waist-to-hip ratio is the most relevant obesity index at each phase of insulin secretion among obese patients." Journal of Diabetes and its Complications **32**(7): 670-676.
- Loh, K., A. Fukushima, X. Zhang, S. Galic, D. Briggs, Pablo J. Enriori, S. Simonds, F. Wiede, A. Reichenbach, C. Hauser, Natalie A. Sims, Kendra K. Bence, S. Zhang, Z.-Y. Zhang, Barbara B. Kahn, Benjamin G. Neel, Zane B. Andrews, Michael A. Cowley and T. Tiganis (2011). "Elevated Hypothalamic TCPTP in Obesity Contributes to Cellular Leptin Resistance." Cell Metabolism **14**(5): 684-699.
- Lumeng, C. N. and A. R. Saltiel (2011). "Inflammatory links between obesity and metabolic disease." The Journal of Clinical Investigation **121**(6): 2111-2117.

- Maffei, M., J. Halaas, E. Ravussin, R. E. Pratley, G. H. Lee, Y. Zhang, H. Fei, S. Kim, R. Lallone, S. Ranganathan, P. A. Kern and J. M. Friedman (1995). "Leptin levels in human and rodent: Measurement of plasma leptin and ob RNA in obese and weight-reduced subjects." Nature Medicine **1**(11): 1155-1161.
- Mahmood, T. and P.-C. Yang (2012). "Western blot: technique, theory, and trouble shooting." North American journal of medical sciences **4**(9): 429-434.
- Marsh, D. J., G. Hollopeter, D. Huszar, R. Laufer, K. A. Yagaloff, S. L. Fisher, P. Burn and R. D. Palmiter (1999). "Response of melanocortin-4 receptor-deficient mice to anorectic and orexigenic peptides." Nature Genetics **21**: 119.
- Martin, T. L., T. Alquier, K. Asakura, N. Furukawa, F. Preitner and B. B. Kahn (2006). "Diet-induced Obesity Alters AMP Kinase Activity in Hypothalamus and Skeletal Muscle." Journal of Biological Chemistry **281**(28): 18933-18941.
- Marty, N., M. Dallaporta, M. Foretz, M. Emery, D. Tarussio, I. Bady, C. Binnert, F. Beermann and B. Thorens (2005). "Regulation of glucagon secretion by glucose transporter type 2 (glut2) and astrocyte-dependent glucose sensors." The Journal of Clinical Investigation **115**(12): 3545-3553.
- Meacham, L. R., C. A. Sklar, S. Li, Q. Liu, N. Gimpel, Y. Yasui, J. A. Whitton, M. Stovall, L. L. Robison and K. C. Oeffinger (2009). "Diabetes mellitus in long-term survivors of childhood cancer. Increased risk associated with radiation therapy: a report for the childhood cancer survivor study." Arch Intern Med **169**(15): 1381-1388.
- Milanski, M., G. Degasperi, A. Coope, J. Morari, R. Denis, D. E. Cintra, D. M. L. Tsukumo, G. Anhe, M. E. Amaral, H. K. Takahashi, R. Curi, H. C. Oliveira, J. B. C. Carvalheira, S. Bordin, M. J. Saad and L. A. Velloso (2009). "Saturated Fatty Acids Produce an Inflammatory Response Predominantly through the Activation of TLR4 Signaling in Hypothalamus: Implications for the Pathogenesis of Obesity." The Journal of Neuroscience **29**(2): 359.
- Miller, T. L., S. R. Lipsitz, G. Lopez-Mitnik, A. S. Hinkle, L. S. Constine, M. J. Adams, C. French, C. Proukou, A. Rovitelli and S. E. Lipshultz (2010). "Characteristics and determinants of adiposity in pediatric cancer survivors." Cancer Epidemiol Biomarkers Prev **19**(8): 2013-2022.
- Moravan, M. J., J. A. Olschowka, J. P. Williams and M. K. O'Banion (2011). "Cranial irradiation leads to acute and persistent neuroinflammation with delayed increases in T-cell infiltration and CD11c expression in C57BL/6 mouse brain." Radiation research **176**(4): 459-473.
- Mori, H., R. Hanada, T. Hanada, D. Aki, R. Mashima, H. Nishinakamura, T. Torisu, K. R. Chien, H. Yasukawa and A. Yoshimura (2004). "Socs3 deficiency in the brain elevates leptin sensitivity and confers resistance to diet-induced obesity." Nature Medicine **10**: 739.
- Mountjoy, K. G., L. S. Robbins, M. T. Mortrud and R. D. Cone (1992). "The cloning of a family of genes that encode the melanocortin receptors." Science **257**(5074): 1248-1251.
- Myers, M. G., Jr., R. L. Leibel, R. J. Seeley and M. W. Schwartz (2010). "Obesity and leptin resistance: distinguishing cause from effect." Trends in endocrinology and metabolism: TEM **21**(11): 643-651.

- Nanda, J. S. and J. R. Lorsch (2014). Chapter Eight - Labeling a Protein with Fluorophores Using NHS Ester Derivatization. Methods in Enzymology. J. Lorsch, Academic Press. **536**: 87-94.
- Neel, J. V. (1962). "Diabetes mellitus: a "thrifty" genotype rendered detrimental by "progress"?" American journal of human genetics **14**(4): 353-362.
- Neill, U. S. (2010). "Leaping for leptin: the 2010 Albert Lasker Basic Medical Research Award goes to Douglas Coleman and Jeffrey M. Friedman." The Journal of Clinical Investigation **120**(10): 3413-3418.
- Norton, W. T., D. A. Aquino, I. Hozumi, F. C. Chiu and C. F. Brosnan (1992). "Quantitative aspects of reactive gliosis: a review." Neurochem Res **17**(9): 877-885.
- O'Neill, L. A. J. (2008). "The interleukin-1 receptor/Toll-like receptor superfamily: 10 years of progress." Immunological Reviews **226**(1): 10-18.
- Oberheim, N. A., X. Wang, S. Goldman and M. Nedergaard (2006). "Astrocytic complexity distinguishes the human brain." Trends in Neurosciences **29**(10): 547-553.
- Oeffinger, K. C., A. C. Mertens, C. A. Sklar, T. Kawashima, M. M. Hudson, A. T. Meadows, D. L. Friedman, N. Marina, W. Hobbie, N. S. Kadan-Lottick, C. L. Schwartz, W. Leisenring and L. L. Robison (2006). "Chronic Health Conditions in Adult Survivors of Childhood Cancer." New England Journal of Medicine **355**(15): 1572-1582.
- Ottaway, N., P. Mahbod, B. Rivero, L. A. Norman, A. Gertler, D. A. D'Alessio and D. Perez-Tilve (2015). "Diet-induced obese mice retain endogenous leptin action." Cell Metab **21**(6): 877-882.
- Ozcan, L., A. S. Ergin, A. Lu, J. Chung, S. Sarkar, D. Nie, M. G. Myers, Jr. and U. Ozcan (2009). "Endoplasmic Reticulum Stress Plays a Central Role in Development of Leptin Resistance." Cell Metabolism **9**(1): 35-51.
- Patel, K. A. and D. G. Schlundt (2001). "Impact of moods and social context on eating behavior." Appetite **36**(2): 111-118.
- Peiser, C., G. P. McGregor and R. E. Lang (2000). "Binding and internalization of leptin by porcine choroid plexus cells." Neuroscience Letters **283**: 209-212.
- Pfuhlmann, K., S. C. Schriever, P. Baumann, D. G. Kabra, L. Harrison, S. E. Mazibuko-Mbeje, R. E. Contreras, E. Kyriakou, S. E. Simonds, T. Tiganis, M. A. Cowley, S. C. Woods, M. Jastroch, C. Clemmensen, M. De Angelis, K. W. Schramm, M. Sattler, A. C. Messias, M. H. Tschop and P. T. Pfluger (2018). "Celastrol-Induced Weight Loss Is Driven by Hypophagia and Independent From UCP1." Diabetes **67**(11): 2456-2465.
- Rahmouni, K., M. A. Fath, S. Seo, D. R. Thedens, C. J. Berry, R. Weiss, D. Y. Nishimura and V. C. Sheffield (2008). "Leptin resistance contributes to obesity and hypertension in mouse models of Bardet-Biedl syndrome." The Journal of clinical investigation **118**(4): 1458-1467.
- Reed, A. S., E. K. Unger, L. E. Olofsson, M. L. Piper, M. G. Myers and A. W. Xu (2010). "Functional Role of Suppressor of Cytokine Signaling 3 Upregulation in Hypothalamic Leptin Resistance and Long-Term Energy Homeostasis." Diabetes **59**(4): 894.

Ridet, J. L., A. Privat, S. K. Malhotra and F. H. Gage (1997). "Reactive astrocytes: cellular and molecular cues to biological function." Trends Neurosci **20**(12): 570-577.

Rodriguez, E. M., J. L. Blazquez and M. Guerra (2010). "The design of barriers in the hypothalamus allows the median eminence and the arcuate nucleus to enjoy private milieus: the former opens to the portal blood and the latter to the cerebrospinal fluid." Peptides **31**(4): 757-776.

Roglic, G., N. Unwin, P. H. Bennett, C. Mathers, J. Tuomilehto, S. Nag, V. Connolly and H. King (2005). "The burden of mortality attributable to diabetes: realistic estimates for the year 2000." Diabetes Care **28**(9): 2130-2135.

Rorato, R., B. d. C. Borges, E. T. Uchoa, J. Antunes-Rodrigues, C. F. Elias and L. L. K. Elias (2017). "LPS-Induced Low-Grade Inflammation Increases Hypothalamic JNK Expression and Causes Central Insulin Resistance Irrespective of Body Weight Changes." International journal of molecular sciences **18**(7): 1431.

Rothman, K. J. (2008). "BMI-related errors in the measurement of obesity." International Journal Of Obesity **32**: S56.

Sanderson, M. J., I. Smith, I. Parker and M. D. Bootman (2014). "Fluorescence Microscopy." Cold Spring Harbor Protocols **2014**(10): pdb.top071795.

Schimmel, W. C. M., E. Verhaak, P. E. J. Hanssens, K. Gehring and M. M. Sitskoorn (2018). "A randomised trial to compare cognitive outcome after gamma knife radiosurgery versus whole brain radiation therapy in patients with multiple brain metastases: research protocol CAR-study B." BMC Cancer **18**(1): 218.

Schreyer, S. A., S. C. Chua, Jr. and R. C. LeBoeuf (1998). "Obesity and diabetes in TNF-alpha receptor- deficient mice." The Journal of Clinical Investigation **102**(2): 402-411.

Schulz, C., K. Paulus, O. Jöhren and H. Lehnert (2012). "Intranasal Leptin Reduces Appetite and Induces Weight Loss in Rats with Diet-Induced Obesity (DIO)." Endocrinology **153**(1): 143-153.

Sheng, J. G., K. Ito, R. D. Skinner, R. E. Mrak, C. R. Rovnaghi, L. J. van Eldik and W. S. T. Griffin (1996). "In vivo and in vitro evidence supporting a role for the inflammatory cytokine interleukin-1 as a driving force in Alzheimer pathogenesis." Neurobiology of Aging **17**(5): 761-766.

Shi, H., M. V. Kokoeva, K. Inouye, I. Tzamelis, H. Yin and J. S. Flier (2006). "TLR4 links innate immunity and fatty acid-induced insulin resistance." The Journal of Clinical Investigation **116**(11): 3015-3025.

Silvestri, L., I. Costantini, L. Sacconi and F. S. Pavone (2016). Clearing of fixed tissue: a review from a microscopist's perspective, SPIE.

Smith, A. M., M. C. Mancini and S. Nie (2009). "Second window for in vivo imaging." Nature Nanotechnology **4**: 710.

Speakman, J. R. (2008). "Thrifty genes for obesity, an attractive but flawed idea, and an alternative perspective: the 'drifty gene' hypothesis." International Journal Of Obesity **32**: 1611.

Stadtmann, H., C. Hranitzky and N. Brasik (2006). "Study of real time temperature profiles in routine TLD read out--influences of detector thickness and heating rate on glow curve shape." Radiat Prot Dosimetry **119**(1-4): 310-313.

Storer, J. B., P. S. Harris, J. E. Furchner and W. H. Langham (1957). "The Relative Biological Effectiveness of Various Ionizing Radiations in Mammalian Systems." Radiation Research **6**(2): 188-288.

Streit, W. J., R. E. Mrak and W. S. T. Griffin (2004). "Microglia and neuroinflammation: a pathological perspective." Journal of Neuroinflammation **1**(1): 14.

Tartaglia, L., M. Dembski, X. Weng, N. Deng, J. Culpepper, R. Devos, G. J. Richards, L. A. Campfield, F. T. Clark, J. Deeds, C. Muir, S. Sanker, A. Moriarty, K. J. Moore, J. S. Smutko, G. G. Mays, E. A. Wool, C. A. Monroe and R. I. Tepper (1995). "Identification and expression cloning of a leptin receptor, OB-R." Cell **83**: 1263-1271.

Teraphongphom, N., C. S. Kong, J. M. Warram and E. L. Rosenthal (2017). "Specimen mapping in head and neck cancer using fluorescence imaging." Laryngoscope Investigative Otolaryngology **2**(6): 447-452.

Thaler, J. P., S. J. Guyenet, M. D. Dorfman, B. E. Wisse and M. W. Schwartz (2013). "Hypothalamic Inflammation: Marker or Mechanism of Obesity Pathogenesis?" Diabetes **62**(8): 2629.

Thaler, J. P., C.-X. Yi, E. A. Schur, S. J. Guyenet, B. H. Hwang, M. O. Dietrich, X. Zhao, D. A. Sarruf, V. Izgur, K. R. Maravilla, H. T. Nguyen, J. D. Fischer, M. E. Matsen, B. E. Wisse, G. J. Morton, T. L. Horvath, D. G. Baskin, M. H. Tschöp and M. W. Schwartz (2012). "Obesity is associated with hypothalamic injury in rodents and humans." The Journal of Clinical Investigation **122**(1): 153-162.

Thaler, J. P., C. X. Yi, E. A. Schur, S. J. Guyenet, B. H. Hwang, M. O. Dietrich, X. Zhao, D. A. Sarruf, V. Izgur, K. R. Maravilla, H. T. Nguyen, J. D. Fischer, M. E. Matsen, B. E. Wisse, G. J. Morton, T. L. Horvath, D. G. Baskin, M. H. Tschop and M. W. Schwartz (2012). "Obesity is associated with hypothalamic injury in rodents and humans." J Clin Invest **122**(1): 153-162.

Tokarz, V. L., P. E. MacDonald and A. Klip (2018). "The cell biology of systemic insulin function." The Journal of Cell Biology **217**(7): 2273-2289.

Trayhurn, P. (1990). "Energy expenditure and thermogenesis: animal studies on brown adipose tissue." Int J Obes **14 Suppl 1**: 17-26; discussion 26-19.

Valdearcos, M., J. D. Douglass, M. M. Robblee, M. D. Dorfman, D. R. Stifler, M. L. Bennett, I. Gerritse, R. Fasnacht, B. A. Barres, J. P. Thaler and S. K. Koliwad (2017). "Microglial Inflammatory Signaling Orchestrates the Hypothalamic Immune Response to Dietary Excess and Mediates Obesity Susceptibility." Cell Metab **26**(1): 185-197.

Valdearcos, M., M. M. Robblee, D. I. Benjamin, D. K. Nomura, A. W. Xu and S. K. Koliwad (2014). "Microglia dictate the impact of saturated fat consumption on hypothalamic inflammation and neuronal function." Cell Rep **9**(6): 2124-2138.

van Waas, M., S. J. Neggers, A. G. Uitterlinden, K. Blijdorp, I. M. van der Geest, R. Pieters and M. M. van den Heuvel-Eibrink (2013). "Treatment factors rather than genetic variation

determine metabolic syndrome in childhood cancer survivors." Eur J Cancer **49**(3): 668-675.

Velloso, L. A. and M. W. Schwartz (2011). "Altered hypothalamic function in diet-induced obesity." International Journal Of Obesity **35**: 1455-1465.

Wang, X., A. Ge, M. Cheng, F. Guo, M. Zhao, X. Zhou, L. Liu and N. Yang (2012). "Increased hypothalamic inflammation associated with the susceptibility to obesity in rats exposed to high-fat diet." Experimental diabetes research **2012**: 847246-847246.

Whish, S., K. M. Dziegielewska, K. Møllgaard, N. M. Noor, S. A. Liddel, M. D. Habgood, S. J. Richardson and N. R. Saunders (2015). "The inner CSF-brain barrier: developmentally controlled access to the brain via intercellular junctions." Front Neurosci **9**: 16.

WHO (2004). "BMI classification."

WHO (2018). "Obesity and overweight."

Wirth, A., M. Wabitsch and H. Hauner (2014). "The prevention and treatment of obesity." Deutsches Arzteblatt international **111**(42): 705-713.

Woods, S. C., E. C. Lotter, L. D. McKay and D. Porte (1979). "Chronic intracerebroventricular infusion of insulin reduces food intake and body weight of baboons." Nature **282**(5738): 503-505.

Xu, Y., Y. Sun, K. Zhou, T. Li, C. Xie, Y. Zhang, J. Rodriguez, Y. Wu, M. Hu, L. R. Shao, X. Wang and C. Zhu (2018). "Cranial Irradiation Induces Hypothalamic Injury and Late-Onset Metabolic Disturbances in Juvenile Female Rats." Dev Neurosci **40**(2): 120-133.

Yeo, G. S. H., I. S. Farooqi, S. Aminian, D. J. Halsall, R. G. Stanhope and S. O'Rahilly (1998). "A frameshift mutation in MC4R associated with dominantly inherited human obesity." Nature Genetics **20**: 111.

Yoo, S., D. Cha, D. W. Kim, T. V. Hoang and S. Blackshaw (2019). "Tanycyte-Independent Control of Hypothalamic Leptin Signaling." Frontiers in Neuroscience **13**(240).

Yoshizumi, T., S. L. Brady, M. E. Robbins and J. D. Bourland (2011). "Specific issues in small animal dosimetry and irradiator calibration." Int J Radiat Biol **87**(10): 1001-1010.

Zabolotny, J. M., K. K. Bence-Hanulec, A. Stricker-Krongrad, F. Haj, Y. Wang, Y. Minokoshi, Y.-B. Kim, J. K. Elmquist, L. A. Tartaglia, B. B. Kahn and B. G. Neel (2002). "PTP1B Regulates Leptin Signal Transduction In Vivo." Developmental Cell **2**(4): 489-495.

Zhang, K., X. Shen, J. Wu, K. Sakaki, T. Saunders, D. T. Rutkowski, S. H. Back and R. J. Kaufman (2006). "Endoplasmic Reticulum Stress Activates Cleavage of CREBH to Induce a Systemic Inflammatory Response." Cell **124**(3): 587-599.

Zhang, X., G. Zhang, H. Zhang, M. Karin, H. Bai and D. Cai (2008). "Hypothalamic IKK β /NF- κ B and ER Stress Link Overnutrition to Energy Imbalance and Obesity." Cell **135**(1): 61-73.

Zhang, Y. P., R. Maffei, M. Barone, M. Leopold, L. Friedman, J.M. (1994). "Positional cloning of the mouse obese gene and its human homologue." Nature **372**: 425-432.

Zhou, Y. and L. Rui (2013). "Leptin signaling and leptin resistance." Frontiers of medicine **7**(2): 207-222.

Zimmer, D. J., R. C. Tsou, K. K. Bence and B. C. De Jonghe (2012). "Deficiency of PTP1B in Leptin Receptor-Expressing Neurons Leads to Decreased Body Weight and Adiposity in Mice." Endocrinology **153**(9): 4227-4237.

8. Abbreviations

Agrp	Agouti-related protein
ARC	Arcuate nucleus of the hypothalamus
BABB	Benzylalcohol-benzylbenzoat
BBB	Blood-brain-barrier
BDNF	Brain-derived neurotrophic factor
BMI	Body mass index
CrI	Cranial irradiation
CSF	Cerebrospinal fluid
DIO	Diet-induced obesity
DMH	Dorsomedial nucleus of the hypothalamus
ER	Endoplasmic reticulum
EX4	Exendin-4
GFAP	Glial fibrillary acidic protein
GhsR	Growth hormone secretagogue receptor
HFD	High-fat diet
Iba1	Ionised calcium-binding adapter molecule 1
ICV	Intracerebroventricular
IL-1	Interleukin-1
IL-6	Interleukin-6
InsR	Insulin receptor
JAK2	Janus kinas 2
JNK1	C-Jun amino-terminal kinase 1
LepR	Leptin receptor
LHA	Lateral hypothalamus
MBH	Mediobasal hypothalamus
MC3/4R	Melanocortin receptor 3 or 4
ME	Median eminence
MetS	Metabolic syndrome
NEFA	Non-esterified fatty acids
NF-kB	Nuclear factor kappa-light-chain-enhancer of activated B-cells
NG2	Neuron-glia antigen 2
NHS	N-hydroxysuccinimide
NPY	Neuropeptide Y
POMC	Pro-opiomelancortin
PTP1B	Protein tyrosine phosphatase 1B
PVN	Paraventricular nucleus of the hypothalamus
qPCR	Quantitative polymerase chain reaction
RG	Reactive gliosis
SHP2	Protein tyrosine phosphatase 2

SOCS3	Suppressor of cytokine signalling 3
STAT3	Signal transducer and activator of transcript 3
STAT5	Signal transducer and activator of transcript 5
T2D	Type 2 Diabetes
TCPTP	T cell protein tyrosine phosphatase
TLD	Thermoluminescent dosimeters
TLR4	Toll-like receptor 4
TNF- α	Tumour necrosis factor alpha
VMH	Ventromedial nucleus of the hypothalamus
WHO	World health organisation

9. List of figures

Figure 1. Prevalence of obesity in adults 18 years and older.....	1
Figure 2. Murine hypothalamic organisation.....	6
Figure 3. Parabiosis experiments performed by Douglas Coleman	8
Figure 4. Leptin receptor signalling mechanism	10
Figure 5. Custom-built irradiation chamber.....	25

10. List of tables

Table 1. Body weight classification defined by the World Health Organisation.....	2
--	---

11. Acknowledgements

Throughout my time as a PhD student I have received a great deal of support from a lot of people and I would like to express my gratitude.

First, I would like to thank Prof. Dr. Matthias Tschöp for giving me the opportunity to perform my PhD at a fantastic cutting edge research institute. The first class environment supported me in all aspects of my project.

I would like to extend my greatest thanks to my direct supervisor and mentor Dr. Paul Pfluger for his support over the past 3 years. Thank you for encouraging my research and for allowing me to grow as a scientist. I thoroughly enjoyed working with you and wish you all the best.

Besides my direct supervisor, I would like to thank the rest of my thesis committee: Prof. Dr. Hans Hauner and Prof. Dr. Preißl, for their time, their scientific guidance and positive nature.

I extend my deepest gratitude to the members of the neurobiology of diabetes research group; Sonja, Katrin, Emily, Raian and Peter. Thank you for all the scientific, technical and emotional support. But most of all, for making the time in the lab a very enjoyable one, which I will miss very much.

Next, I would like to thank the entire IDO for making me feel welcome from the first day and providing the ideal setting for scientific discussion and a pleasant place to work.

Finally, I am eternally grateful to my family, for providing me with unfailing support, for their continuous encouragement throughout my years of study, especially during my PhD. This achievement would not have been possible without them.

Lastly, to Laura, for her never-ending love, support and patience.

